Sede Amministrativa: Università degli Studi di Padova

Dipartimento di Ingegneria Meccanica – Settore Materiali

Scuola di Dottorato di Ricerca in Scienza e Ingegneria dei Materiali

XXIV Ciclo

Rubber compounds for industrial applications

Direttore della Scuola: Ch.mo Prof. Gaetano Granozzi

Supervisore: Ch.mo Prof. Massimo Gugliemi

Correlatore: Prof. ssa Giovanna Brusatin

Dottoranda: Jlenia Bottazzo

Contents

Sintesi

Dopo la scoperta del processo di vulcanizzazione, le gomme hanno invaso la nostra vita e attualmente occupano un posto significativo nel mondo industriale tanto che per molte applicazioni non ci sono materiali alternativi ad esse.

A differenza di quanto si potrebbe pensare, un oggetto di gomma è una sistema piuttosto complesso. Infatti, esso è in genere costituito da uno o più elastomeri e da molti altri additivi, quali ad esempio cariche rinforzanti, plastificanti, antidegradanti, agenti vulcanizzanti, etc. La realizzazione di un prodotto finito in gomma prevede una serie di operazioni. La prima di queste prevede la miscelazione dell'elastomero/i con diversi additivi ad una specifica temperatura per un tempo prefissato. Tale operazione è significativa nel determinare il grado di dispersione degli additivi nella matrice, influenzando quindi le proprietà del prodotto finale. Successivamente si verifica l'operazione di formatura durante la quale viene data una forma definita alla mescola. Infine con il processo di vulcanizzazione l'oggetto acquisisce la caratteristica proprietà di ritorno elastico, tipica delle gomma.

Le proprietà finali di un prodotto di gomma dipendono innanzitutto dall'elastomero di partenza, tuttavia possono essere ampiamente manipolate variando la tipologia e la concentrazione degli additivi aggiunti e le fasi di lavorazione.

Il fatto di essere un sistema multicomponente e la complessità delle fasi di produzione sono i motivi principali che hanno ritardato lo studio e lo sviluppo dei nanocompositi a base elastomera rispetto a quelli polimerici. Tuttavia, negli ultimi dieci anni il numero dei lavori scientifici sui nanocompositi elastomerici è ampiamente aumentato. Il continuo interesse deriva dal notevole miglioramento delle proprietà fisico-meccaniche che si osserva quando additivi nanodimensionali sono introdotti in una matrice elastomerica. Il miglioramento ottenuto dipende dalla dispersione a livello nanometrico che tali riempitivi possono raggiungere, contrariamente ai più comuni silice e nero fumo che si disperdono su scala micrometrica.

Ad oggi, le nanocariche maggiormente studiate per la loro disponibilità in natura e il basso costo sono le nanoargille. Numerosi studi hanno dimostrato che l'aggiunta di piccole quantità di silicati a strati (< 10 wt.%) migliora le proprietà meccaniche, riduce la permeabilità ai gas e il rigonfiamento in solventi, aumenta la stabilità termica e la resistenza alla fiamma.

La borsa di studio di questo dottorato è stata finanziata dalla ditta "IVG Colbachini" di Cervarese Santa Croce, Padova.

L'azienda, da più di 40 anni, realizza tubi industriali in gomma per la conduzione di polveri, granuli, gas, liquidi. I prodotti di "IVG Colbachini" trovano applicazione nei settori più diversi, tra i quali l'industria chimica e agro-alimentare, l'edilizia, la cantieristica navale e da diporto, le apparecchiature ferroviarie, le lavorazioni dei metalli.

Il lavoro di tesi svolto è stato dedicato allo studio e all'ottimizzazione di mescole elastomeriche prodotte in "IVG Colbachini".

Questa tesi consta di 6 capitoli e di seguito saranno riassunti brevemente gli argomenti principali trattati in ciascun capitolo.

Il Capitolo 1 evidenzia le differenze sostanziali tra composito convenzionale e nanocomposito, fornendo anche una classificazione di quest'ultima categoria di materiali. Inoltre spiega quali caratteristiche di un *filler* sono di fondamentale importanza per la realizzazione di un nanocomposito e come ciascuna di esse influenzi le proprietà del materiale finale.

Nel Capitolo 2 è contenuta una presentazione delle nanoargille e dei nanocompositi elastomerica additivati con *filler* a strati. In particolare si descrivono la struttura chimica di quest'ultimi e l'importanza del modificante organico. A questo si aggiunge un quadro dei metodi di sintesi di questi nanocompositi e delle loro proprietà tipiche riportate in letteratura, quali le prestazioni meccaniche, l'effetto barriera ai gas e la resistenza alla fiamma.

Il Capitolo 3 illustra passo passo l'arte della lavorazione della gomma. In particolare si introduce il concetto di "ricetta elastomerica" e come viene in genere espressa. Vengono specificate le tipologie, le caratteristiche e le funzioni dei diversi componenti di una "ricetta". Inoltre si descrivono le varie fasi di produzione di un oggetto in gomma, partendo dalla miscelazione degli ingredienti, passando per la formatura, arrivando fino al processo di vulcanizzazione. In questo capitolo vengono infine riportate alcune possibili applicazioni di prodotti in gomma.

Nel Capitolo 4 si introducono i materiali impiegati per la produzione delle formulazioni, oggetto di questo lavoro di tesi, le procedure sperimentali e le tecniche di caratterizzazione utilizzate.

Il Capitolo 5 illustra le prove condotte su una mescola elastomerica a base di etilene vinil acetato, con lo scopo di migliorarne le proprietà di resistenza alla fiamma. Vengono quindi riportati i risultati ottenuti e proposte alcune interpretazioni di essi.

Nel Capitolo 6 ci si è concentrati sullo studio delle proprietà meccaniche di un *blend* costituito da gomma naturale e polibutadiene. In particolare, i dati sperimentali ottenuti da mescole contenenti riempitivi tradizionali, come silice e nero fumo, sono stati confrontati con quelli ricavati da *compound* con *filler* innovativi, quali le nanoargille.

Abstract

Since the discovery of vulcanization, rubbers have invaded our life and nowadays occupie a significant place in the industrial world. In fact, in most applications there are no alternative materials to them.

Despite what it could be thought, a rubbery object is a very complex system. In fact, it is generally based on only one or more rubbers and on several other additives, such as reinforcing fillers, plasticizers, antidegradants, vulcanizing agents. Different production phases are required to realized a rubbery product. The first is the rubber compounding with the additives, which occurs at a defined temperature for a fixed time. The dispersion degree achieved by the fillers in the elastomeric matrix and consequently the final product properties are strictly dependent on this first step of production. After the mixing, the forming operations follow: the compound will retain the shape imposed. Finally, vulcanization process provides the material its 'elastic' recovery behaviour.

The final properties of a rubber product depend mainly on the type of rubber chosen, however they can be further manipulated by varying the additives used and their concentrations, and the processing steps.

The special character of rubber, being a multicomponent system, and the complexity of the production phases delayed the study and the development of rubber nanocomposites, in respect to the polymeric ones. However, in the ten past years, the reports published that deal with rubber nanocomposites have been raise.

The ongoing R&D interest is mostly due to the significant physico-mechanical properties improvement which is observed when the nanoclays are added to a rubber matrix. This enhancement depends on the nanometric-scale dispersion that the nanoclays can achieve in the compound; contrary to the conventional fillers, such as carbon black and silica, which carry out a micrometric-scale dispersion.

Nowadays, the nanoclays are the most studied nano-sized fillers because there are easily available in nature and cheap.

Several research works have demonstrated that the addition of even low amounts of layered nanofillers (< 10 wt.%) improves the mechanical properties, decreases gas permeability and swelling in solvents, increases thermal endurance and flame resistance.

5

The company, for over 40 years, has been involved in the production of industrial rubber hoses to convey powders, granular, liquid or gas materials. The "IVG Colbachini" products are used in different sectors, such as food, chemical, agricultural, construction, rail, naval and steel industries.

The thesis work was aimed at the study and the optimization of rubber compounds produced in "IVG Colbachini".

This thesis consists of 6 chapters and subsequently the main topics dealt with in each chapter will be concisely summarized.

Chapter 1 highlights the significant differences between a conventional composite and a nanocomposite, giving also a classification of this latter class of materials. In addition, it explains which filler features are the most important to obtain a nanocomposite and how each of these can influence the final product properties.

In Chapter 2 nanoclays and rubber nanocomposites loaded with layered fillers are introduced. Particularly, the chemical structure of these latter and the organo-modification importance are described. In addition there is a summary of the rubber/clay nanocomposite synthesis methods and their characteristic properties present in literature, such as mechanical performance, barrier effect and flame resistance.

Chapter 3 explains step by step the art of rubber compounding. In particular, the concept of recipe and how it is indicated are introduced. Types, features and functions of recipe diverse ingredients are specified. In addition, the different processing steps are described, starting from the component mixing, proceeding with the forming, until to the vulcanizing. Finally, some applications of rubber products are summarized.

Chapter 4 deals with materials used for the formulations subject of this thesis, experimental procedures and characterization techniques applied.

Chapter 5 is devoted to tests carried out on an ethylene vinyl acetate based rubber compound, with the aim to improve its flame retardant properties. The obtained results are indicated and some whose interpretations are presented.

Chapter 6 surveys the mechanical performances of a natural rubber/polybutadiene blend. Particularly, the experimental data obtained from the rubber compounds filled with conventional fillers, such as silica and carbon black, are compared with the ones found for the rubber compounds loaded with innovative fillers, like the nanoclays.

Chapter 1

Polymeric composites: state of the art

1.1 Introduction

The addition of both natural and synthetic fillers and reinforcements in polymeric matrices is a practice widely diffused in the polymer industry for the production of high-performances plastics. In fact a multiphase material, normally called composite, offers unusual combinations of properties that is difficult to attain separately from individual components.

It is very interesting to consider the changes in the role of particulate fillers as the time goes by. While in the early days fillers were added to the polymer to decrease price, in recent years the increasing technical requirements as well as soaring material and compounding costs require the utilization of all possible advantages of fillers.

Fillers can improve the composite performances [1], for example increasing tensile and tear strength without losing elasticity, or extending the barrier effect to gas and vapors. In addition, fillers can originate new functional properties not possessed by the matrix polymer at all like flame retardancy or conductivity.

The properties of all heterogeneous polymer systems are determined by the same four factors: component properties, composition, structure and interfacial interactions. Although an enormous variety of fillers is nowadays used and new fillers and reinforcements continually emerge, the effect of the four factors above mentioned is universal and valid for all particulate filled materials.

About the component properties, numerous filler characteristics influence the composite performance, in particular particle size, size distribution, specific surface area and particle shape. On the other hand, the main matrix property is stiffness.

The composition is related to the possibility to vary the filler content in a wide range. However, an optimum amount exists for each specific compound realized and excessive filler contents provoke the detriment of physico-mechanical properties. In addition, the improvement of a specific property achieved with a determined filler content may be accompanied by a deterioration of other performances.

The structure of filled polymers is considered simple, unfortunately a homogeneous distribution of particles is very difficult to achieve. On the contrary, particle related structures, such as aggregation

and orientation of anisotropic filler particles, usually develop in the composites.

The filler/matrix but also filler/filler interactions which occur into a composite are very important to control. In fact, the former cause the development of an interphase with properties different from those of both components, while the latter induce aggregation phenomena.

1.2 Nanocomposites: a new class of materials

Nanotechnology is the study and control of matter at dimensions of roughly 1 to 100 nanometers (nm), where unique phenomena enable novel applications [2].

Nanoscience can be considered as a revolutionary science in the multidisciplinary area. In fact, the development and the success achieved until now depend on the efforts from chemistry, physics, material science, electronics and biosciences.

In the field of nanotechnology, polymer matrix based nanocomposites have become a prominent area of current research and development and they have been defined as a promising new class of composites. They can be obtained by dispersing into a polymer matrix organic or inorganic particles with at least one dimension in the nanometer range (nanofillers). The fundamental length scales dominate the morphology and properties of these materials and the uniform dispersion of nanoscopically-sized particles can lead to a very large interfacial area. Because of their nanometer size features nanocomposites possess unique properties typically not shared by their more conventional microcomposite counterparts and, therefore, offer new technology and business opportunities [3].

1.2.1 Kinds of nanofillers

Nanocomposites can be classified according to the number of dimensions in the nanometer range of dispersed particles (Figure 1.1) [4].

Isodimensional nanoparticles, such as silica, carbon black, zinc oxide, polyhedral oligomeric silsesquioxanes (POSS), semiconductor nanoclusters, have three dimensions in the order of nanometers. When only two dimensions are nanometric while the third is larger, forming an elongated structure, we are dealing with nanotubes or whiskers. Examples are carbon nanotubes, cellulose whiskers, boron nitride tubes, gold or silver nanotubes. The last group is characterized by only one dimension in the nanometer range.

In this case the filler is disk-like nanoparticle and is one to a few nanometers thick while it is hundreds to thousands nanometers long. Layered silicates, layered graphite flakes and layered double hydroxides belong to this group [4].

0D   2D   1D
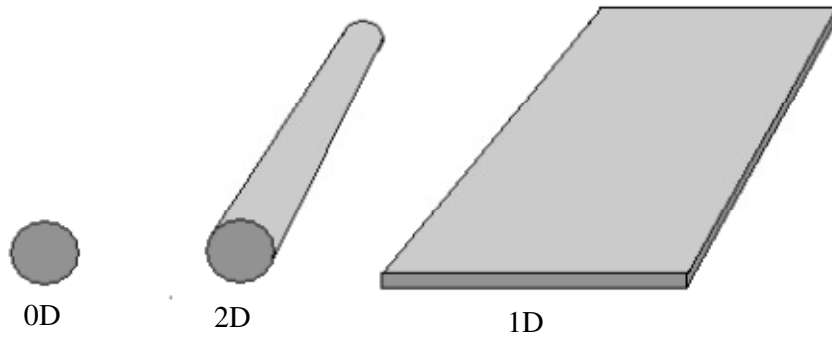
Fig. 1.1 Class of nanofillers.

Isodimentional fillers

Carbon black and silica are the widely used spherical fillers for polymer nanocomposite production. Carbon black consists essentially of elemental carbon in the form of near-spherical particles coalesced in aggregates of colloidal size, obtained by incomplete combustion or thermal decomposition of hydrocarbons [5].

Unfortunately, carbon black seldom exists as singles particles but instead as aggregates. A low structure black has an average of 30 particles per aggregate, whereas a high structure black may average up to more than 200 particles per aggregate (Figure 1.2) [6].

The aggregates tend to coalesce, due to Van der Waals forces, to form agglomerates, which size can vary from less than a micrometer to a few millimeters (Figure 1.2) [5].

20nm   100nm   10mm
(a)   (b)   (c)

Fig. 1.2: Characteristic sizes of fillers: (a) prymary particle, (b) aggregate, (c) agglomerate.

Silica, like carbon black, consists of aggregates of spherical particles fused together. It is made up of silicon and oxygen arranged in a tetrahedral structure of a three-dimensional lattice.

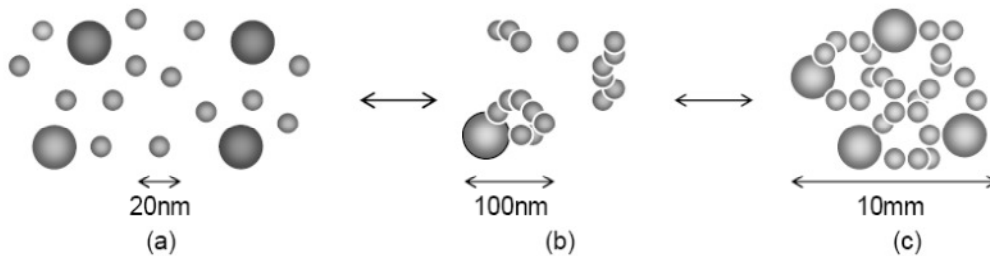Silicas are obtained with the precipitation process and, depending on the production parameters, they can be assigned to one of three groups: conventional silica (CV); semi-highly dispersible silica (semi-HD); highly dispersible silica (HD).

It was found that the HD silicas show a high structural level and are less fragile compared to those of the CV silicas. In addition, aggregates of the HD silicas have a more branched structure with 3-4 major branches on average [7]. This means that the HD silica is highly capable of dispersing during the mixing process.

The surface of silica and siliceous fillers contain silanol groups which have a higher acidity than hydroxyl groups of aliphatic silanols and than hydroxyl groups of hydrocarbon alcohols. So they have the tendency to form hydrogen bonds with many compounds like water, amines, alcohols and silanols [3].

Other spherical fillers, which have attracted great interest in recent year, are polyhedral oligomeric silsesquioxanes (POSS) [8-10]. They are considered as the smallest particles possible for silica. Polyhedral oligomeric silsesquioxane possesses two unique structural features: the chemical composition is a hybrid, intermediate ($RSiO_{1.5}$) between that of silica (SiO_2) and silicones (R_2SiO); and POSS molecules are nanometric and equivalent in size to most polymer segments and coil.
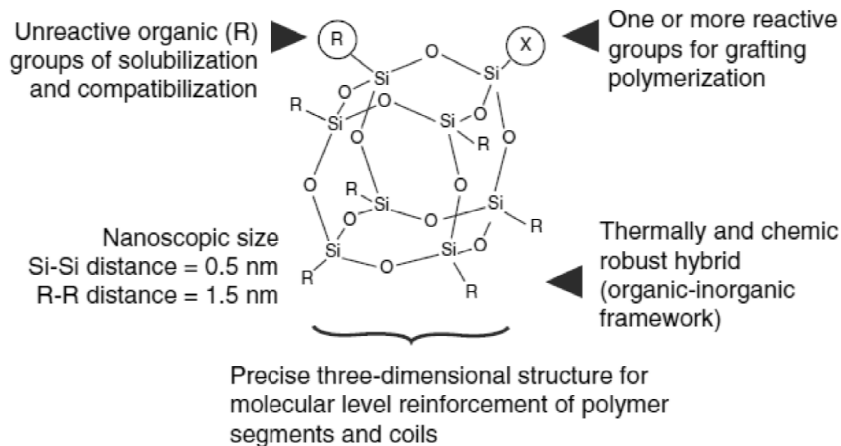

Fig. 1. 3: Structure of a POSS.

The anatomy of POSS molecule is displayed in Figure 1.3. It appears as a three-dimensional silicone and oxygen cage structure with unreactive groups but also one or more reactive groups for grafting to polymer chains.

Tubolar fillers

Among different types of tubular fillers, carbon nanotubes are the most widely used in academia and industry to produce polymer nanocomposites. As the name indicates, nanotubes are cylindrical in shape with at least one end capped with a hemisphere of the buckyball structure. Carbon nanotubes can be classified in single-wall (SWNT) or multiwall (MWNT) based on the number of walls rolled [3]. Carbon nanotubes have received great attention for their mechanical, electrical and thermal properties, which are a consequence of their bonding nature. A new class of naturally occurring nanotubes (silicates with a nanotubular structure) named halloysite nanotubes (HNTs) have been reported and used as reinforcing filler in various polymer matrices [3, 11, 12]. HNTs are aluminosilicates with nanodimensional tubular structure composed of siloxane groups on the surface along with a few hydroxyl groups; they possess a better dispersion property and the ability to form hydrogen bonding with the functionalized polymer matrix [13, 14]. Other tubolar nanofillers are cellulose nanofibers which are obtained from wood after suitable chemical treatment [3]. Cellulose chains aggregate to form microfibrils with a diameter ranges from 2 to 20 nm with lengths up to several tens of microns.

Layered fillers

Layered clays are composed of platy very fine particles called layers (Figure 1.4) [15]. The neighboring layers are stacked and held together by weak Van der Waals bonds. The gap between the layers is called gallery or interstratum. Layered fillers were used in this PhD activity and an in-depth description will be provided in the Chapter 2.
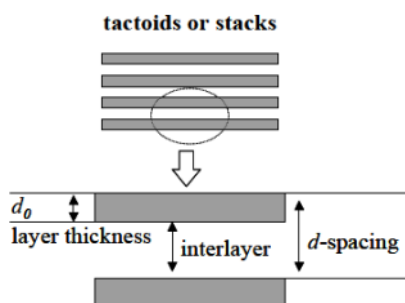

Fig. 1.4 Structure of layered clay.

1.3 Filler features and their effect on composite properties

A large variety of fillers is used nowadays in composites and one of their principal feature is the diverse chemical composition. However, a lot of other characteristics of a filler influence the final composite performance. The most important filler characteristics are particle size, size distribution, specific surface area and particle shape [3].

1.3.1 Particle size

One of the first information generally considered about a filler is the average particle size [3, 16]. The latter has a significant influence on composite properties, in fact strength and sometimes modulus increase, while deformability and impact strength usually decrease with decreasing particle size [16].

However, the knowledge of the particle size distribution is equally important for the characterization of any filler. In fact, the aggregation tendency of fillers increases with decreasing particle size. Extensive aggregation leads to insufficient homogeneity, rigidity and low impact strength. But also aggregated filler particles act as crack initiation sites in impact.

1.3.2 Specific surface area and surface energy

The specific surface area is strictly related to the particle size, however it is a very important filler feature since it influences directly the properties of the composite. In fact, from the specific surface area depends on the area of the matrix/filler interface.

The surface free energy of fillers determines both matrix/filler and filler/filler interaction. The former has a pronounced effect on the mechanical properties of the composite; the latter influences aggregation [16].

1.3.3 Particle shape

The shape of the particles has pronounced significance. In particular, the reinforcing effect of the filler increases with the anisotropy of the particle, that is with the increase of the aspect ratio (average length/diameter ratio).

Fillers with plate-like geometry like talc, mica, or layered silicates reinforce polymers more than spherical fillers and the influence of glass fibers is expected to be even stronger [16]. The filler shape also affects the barrier properties. In fact, fillers with high aspect ratio reduce gas permeability and solvent diffusion more effectively than spherical fillers.

1.4 Interfacial interactions

Interfacial interactions developed in a filled polymer matrix are diverse: interactions between matrix and filler and interactions between filler particles [3]. The control of the interactions in a composite is very important because these influence significantly not only mechanical properties but also processability and appearance of the final product. It is obvious that to achieve the better performance is necessary to limit the filler/filler interactions because they could provoke aggregation phenomena.

Experience has shown that the probability of aggregation increases with decreasing particle size of the filler. Filler aggregation represents a problem because it induces a detrimental in the properties of composites. It is well-known that tensile strength but also the fracture resistance of composites containing aggregated particles drastically decreases with increasing number of aggregates. Aggregates may act as fracture initiation sites and depending on aggregate strength they may break under the effect of external load, which results in the failure of the product [16].

The best performance of a composite can be achieved minimizing interactions between the fillers. A way to attain this goal is the surface modification of the fillers (see 1.5) which permits to change the polarity of a particle increasing the compatibility between matrix and filler, and improving the wetting of the latter by the polymer.

The adsorption of polymer chains onto the active sites of the filler surface results in the development of a layer, called interphase, which has properties different from those of the polymer matrix. The thickness of the interphase is related to the type and the strength of the interactions.

1.5 Enhance matrix/filler interaction: surface modification

The easiest way to change interfacial interactions is the filler surface modification [3, 16, 17]. Surface treatment is a fundamental step during composite production because it permits to modify both filler/filler and matrix/filler interactions, and as consequence to vary the final properties of the composite.

The most common method to modify the fillers is coating their surface with a small molecular weight organic compounds. Stearic acid and their metallic salts are good examples of surface active agents, generally used for the coverage of calcium carbonate. The principle of the treatment is the preferential adsorption of the surfactant onto the surface of the filler.

In other that the treatment is efficient, a crucial step is the determination of the optimum amount of surfactant to use. In fact, insufficient amount does not achieve the desired effect, while excessive quantities lead to the deterioration of the physical-mechanical properties. The optimum amount is generally influenced to diverse parameters, such as the type of the interaction, the surface area occupied by the coating molecule, its alignment to the surface.

In addition to non-reactive treatment, reactive surface modification may be applied. In this condition, a coupling agent is added to the compound and it reacts and forms covalent bonds with fillers and matrix.

Silane coupling agents are successfully applied for fillers and reinforcements which have reactive –OH groups on their surface [3]. The most common is the reaction between organosilane and silica which permits to make silica compatible with non polar polymer. The final effect depends strictly on the kind and on the amount of the silane used. Long chains cover the silica surface more efficiently and/or form self-oriented layers that shield the surface than short chain silanes.

An advantage of silane coupling agents is their double reactivity since they are capable of reacting both with filler but also with matrix.

References

[1] R.F. Gibson, *Composite Structures*, **92**, 2793 (2010).

[2] V.E. Borisenko and S. Ossicini, *What is What in the Nanoworld: A Handbook on Nanoscience and Nanotechnology*, Wiley-VCH (2008).

[3] T. Sabu and S. Ranimol, *Rubber Nanocomposites: Preparation, Properties and Applications*, John Wiley & Sons (2010).

[4] Q.H.Zeng, A.B. Yu, G.Q. Lu and D.R. Paul, *J. Nanosci. Nanotechnol.*, **5**, 1574 (2005).

[5] B. Rodgers, *Rubber Compounding: Chemistry and Applications*, Marcel Dekker (2004).

[6] J.R. White and S.K. De, *Rubber Technologist's Handbook*, Rapra Technology (2001).

[7] D.W. Schaefer, *J. Appl. Crystallogr.*, **33**, 587 (2000).

[8] C. Sanchez, G.J. de A.A. Soler-Illia, F. Ribot, T. Lalot, C.R. Mayer and V. Cabuil, *Chem. Mater.*, **13**, 3061 (2001).

[9] U. Schubert, *Chem. Mater.*, **13**, 3487 (2001).

[10] C. Sanchez, B. Lebeau, F. Ribot and M. In, *J. Sol-Gel Sci. Tech.*, **19**, 31 (2000).

[11] M.X Liu, B.C. Guo, M.L. Du, X.J. Cai and D.M. Jia, *Nanotech.*, **18**, 455703 (2007).

[12] M.L Du, B.C. Guo, M.X. Liu and D.M. Jia, *Polym. J.*, **38**, 1198 (2006).

[13] E. Joussein, S. Petit, J. Churchman, B. Theng, D. Righi and B. Delvaux, *Clay Miner.*, **40**, 383 (2005).

[14] Y.P Ye, H.B. Chen, J.S. Wu and L. Ye, *Polymer*, **48**, 6426 (2007).

[15] M. Alexandre and P. Dubois, *Mater. Sci. Eng*, **28**, 1 (2000).

[16] János Móczó and Béla Pukánszky, *J. Ind. Eng. Chem.*, **14**, 535 (2008).

[17] L. Betega de Paiva, A.R. Morales and F.R.Valenzuela Díaz, *Appl. Clay Sci.*, **42**, 8 (2008).

Chapter 2

Rubber-clay nanocomposites

2.1 Introduction

Nanoreinforcement of rubbers has a long and solid background since a plethora of compounding recipes, which contain particles of nanodimension range, like carbon black and silica grades, have been developed by both academia and industry [1]. However, recently several other kinds of nanofillers have received attention for reinforcement characteristics in rubbers and, amongst all, the nanoclays have been more widely investigated probably because they are easily available in nature and cheaper.

The ongoing R&D interest is mostly due to the remarkable properties improvement which is observed when nanoclays are added to a rubber matrix. This enhancement depends on the nanometric-scale dispersion that the nanoclays can achieve in the compound; contrary to the conventional fillers, such as carbon black and silica, which carry out a micrometric-scale dispersion.

2.2 Layered clays

Layered clays are constituted by plate-shaped very fine particles. The clay particles can be delaminated into discrete nanosized sheets in a polymeric matrix or in absence of delamination, the particles can have dimensions in the microscale [1].

The layered clays mainly used in nanocomposites belong to the structural family of the 2:1 phyllosilicates. The crystal structure consists of two-dimensional layers where a central octahedral sheet of alumina or magnesia is sandwiched between two silica tetrahedron sheets (Figure 2.1). The layer thickness is around 1 nm and the lateral dimensions of these layers may vary from 300 Å to several microns and even larger depending on the silicate [2]. Stacking of the layers leads to a regular Van der Waals gap between the layers called the interlayer or gallery.

Isomorphic substitution of Al with Mg, Fe, Li in the octahedron sheets and/or Si with Al in tetrahedron sheets generates excess negative charge in the layers, which is counterbalanced by exchangeable metal cations situated in the galleries (such as Na^+, K^+,

Ca^{2+}). Montmorillonite (MMT), hectorite and saponite are the most commonly 2:1 phyllosilicates and they are defined as cationic clays.
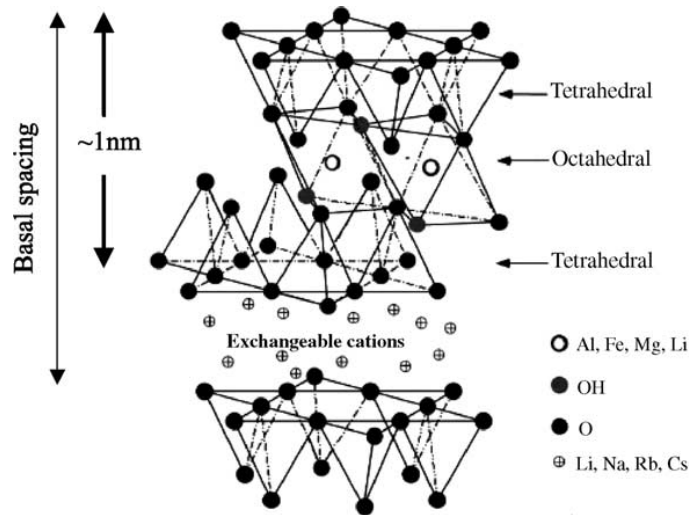
Fig. 2.1 Structure of 2:1 phyllosilicates [3].

On the other hand, it is also possible to have positively charged layers with anions intercalated in the interlayer regions together with water molecules so as to form anionic clays. Layered double hydroxides (LDHs), which have the structure of mineral brucite ($Mg(OH)_2$), are an example of anionic clays. Brucite consists of an hexagonal close packing of hydroxyl ions with alternate octahedral sites occupied by Mg^{2+} ions (Figure 2.2).

Fig. 2.2 Schematic representation comparing the crystal structure of brucite (a) and LDH (b).

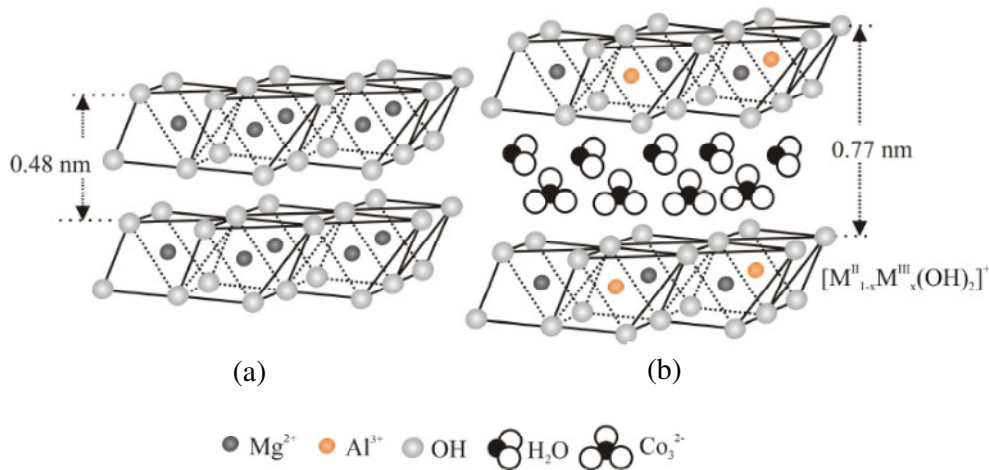The metal hydroxide sheets in brucite crystal are neutral in charge and stack one upon another by Van der Waals interactions. When a fraction of the Mg^{2+} ions in brucite is substituted by trivalent cations such as Al^{3+}, the resultant hydroxide layers acquire a positive charge; so various anions are intercalated in the interlayer regions for neutralizing the excess positive charge.

The spaces between the layers in LDH also contain some water molecules for the stabilization of the crystal structure. The presence of anions and water molecules leads to an enlargement of the basal spacing from 0.48 nm in brucite to about 0.77 nm in LDH [4].

2.3 Organic modification of clays

One of the drawbacks of clays is their hydrophilic nature that makes difficult their dispersion in hydrophobic matrix. Therefore, the clays can be organically modified in order to render them more compatible with organic polymers [5]. Such modified clays are commonly referred to as organo-clays. Another key aspect of surface modification is to swell the interlayer space up to a certain extent and hence to reduce the layer-layer attraction, allowing a favourable diffusion and accommodation of the chains of polymer into the interlayer galleries [5].

Several routes can be employed to modify clays, such as adsorption, ion exchange with inorganic cations and organic cations, binding of inorganic and organic anions (mainly at the edges), grafting of organic compounds, reaction with acids, pillaring by different types of poly(hydroxo metal) cations, intraparticle and interparticle polymerization, dehydroxylation and calcination, delamination and reaggregation of smectites, and lyophilisation, ultrasound and plasma [6].

Among all the ion exchange is the most popular and the most easy technique to modify the clays (Figure 2.3). It consists in exchange interlayer ions of the clay by organic ions in aqueous solution. A variety of organic ions can be used for the modification but the choice has to be made in relation of the clay nature. For example, MMT is anionic in nature and, therefore, this clay is modified by cationic surfactants, like ammonium and phosphonium compounds. On the other hand, having cationic layer charges, LDH is modified by anionic surfactants, like carboxylates, sulfonates [4].
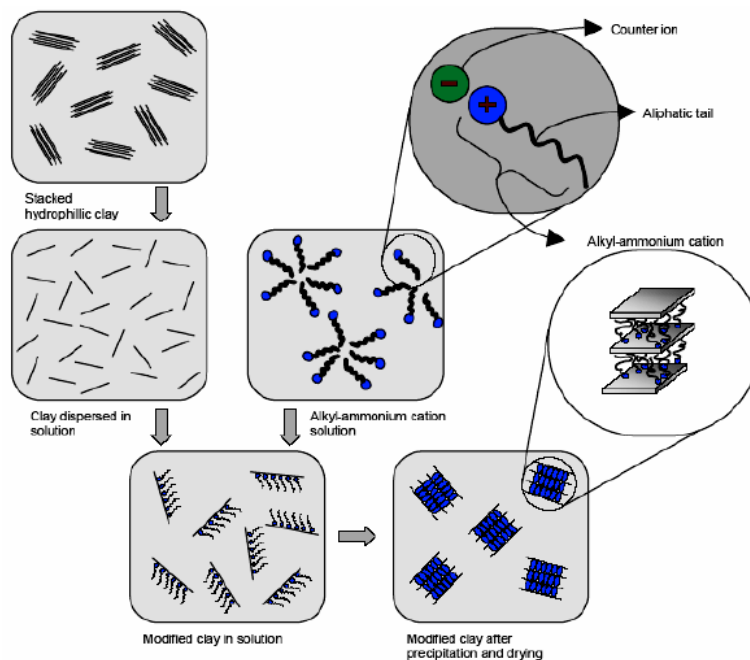
Fig. 2.3 Organic modification by ion exchange of pristine nanoclays.

2.4 Preparation of rubber-clay nanocomposites

During the early research activities (1960-1970) on polymer/clay nanocomposites less attention was put on rubbers. While in the "hot" period of 1990s only sporadic works had rubbers/layered silicates as subject. However, in the ten past years, the reports published that deal with rubber nanocomposites have been raise. Ethylene-propylene-diene rubber [7], natural rubber [8, 9] and epoxidized natural rubber [10, 11], silicon rubber [12], nitrile [13] and hydrogenated nitrile rubbers [14], fluoroelastomers [15] have been used as matrices in clay-filled systems.

The reason for this late development is essentially due to the complexity of vulcanized rubbers. In fact, being a multicomponent system, the analysis of the parameters affecting the rubber nanocomposite formation becomes complicated.

A nanocomposite is not always obtained when nanoclays are added in a rubber matrix. In fact, depending on the nature of the components, the method of preparation and hence on the strength of interfacial interactions developed between matrix and clays, three main kinds of composites may be produced (Figure 2.4).

When the rubber chains are not able to intercalate into the gallery spaces of the clay, a phase separated composite is obtained, which shows the same properties of a traditional microcomposite. On the other hand, intercalated nanocomposites are produced when

polymer chains are inserted into the gallery of nanoclay, resulting in a well ordered multilayer morphology stacking alternately polymer layers and clay platelets and a repeating distance of a few nanometers [5]. The last case is that of an exfoliated or delaminated nanocomposites, in which the clay platelets are completely and uniformly dispersed in a continuous rubber matrix [5]. The totally exfoliated nanocomposites is very difficult to produce, generally intercalated and exfoliated structures are present at the same time.
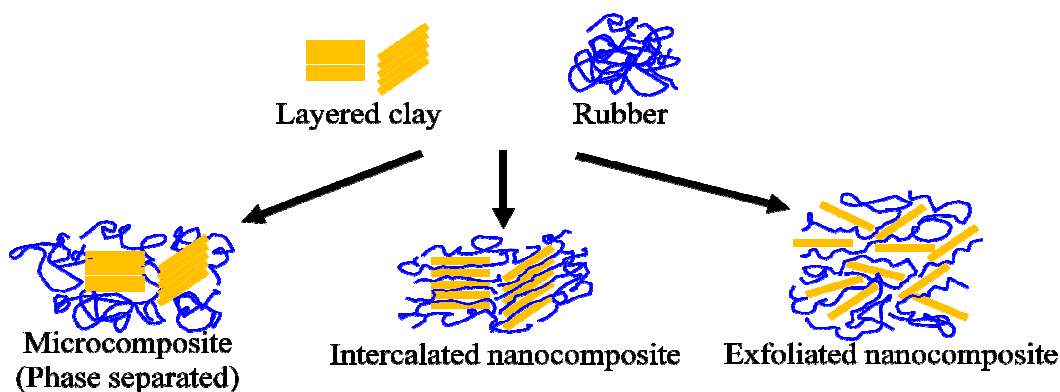

Fig. 2.4 Scheme of different types of composite arising from the interaction of layered silicates and polymers: phase separated microcomposite, intercalated nanocomposite and exfoliated nanocomposite.

Three are the methods commonly used to prepare rubber-clay nanocomposites: solution mixing, latex compounding and melt mixing.

2.4.1 Solution mixing

In this method, dry rubber is dissolved in a suitable solvent along with the nanoclays or mixed together after dissolution in suitable solvents. Then, the solvent is evaporated to obtain the nanocomposite.

Sadhu et al. [16] prepared a series of rubber nanocomposites by mixing octadecyl amine modified sodium MMT clay and styrene-butadiene rubber with different styrene content (15, 23 and 40 wt.%). The authors varied the solvent, the cure conditions, and the cure system to determine their effect on the nanocomposite properties. It was observed that the nature of the solvent strongly influenced the mechanical properties of the rubber/clay compound. In particular, the tensile strength and the modulus were higher for the toluene-cast sample, while the highest elongation at break was obtained for the chloroform-cast sample. The cure system had a significant effect on the elongation at break, in fact it is

higher with sulphur curing. In addition, the authors cured the samples at 160°C for 10, 15, 30, and 60 minutes, finding that the mechanical properties reached the optimum with a cure time of 15 min.

López-Manchado et al. [17] compared natural rubber/organo-MMT nanocomposites produced by solution and mechanical mixing. It was found that both methods permit to carry out an optimal dispersion of the filler. However, bound rubber measurement showed that a higher amount of rubber is fixed to the clay with the solution mixing procedure. Consequently, the dynamical mechanical properties, the compression set and the hardness of the nanocomposite synthesized by solution mixing are more improved in relation to mechanical compounded-nanocomposite.

2.4.2 Latex compounding

The latex is an aqueous dispersion of rubber particles in the submicron-micron range. This mixing technique is particularly suitable for pristine clays which are strongly hydrophilic. Water can act as a swelling agent owing to the hydration of the intergallery cations, making easier the clay exfoliation under stirring.

The clay/latex mixture is casted in a mold and left to dry. In this case, the nanocomposite is not vulcanized; however it is possible to add the curative agents, previously dispersed in water, to the clay-containing rubber latex. After the casting and drying, the material is thermal treated for the vulcanization.

Blending of rubber latices is a versatile way to produce rubber articles of enhanced performance, at the same time lowering the proportion of the most expensive component. Varghese et al. [18] prepared polyurethane rubber (PUR)/natural rubber (NR) blend with clays from the related latices, producing films of nanocomposites with properties similar to those of PUR-based matrix. This result is of great economic significance, as NR latex is cheaper then PUR latex and is found abundance in nature.

2.4.3 Melt intercalation

From an industrial standpoint, the melt compounding is the most direct, most cost-effective, and environment friendly method (no organic solvent is involved) to synthesize layered silicate/rubber nanocomposites. This involves equipments like internal mixer and open mills.

Since Vaia et al. [19] reported mixing polymers with clays without the use of organic solvents, there has been vigorous research in this field.

Direct melt intercalation of polymers in organo-silicates is primarily driven by enthalpic polymer-host interactions whereas the driving force for polymer intercalation from solution is the entropy gained by desorption of small molecules from the host galleries [19]. The role of the alkyl ammonium cations in organo-silicates is to lower the host's surface energy and thereby to improve the wetting-out by the polymers.

Nah et al. [20] prepared NBR hybrid nanocomposites with organo-clays by melt mixing using an internal mixer. The authors found that the sample properties were compared with those of conventional rubber compounds filled with carbon black and silica. On the basis of XRD and TEM, the authors found that when the organoclay content was below 2 phr, the NBR hybrids formed an exfoliated structure, but they formed an intercalated nanocomposite with increasing organo-clay amount. The organo-clay nanocomposite showed a simultaneous improvement in ultimate strength and stiffness, which generally follow a trade-off relation in rubbery materials. The organo-clay nanocomposite showed much higher hysteresis and tension set compared to pristine MMT, silica and carbon black filled compounds. This result is due to the greater chain slipping on the surfaces and interfaces of intercalated organo-clays and reduced recovery during cyclic deformation.

Tian et al. [21] reported the preparation, by direct mill mixing, of low-cost SBR nanocomposites based on attapulgite (AT), a natural fibrillar silicate. Investigating the structure of the composite, it was found that most AT separated into dispersed units with diameters less than 100 nm in SBR. However, a few dispersion units as large as 0.2–0.5 μm were also observed. The authors demonstrated that the pretreatment of AT with the silane coupling agent Si69 improves the dispersion of AT and enhances the chemical interfacial adhesion. At the same loading, AT (pretreated with Si69) showed better reinforcing effect on SBR than some kinds of carbon black.

In most of reported studies rubber nanoclays nanocomposites (RCNs) prepared by melt compounding, the full exfoliation of organoclay layers in rubber matrix was not obtained. There are many factors affecting the morphology of RCNs during melt compounding, such as the type of intercalates, compounding condition (shear rate and temperature) and the polarity of matrix rubber. Some of these parameters were investigated by Gatos et al [22] in a sulfur-cured ethylene propylene diene rubber (EPDM) containing 10 phr organo-clay. The parameters varied were linked to processing (mixer type, temperature) and rubber recipe (compatibilizer, accelerator). The authors demonstrated that increasing shear rate and temperature improve mechanical properties because of a better clay

dispersion is achieved. In addition, using a compatibilizer is possible to change the polarity of the rubber and the overall effect of the compatibilizer was found to be superior to the one of processing condition.

2.5 Properties of rubber-clay nanocomposites

In recent years rubber-clay nanocomposites have attracted considerable attention in both academic and industrial due to their improved performance compared to matrices containing micron-sized fillers. In particular, mechanical properties enhancement has been observed. Thermal stability and fire retardancy through char formation are other interesting and widely searched properties displayed by rubber nanocomposites. These new materials have also been studied and applied for their superior barrier properties against gas and vapor transmission.

2.5.1 Mechanical performance

When submitted to a mechanical stimulus, elastomers show a viscoelastic response. Figure 2.5 displays a typical stress-strain curve of a rubber. At low strain, unfilled elastomers have a linear behaviour, defined by a modulus independent of the applied stress level. The introduction of nanosized fillers in a rubber matrix leads, at strain below 100%, to a non linear mechanical behaviour. This phenomenon, observed in all the filled elastomers, is known as Payne effect [1].
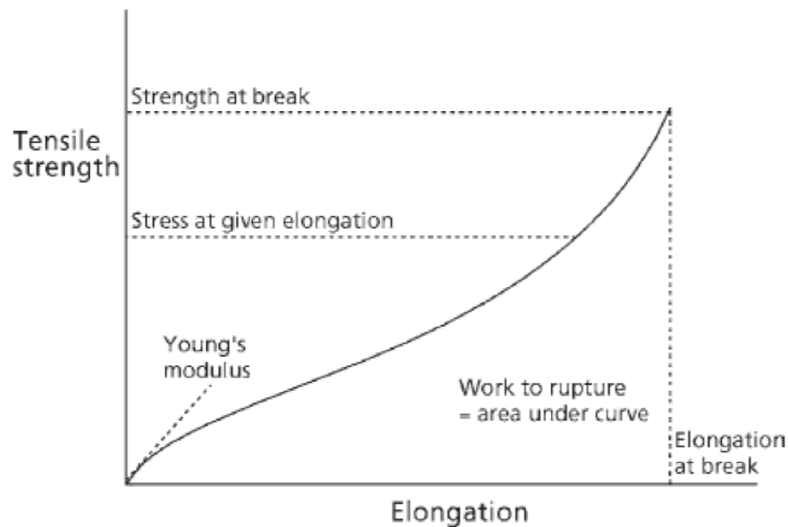

Fig. 2.5 Typical rubber stress-strain curve.

At higher strain level, rubbers exhibit a rapid increase of the stress (Figure 2.5). This behaviour is related to the limited extensibility of the chains between cross-links.

Like at small strain, the addition of fillers induces an increase of the stress level of the material at a given strain, as shown in Figure 2.6.
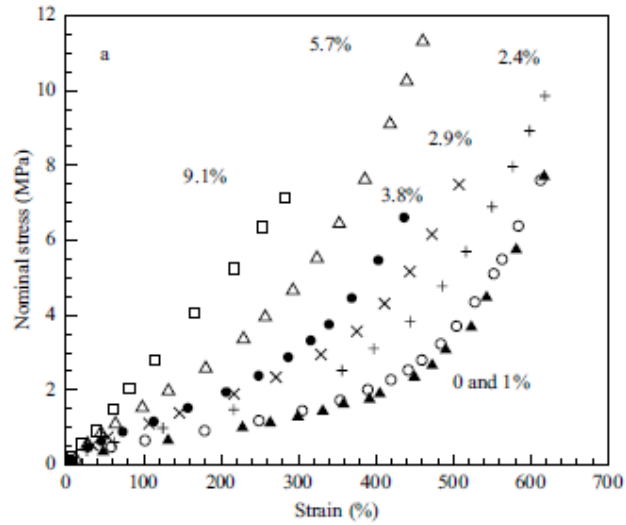

Fig. 2.6 Stress-strain curves of pure NR and NR/MWNTs composites [23].

Another phenomenon observed in filled rubbers is the so-called Mullin effect (Figure 2.7) [1]. A sample is stretched at a maximum deformation (ε_{max}) and then it is unloaded for between half an hour and several days. When a new loading is applied the stress-strain curve appears below the first curve obtained. For a deformation above (ε_{max}), the second curve joins the first one.
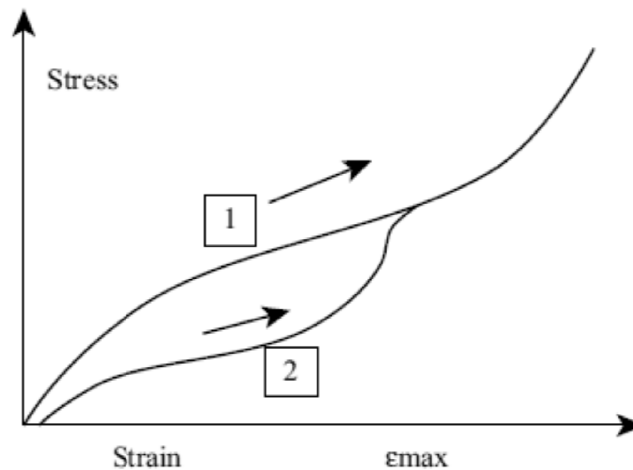

Fig. 2.7 The Mullin effect on stress-strain curves in reinforced elastomers [1].

25

The main interest in rubber/clay nanocomposites until now has concerned the improvement of mechanical properties of the rubber matrices at a relatively low filler content. Thus, layered silicate can be considered as a potential substitute of the conventional reinforcing fillers: carbon black and silica, which have to be mixed at high concentration.To this end, natural rubber with 10 phr of pristine (PC) and octadecylamine modified (OC) montmorillonite were compared with 10 and 40 phr carbon black (CB) as filler by Arroyo et al. [24]. The formation of a conventional composite was produced by using the unmodified MMT and a low reinforcing effect was obtained. On the other hand, a significant enhancement in the mechanical properties was observed with the organo-clay. Increment of above 350% in the strength was produced without loss in the elongation at break, kept at the same value of pure natural rubber.

Curing characterization demonstrated that nanocomposites with the organo-clay has a higher number of cross-links than carbon black nanocomposites. This influences strongly the mechanical properties of the compound which are significant improved (Table 2.1). In particular, the mechanical performances of 10 phr organo-clay-filled NR rubber filled was comparable with the ones of 40 phr carbon black-filled compound (Table 2.1).

Table 2.1 Properties of the studied compounds [24].

Property	NR	NR-PC (10 phr)	NR-OC (10 phr)	NR-CB (10 phr)	NR-CB (40 phr)
Modulus 100% (MPa)	0.59	0.53	1.72	0.83	1.60
Modulus 300% (MPa)	1.33	1.38	4.31	2.53	5.52
Modulus 500% (MPa)	2.60	2.90	9.73	-	-
Maximum strength (MPa)	4.25	3.60	15.0	4.93	10.3
Elongation at break (%)	>700	555	>700	464	434
Hardness (shore A)	28.8	20.7	43.5	30.5	38.3
Rebound resilience (%)	63.0	58.0	62.5	58.5	50.5
Compression set (%)	17.5	27.9	22.4	28.7	42.8
Abrasion loss (mm^3)	286.2	-	217.5	282.0	199.3
Density (g/cm^3)	0.975	1.030	1.004	1.014	1.081

The effect of clay modification on organo-montmorillonite/NBR nanocomposites was studied by Kim et al. [25]. Different nanocomposites were prepared through a melt

intercalation process. XRD showed that the basal spacing in the clay increased, which means that the NBR matrix was intercalated in the clay galleries. The tensile test demonstrated that nanocomposites achieved superior mechanical performance than conventional composites. This high reinforcement effect implies a strong interaction between matrix and clay interface that can be attributed to the nanoscale and uniform dispersion of silicate layers in the NBR matrix.

It is very important to highlight that the final properties of a rubber/nanoclay compound depends strongly on organoclay type and loading. To this end, Gatos et al. [26] observed a different trend with respect to the type of MMT organic modifier for the nanocomposites. The authors prepared ethylene-propylene-diene (EPDM) rubber based compounds, containing maleic anhydride grafted EPDM and MMTs modified with primary or quaternary amine.

As shown in Figure 2.8, the EPDM-MA/MMT-PRIM presented a plateau as a function of increasing organoclay content, whereas for the EPDM-MA/MMT-QUAT the ultimate tensile strength went through a maximum. Significant differences were also observed in the elongation at break values versus clay loading traces. The EPDM-MA/MMT-PRIM nanocomposite above 10 phr organoclay content had surprisingly high strain values. On the contrary, for the EPDM-MA/MMT-QUAT a decrease in the elongation at break was observed. This behaviour is likely related with agglomeration phenomena.
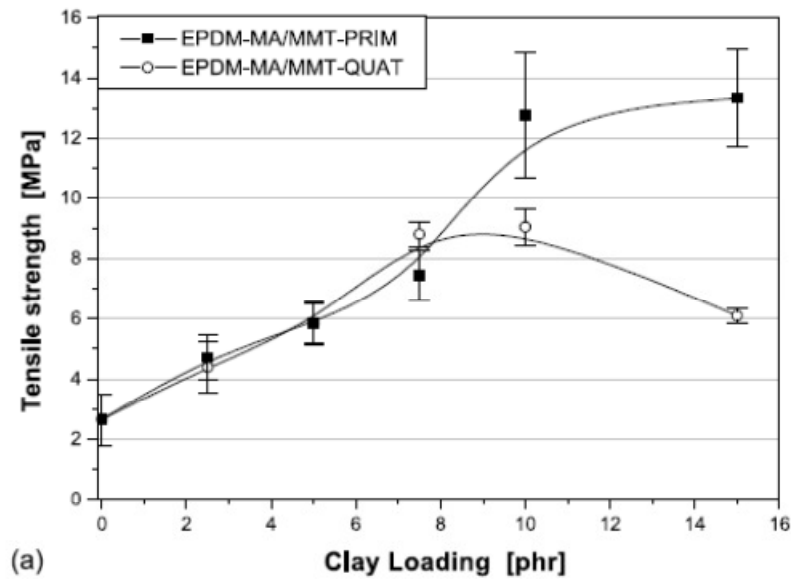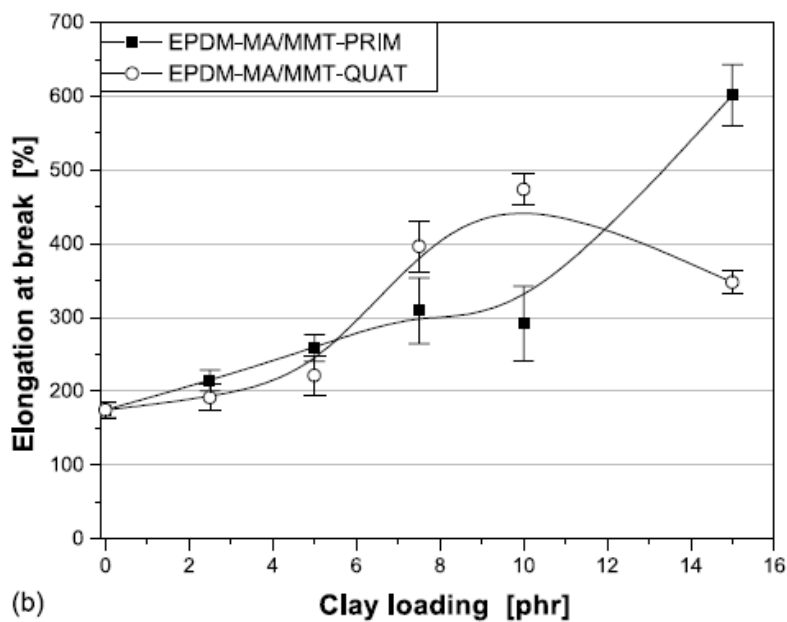
Fig. 2.8 (a) Tensile strength and (b) elongation at break vs. clay loading for the EPDM-MA/MMT-PRIM and EPDM-MA/MMT-QUAT nanocomposites [26].

Similar stress-strain curve has been reported for various rubber nanocomposites [27, 28]. Usually, at relatively low organic content, favourable matrix/clay interactions are achieved and both tensile strength and elongation at break increase. However, further increase in the loaded clay amount produces a plateau (saturation) or a reduction in the ultimate stress and strain values.

Tensile strength improvement, associated with an increase in the elongation at break values, is a rather unexpected phenomenon for rubber/organo-clay nanocomposites, nevertheless, it was found also in other rubber compounds. This phenomenon was explained by a synergistic effect of platelet orientation and chain slippage [29]. The orientation can increase the loading capability of organoclay (OC), and the slippage makes it possible for the highly strained molecular chains to relieve the tension caused by the stretching so that they will not break prematurely, resulting in a higher strain-at-break and strength.

In Figure 2.9, poor and good dispersion of the same amount of layered silicate is showed under high deformation of the compound [30].
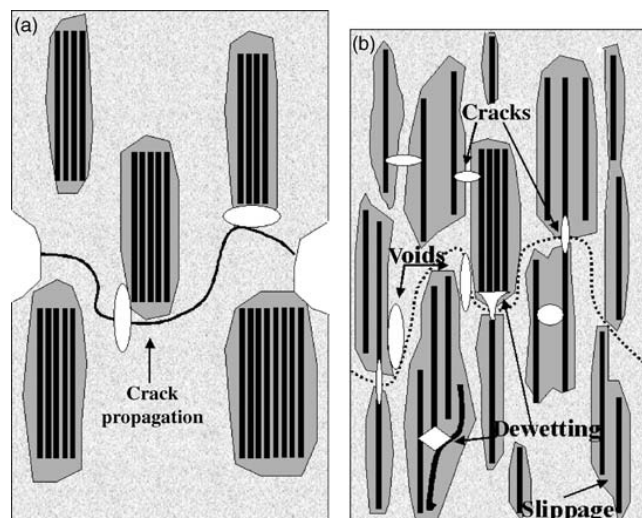
Fig. 2.9 Scheme of failure development in rubber/organoclay mixes with poor (a) and good (b) dispersion of the clay layers due to high strain at uniaxial loading: (a) fast crack growth after surface cracking and (b) slow crack growth via void coalescence [30].

Although the filler volume in both cases is the same (cf. same number of plates in Figure 2.9 (a) and (b)), the effective filler volume values differ from one another as a function of the dispersion grade. The latter may affect the bound rubber content, generates a rubber shell in the vicinity of the silicate platelets (cf. dark gray areas in Figure 2.9 indicate a different rubber cross-linking density compared to the bulk) and influences the occlusion of rubber within the clay galleries.

According to this model a modulus increase is expected even at low organoclay content when the clay layers are well dispersed (well intercalated and exfoliated).

The failure of rubber specimens upon tensile loading starts with crack initiation. In rubber/layered silicate nanocomposites, first the orientation of the clay platelets takes place during uniaxial drawing [30]. Generally, an elastomeric network suffers higher stresses up to break if it is capable of dissipating the input energy (e.g., by converting into heat). At sufficient high strain, cracks can be generated by the fillers (via voiding, dewetting phenomena, chain slippage, and so on.). As the dispersion of the platelets allows the creation of voids (subcritical cracks) in their vicinity (Figure 2.9 (b)), the amount of dissipated energy is high enough to withstand higher values of strain than before. Note that shortening the stack-stack distance can lead to greater resistance to crack propagation. Furthermore, the increased length of the crack path, as the crack travels along a "zig-zag" route, can also be considered as a further mechanism of energy

dissipation. This suggested model can explain the increase in both tensile strength and elongation at break for rubber/clay nanocomposites [30].

The majority of the reports on rubber/nanoclay compounds shows a deterioration of the mechanical performance with increasing filler loading [27, 28]. This behaviour is explained by the formation of agglomerates, which favour the initiation of catastrophic failure. However, some experimental studies on highly-filled nanocomposites were presented and some novel and interesting phenomena were observed. Lu et al. [31] affirmed that in highly filled intercalated rubber/clay nanocomposites, the dispersion homogeneity of the individual silicate layers would be much better than that in the conventional intercalated RCNs with low clay contents, and akin to that in the exfoliated RCNs.
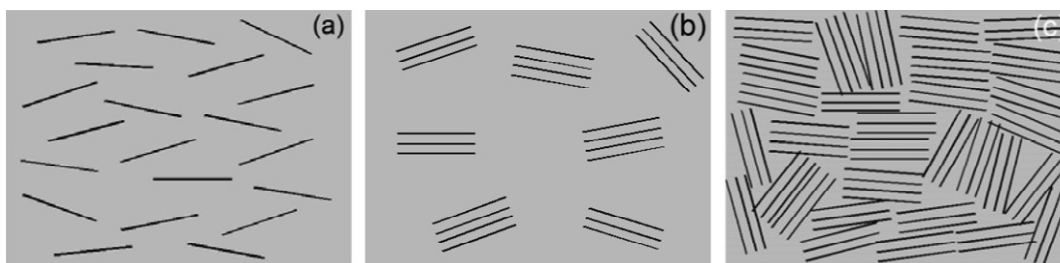

Fig. 2.10 Schematic illustration of dispersion of clay layers in polymers: (a) exfoliated nanocomposite; (b) low concentration (conventional) intercalated nanocomposite; and (c) highly filled intercalated nanocomposite [31].

The highly filled nanocomposites obtained had very high storage modulus at both ambient and high temperatures making them promising substitutes for fiber reinforced rubber composites. This increase was due to the formation of strong clay layers network structures. In fact, in highly filled RCNs, the platelet-platelet distance is very small (Figure 2.11), so that the interactions between clay layers easily occur because of the hydrogen bonding amongst Si–OH located on the edge of the clay layers, and one rubber chain possibly penetrates different silicate galleries and is thus constrained.

As shown in Figure 2.11, the shapes of strain-stress curves of RCNs significantly change with increasing the clay loading. This difference in strain-stress behaviour is likely due to the difference in the density of filler-filler networks and the extent of interfacial interactions among rubber chains and silicate layers. In addition, this highly filled RCNs exhibited excellent gas barrier properties with a reduction of 72-88% in gas permeability compared to neat rubbers.
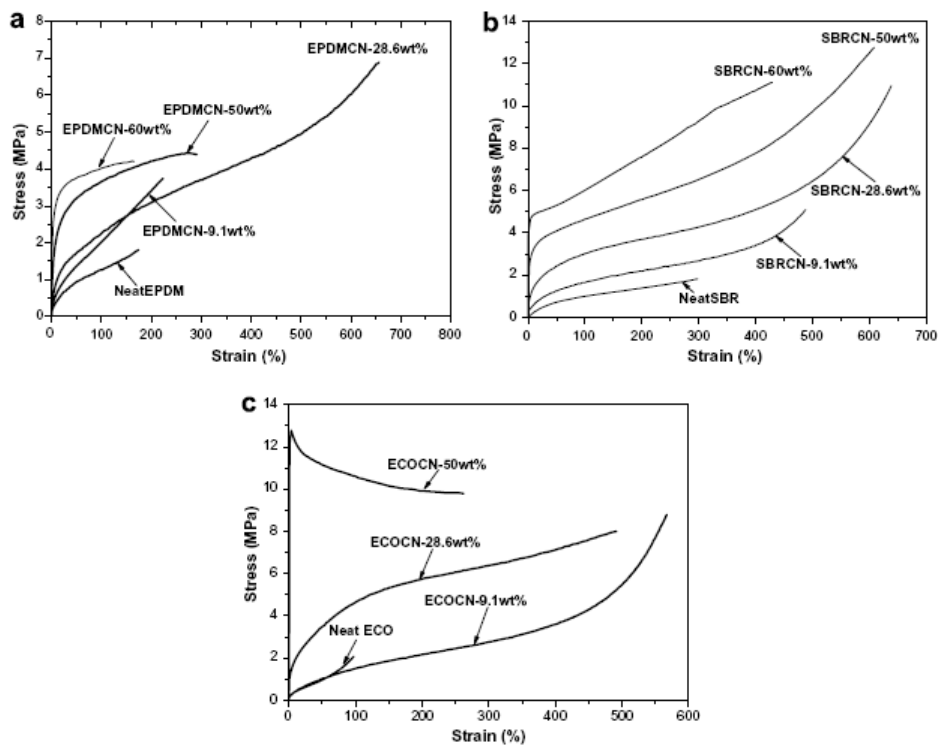
Fig. 2.11 Stress-strain curves of RCNs with different OMC contents and their neat rubber counterparts.

2.5.2 Fire resistance

The dispersion of nanoclays in a rubber matrix can improve the fire resistance of vulcanizates. It seems that the carbonaceous char produced superficially during combustion is reinforced by silicates, creating an excellent physical barrier which protects the substrate from heat and oxygen transfer into the material, and slows down the escape of flammable volatiles generated during polymer degradation [32]. The reduction in peak heat release rate (pHRR) is generally the first sign of an improvement in fire resistance properties. The reduction in peak HRR is important for fire safety, as peak HRR represents the point in a fire where heat is likely to propagate further, or ignite adjacent objects [33]. Khanlari et al. [34] showed that the addition of organo-MMT (OMMT) increased the thermal stability of the natural rubber (NR), based on thermogravimetric analysis. Moreover, this was accompanied with improved flame retardancy. The cone calorimeter results demonstrated that, by adding 3 wt. % of OMMT to NR, the peak value of heat release rate (pHRR) is 54.28% lower than the pure NR (Figure 2.12). In addition, NR with 5 and 7 wt.% clay content exhibit more than 55% and 58% decrease in HRR peak value, respectively. This flame retardant character is traced to the response of a char

layer, which develops on the outer surface of the sample during combustion. This char layer behaves as an excellent insulator and a mass transport barrier, slowing the oxygen supply as well as the escape of the combustion products during decomposition.
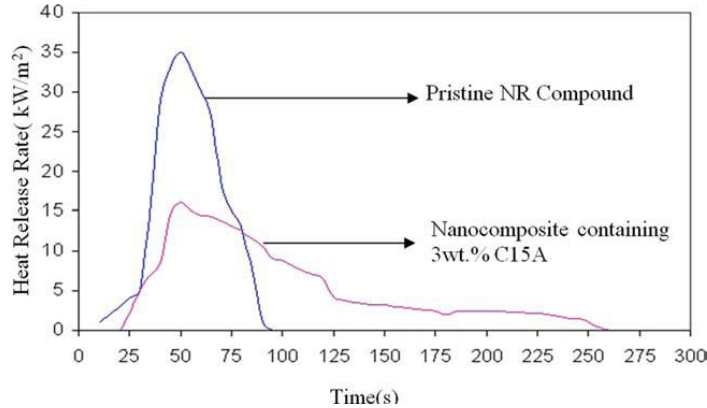

Fig. 2.12 Comparison of the heat release rate (HRR) plots of pristine natural rubber and a typical nanocomposite at 50 kW/m^2 heat flux [34].

The flammability of montmorillonite/styrene-butadiene rubber (SBR) nanocomposites, prepared by the technique of cocoagulating rubber latex and clay aqueous suspension, was investigated by Zhang et al. [35]. Cone calorimeter results (Figure 2.13) demonstrated that the HRR of SBR decreased 27% with the introduction of nanoclay. The nanocomposite exhibited the longest time to ignite, the lowest mass loss rate and the largest amount of char upon combustion compared with pure SBR. MMT/SBR microcomposite was also prepared and it was demonstrated that its flammability properties were intermediated between the ones of pure SBR and those of the nanocomposite.
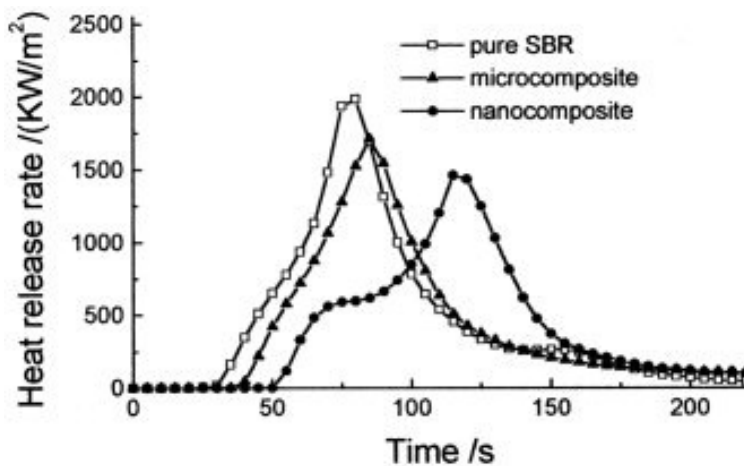

Fig. 2.13 Comparison of the heat release rate (HRR) plot for pure SBR and its composites [35].

2.5.3 Barrier properties

Several studies demonstrated that nanoclays highly improve barrier properties of nanocomposite films. This behaviour is due by creating a "tortuous path" (Figure 2.14) that retards the progress of the gas molecules through the matrix.
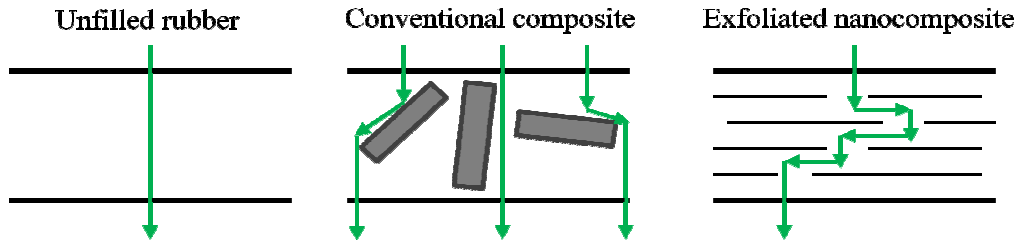

Fig. 2.14 Formation of "tortuous path" in exfoliated nanocomposites.

Kim et al. [36] prepared organo-montmorillonite/acrylonitrile-butadiene rubber (NBR) nanocomposites by a melt intercalation process. It was demonstrated that the clay content and the silane coupling agent amount are the dominating factors in determining the individual water-vapour permeability of the composites (Figure 2.15). In fact, the organoclay decreases the rate of transport by increasing the average path length required to cross the specimen, while the coupling agent enhances the clay dispersion and the inter-chain attraction.
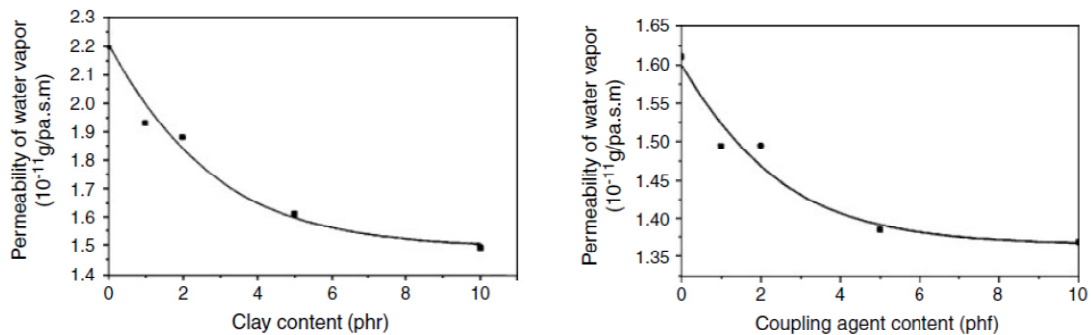

Fig. 2.15 Permeability of water vapour as a function of the: (a) clay content, (b) coupling agent content [36]

The role of the aspect ratio of the layered silicate platelets on the barrier properties of hydrogenated nitrile rubber (HNBR)/layered silicate nanocomposites was investigated by Gatos et al. [37]. To examine this effect, two kinds of clays with different aspect ratio

bearing however the same type of intercalant were used. The results showed that with organo-fluorohectorite lower oxygen permeation values, both in dry and wet conditions, were obtained. This can be traced to highest aspect ratio, compared to organo-montmorillonite, and thus to a more extended tortuous path.

The authors demonstrated also the importance of the clay dispersion degree. In fact, the unmodified fluorohectorite which is dispersed in micro-scale reduces slightly the permeability of the film (Figure 2.16).
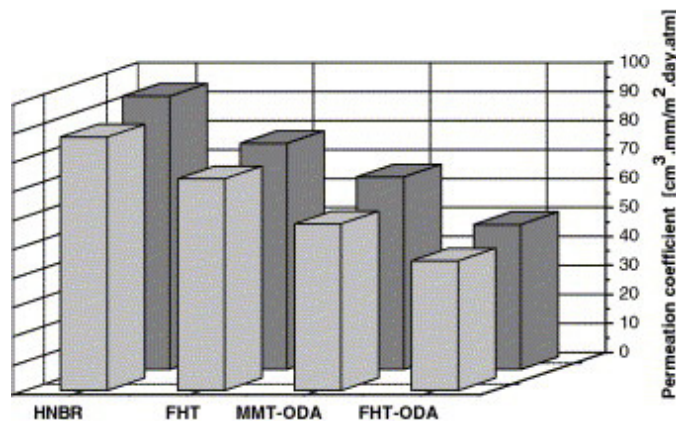

Fig. 2.16 Oxygen permeability measurements for the HNBR vulcanizates as a function of the filler aspect ratio (dry and wet conditions) [37].

Recently, a study on silicon rubber/organo- MMT nanocomposites, prepared by melt blending, was proposed [38]. This work disclosed that the type and loading of OMMT have a strong influence on the dispersion state of the clays in the rubber matrix. Consequently, different mechanical and barrier properties were obtained changing the nanoclay loaded in the rubber compound. In particular, it was demonstrated that the layered silicate, named I.44P, permitted to decrease the N_2 gas permeability coefficients of the composite more than 16%, compared with pure silicon rubber. Among the five clays tested, the I.44P OMMT showed the best dispersion state, forming the most tortuous gas diffusion pathways, which contributed to retard significantly the penetrating progress of gas molecules through materials.

2.5.4 Cross-linking

Several works have demonstrated the effect of the nanoclays on the vulcanization process. In particular, while the unmodified clays induce cure retardation due to absorption of curative by clay, the organoclays show an acceleration action on rubber

34

curing [39, 40]. It was suggested that the tethered primary amine of the organoclay leaves the clay surface in order to participate in the formation of a zinc-containing intermediate complex (vulcanization intermediate) having catalytic activity for curing (Figure 2.17).
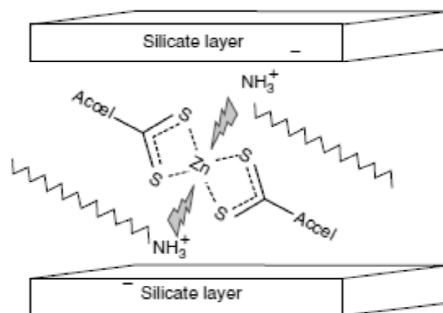

Fig. 2.17 Scheme of the interaction between the sulfur-rich Zn complex and the primary amine intercalant within the silicate gallery [37].

This occurs either by causing rubber cross-linking inside the galleries, inducing better clay dispersion via layers separation or delamination/exfoliation, or by migration into the rubber matrix, resulting in confinement or deintercalation of the galleries [1].

The term confinement indicates the collapse of the layers up to the initial basal spacing of the organoclay in the nanocomposite. A further collapse is termed deintercalation, that means extraction of the initial intercalant. The confinement/deintercalation phenomena were observed frequently for primary amine intercalated clay/rubber during sulphur vulcanization. By contrast, confinement/deintercalation phenomena were noticed when clays with quaternary amine were used [30] or in rubber vulcanized with peroxide [14].
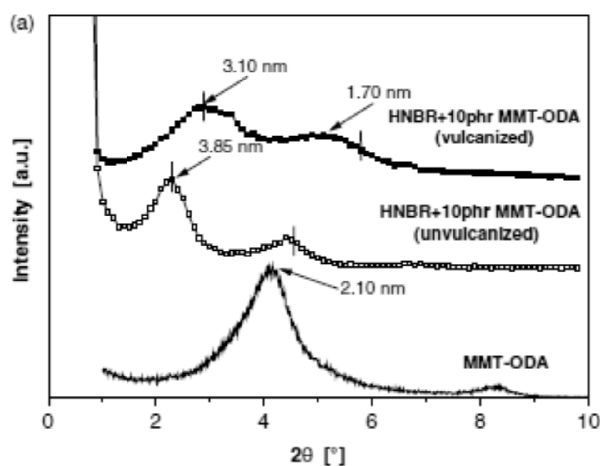
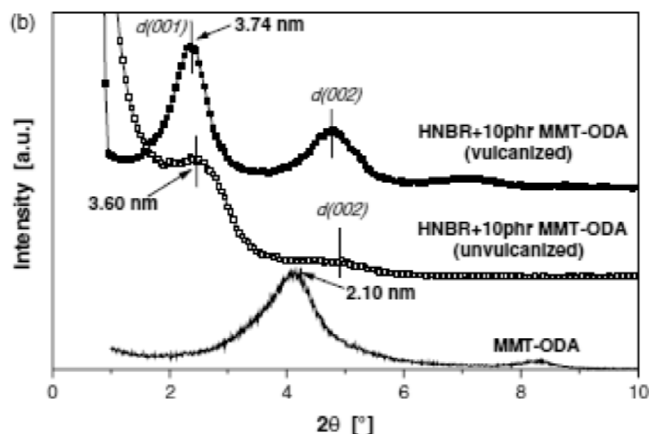**Fig. 2.18** XRD spectra of HNBR reinforced with MMA-ODA using different types of curing system, before and after vulcanization: (a) HNBR mixed with sulphur curatives [30] and (b) HNBR mixed with peroxide curatives [14].

Gatos et al. [14, 30] showed, using the same organoclay and rubber matrix, that highly intercalated clay structure were obtained in peroxide-cured system, while deintercalation occurred in sulphur-cured rubber compounds (Figure 2.18).

Wang et al. [41] observed that, by altering temperature, pressure, and treatment time, intercalated structures and their spatial distributions in the hydrogenated nitrile rubber (HNBR) were extensively modified. The authors contended that the exfoliation states of nanoclays are thermodynamically unfavourable and unstable, the de-intercalation appeared easily because of the molecular relaxations of HNBR chains and aliphatic chains of organic modified agents, which lead to the exfoliation, intercalation, and aggregation of organoclays populations co-existing in the HNBR matrix (Figure 2.19).
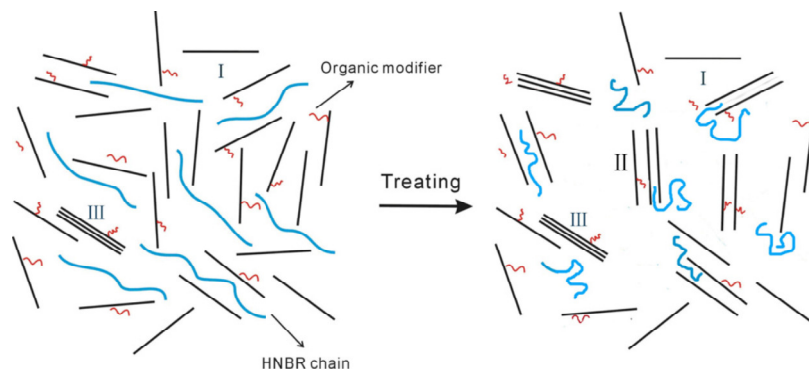

Fig. 2.19 Structure sketch of HNBR/OCNs compound before and after treating [41].

2.5.6 Wear behaviour

Another property of rubber/nanoclays which has received great attention recently is the wear behaviour. In fact, despite the wear performance of rubber/nanoclays has been scarcely studied until now, it seems to be a promising topic.

Gatos et al. [42] sustained that the incorporation of layered silicates in rubber can affect the wear performance of the related vulcanizates favorably or unfavorably. The final outcome depends on those parameters, which affect the abrasive, fatigue and adhesive wear components.

In particular, the authors demonstrated that the dispersion and the orientation of the clay platelets in the rubber matrix are crucial. Alignment of the clay platelets in plane, that is parallel to the sliding direction may be disadvantageous. The specific wear rate of HNBR (Figure 2.19 (a)) and EPDM (Figure 2.19 (b)) reinforced by 10 phr organoclay was reduced and enhanced, respectively. The basic difference between the related rubber compounds lies in their silicate dispersion. In fact, while HNBR/organoclay had a two-dimensional (2D; in-plane) platelet alignment, EPDM/organoclay exhibited a more random distribution of the platelets (3D dispersion). The 2D clay alignment triggers a mechanism during sliding, which has some similarities with a 'can-opening' process. This reduces the resistance to wear markedly.
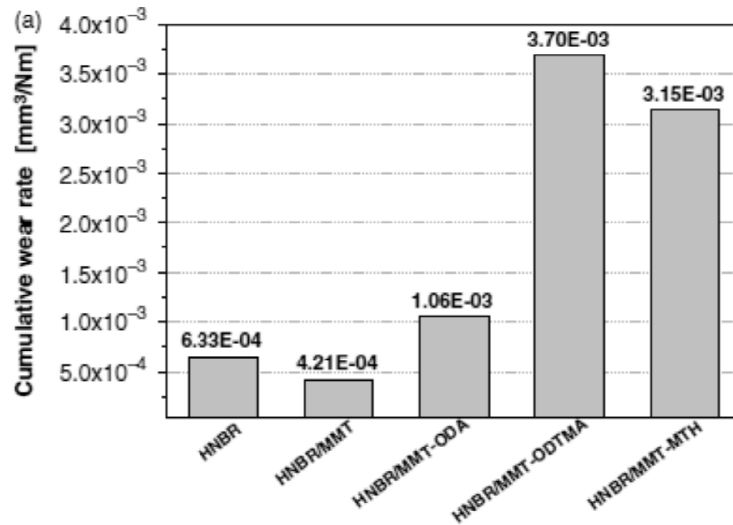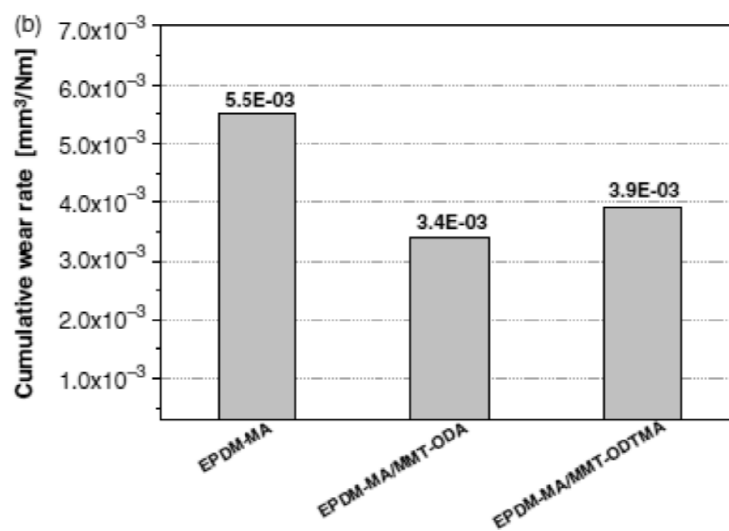
Fig. 2.20 Specific wear rate of (a) HNBR and (b) EPDM-MA, unfilled and filled with various organoclays (10 phr) [42].

References

[1] T. Sabu and S. Ranimol, *Rubber Nanocomposites: Preparation, Properties and Applications*, John Wiley & Sons (2010).

[2] M. Alexandre and P. Dubois, *Mater. Sci. Eng*, **28**, 1 (2000).

[3] S.S. Ray and M. Okamoto, *Prog. Polym. Sci.*, **28**, 1539 (2003).

[4] A. Das, F.R. Costa, U. Wagenknecht and G. Heinrich, *Eur. Polym. J.*, **44**, 3456 (2008).

[5] Q.H.Zeng, A.B. Yu, G.Q. Lu and D.R. Paul, *J. Nanosci. Nanotechnol.*, **5**, 1574 (2005).

[6] L. Betega de Paiva, A.R. Morales and F.R.Valenzuela Díaz, *Appl. Clay Sci.*, **42**, 8 (2008).

[7] H. Zheng, Y. Zhang, Z. Peng and Y. Zhang, *Polym. Test.*, **23**, 217 (2004).

[8] S. Joly, G. Garnaud, R. Ollitrault, L. Bokobza and J.E. Mark, *Chem. Mater.*, **14**, 4202 (2002).

[9] C.A. Rezende, F.C. Bragança, T.R. Doi TR, L.T. Lee, F. Galembeck and F. Boué, *Polymer*, **51**, 3644 (2010).

[10] Y.T. Vu, J.E. Mark, L.H. Pham and M. Engelhardt, *J. Appl. Polym. Sci.*, **82**, 1391 (2001).

[11] S. Varghese, J. Karger-Kocsis and K.G. Gatos, *Polymer*, **44**, 3977 (2003).

[12] B. Pradhan, S.K. Srivastava, R. Ananthakrishnan and A. Saxena, *J. Appl. Polym. Sci.*, **119**, 343 (2011).

[13] W.G. Hwang, K.H. Wei KH and C.M. Wu, *Polymer*, **45**, 5729 (2004).

[14] K.G. Gatos, L. Százdi, B. Pukánszky and J. Karger-Kocsis, *Macromol. Rapid Commun.*, **26**, 915 (2005).

[15] M. Maiti and A.K. Bhowmick, *J. Polym. Sci. B Polym. Phys.*, **44**, 162 (2006).

[16] S. Sadhu, A.K. Bhowmick, *J. Appl. Polym. Sci.*, **92**, 698 (2004).

[17] M.A. López-Manchado, B. Herrero and M. Arroyo, *Polym. Int.*, **53,** 1766 (2004).

[18] S. Varghese, K.G. Gatos, A.A. Apostolov and J. Karger-Kocsis, *J. Appl. Polym. Sci.*, **92**, 543 (2004).

[19] R.A Vaia, H. Ishii and E.P.Giannelis, *Chem. Mater*, **5**, 1694 (1993).

[20] C. Nah, H.J. Ryu, W.D. Kim and Y.W. Chang, *Polym. Int.*, **52**, 1359 (2003).

[21] M. Tian, C. Qu, Y. Feng, and L. Zhang, *J. Mater. Sci.*, **38**, 4917 (2003).

[22] K.G. Gatos, R. Thomann and J. Karger-Kocsis, *Polym. Int.*, **53**, 1191 (2004).

[23] L. Bokobza and M. Kolodziej, *Polym. Int.*, **55**, 1090 (2006).

[24] M. Arroyo, M.A. López-Manchado and B. Herrero, *Polymer*, **44**, 2447 (2003).

[25] J. Kim, T. Oh and D. Lee, *Polym. Int*., **52**, 1058 (2003).

[26] K.G. Gatos and J. Karger-Kocsis, *Polymer*, **46**, 3069 (2005).

[27] A. Mousa and J. Karger-Kocsis, *Macrom. Mater. Eng.*, **286**, 260 (2001)

[28] Y.W. Chang, Y. Yang, S. Ryu and C. Nah, *Polym. Int*., **51**, 319 (2002).

[29] Y.P. Wu, Y. Ma, Y.Q. Wang and L.Q. Zhang, *Macrom. Mater. Eng.*, **289**, 890 (2004).

[30] K.G. Gatos, N.S. Sawanis, A.A. Apostolov, R. Thomann and J. Karger-Kocsis, *Macrom. Mater. Eng.*, **289**, 1079 (2004).

[31] Y.L. Lu, Z. Li, Z.Z. Yu, M. Tian, L.Q. Zhang and Y.W. Mai, *Compos. Sci. Tech.*, **67**, 2903 (2007).

[32] P. Kiliaris and C.D. Papaspyrides, *Prog. Polym. Sci.*, **35**, 902 (2010).

[33] A.B. Morgan, *Polym. Adv. Technol.*, **17**, 206 (2006).

[34] S. Khanlari and M. Kokabi, *J. Appl. Polym. Sci.,* **119**, 855 (2011).

[35] H. Zhang, Y. Wang, Y. Wu, L. Zhang and J. Yang, *J. Appl. Polym. Sci.*, **97**, 844 (2005).

[36] J. Kim, T. Oh and D. Lee, *Polym. Int*., **53**, 406 (2004).

[37] K.G. Gatos and J. Karger-Kocsis, *Europ. Polym. J.*, **43**, 1097 (2007).

[38] C. Jia, L.Q. Zhang, H. Zhang and Y.L. Lu, *Polym. Compos.,* **32**, 1245 (2011).

[39] M. Song, C.W. Wong, J. Jin, A. Ansarifar, Z.Y. Zhang and M. Richardson, *Polym. Int.*, **54**, 560 (2005).

[40] M.A López-Manchado, M. Arroyo, B. Herrero and J. Biagiotti, *J. Appl. Polym. Sci.*, **89**, 1 (2003).

[41] X. Wang, A. Huang , D. Jia and Y. Li, *Europ. Polym. J.*, **44**, 2784 (2008).

[42] K.G. Gatos,K. Kameo and J. Karger-Kocsis, *eXPRESS Polym. Lett.*, **1**, 27 (2007).

Chapter 3

Fundamentals of rubber compounding

3.1 Rubber compounding

World rubber consumption in 2010 was in the range of 24.5 million tonnes. The dominant market for rubbers is in the automotive industry, in the manufacture of tires and inner tubes. Other industrial rubber goods include various belts, hoses, oil seals, gaskets and so on.

Rubber compounding is the art and science of selecting various compounding ingredients and their quantity to mix and produce a useful rubber formulation that can be processed, meets or exceeds the customer's final product requirements, and can be competitively priced.

The heart of the rubber compounding is the formulation, usually referred in the industry as a recipe. A generalized rubber formula is given in Table 3.1. Rubber formulas are almost never publicized by manufactures.

Table 3.1 A generalized rubber recipe [2].

Ingredient	phr
Crude rubber	100
Filler	50
Softener	5
Antioxidant	1
Stearic acid	1
Zinc oxide	5
Accelerator	1
Sulphur	2
Total	*165*

Rubber compounds are generally based on only one rubber or on a blend of two or more raw rubbers to achieve the best balance properties. The total of the crude rubbers in a

given recipe is generally defined as 100 parts. All other non-rubber ingredients are rationed against the 100 parts of rubber (phr).

Each ingredient has a specific function, either in processing, vulcanization or end use of the product. The various ingredients may be classified according to their specific function in the following groups [2]:

- fillers (carbon blacks and non-black fillers);
- plasticized and softeners (extenders, processing aids, special plasticizers);
- age resistors or antidegradants (antioxidants, antiozonants, special age resistors, protective waxes);
- vulcanizing and curing ingredients (vulcanizing agents, accelerators, activators);
- special-purpose ingredients (colouring pigments, blowing agents, flame retardants, odorants, antistatic agents, retarders).

However, many ingredients are capable of functioning in more than one manner.

3.1.1 Rubbers

Crude rubbers are typically categorized as amorphous polymers with very high molecular weight (Mn > 100,000), having a random-coil arrangement. They can be cross-linked to form a tridimensional network. Whose glass transition temperature is sub-ambient and, amongst other properties, rubbers have the ability to be extensively and on release of stress, return to their original length.

The main characteristics of elastomers, which make these materials indispensable in several industrial sectors, are their elasticity, flexibility, and toughness. Beyond these common features, each rubber has its own unique properties. Although the processing and final properties of rubber articles are highly dependent on the base elastomer, the properties can be extensively manipulated by appropriate choice of compounding ingredients.

Rubbers can be divided in two types: natural and synthetic. Natural rubber (NR) belongs to the first group, it is known also as *cis*-1,4 polyisoprene and is produced from the latex of a large variety of plants in many regions of the world. However the most widely exploited commercial source of NR is the *Hevea brasiliensis* tree. Natural rubber latex is a colloid with a specific gravity of 0.96 to 0.98 and a pH in the range of 6.5 to 7.0. The dispersed phase is mainly rubber and the dispersion medium is water. In addition to rubber and water, latex contains small quantities of proteins, resins including fats, fatty acids, other lipids, sterol and sterol esters, carbohydrates and mineral matter [3].

Additional information about natural rubber will be provided in Chapter 4.

The second group constituted by synthetic rubbers is very broad so only some kinds of elastomers will be introduced subsequently.

The first to mentioned is synthetic polyisoprene rubber (IR) which, depending on the polymerization conditions, can exists as different isomeric forms. 1,4-IR can exist in cis or trans forms depending on the orientation of the substituents across the enchained double bond. These isomers are the most important while the other forms, 1,2-IR and 3,4-IR, are of less importance. The IR vulcanizates show aging properties and resistance to chemicals similar to those of NR vulcanizates, while the physical properties are not as good as those of NR [3].

Other general-purpose elastomers, such as NR and IR, are styrene-butadiene rubber (SBR) and butadiene rubber (BR).

SBR denotes a copolymer of styrene and butadiene, typically containing about 23% styrene. It does not develop high tensile strengths without the aid of reinforcing fillers. The tread-wear and heat-ageing properties of SBR are superior to those of NR, but the resilience and low-temperature behaviour are inferior. SBR was produced for the first time during the Second World War as a substitute for NR. This kind of rubber is generally used in many applications, particularly the principal end uses are passenger car tyres (45% of the worldwide capacity), truck and bus tyres (9%), retread tyres (16%), other automotive (6%) and mechanical goods (16%) [3].

An in-depth description of polybutadiene rubber will be presented in Chapter 4.

In many applications, general purpose elastomers are unsuitable for their insufficient resistance to swelling, aging, and/or elevated temperatures. Special-purpose elastomers have been developed to meet these needs. Two of most important properties of elastomers are the ability to withstand weathering due to oxygen, ozone, and light and the capability to resist to organic fluids [4].

Elastomers with strong polarity are more resistant to nonpolar organic fluids than those that are hydrocarbon-based. For example, increasing the acrylonitrile concentration in acrylonitrile-butadiene rubber (NBR) improves its resistance to swelling in oil, at the expense of others properties, such as crack resistance, elasticity, and low-temperature properties.

Some special-purpose elastomers show a high temperature resistance. A common example is constituted by silicone rubbers (Q). These are based on chains of silicon-oxygen-silicon in place of the carbon-carbon linkage. The other heat-resistance elastomer

are fluocarbon elastomers (FKM) which derive from perfluorinated versions of common polyolefin, such as polypropylene and polyethylene. Their thermal resistance arises from non reactivity of the carbon-fluorine bond [4].

In addition fluorocarbon elastomers, besides polychloroprene rubbers, show high fire resistance properties.

3.1.2 Fillers

Fillers are compounding ingredients, usually in powder form, added to crude rubber in large proportions (typically 30 phr). They include two major groups: carbon black and non-black fillers.

Carbon black consists essentially of elemental carbon in the form of near-spherical particles coalesced in aggregates of colloidal size, obtained by incomplete combustion or thermal decomposition of hydrocarbons [5]. The carbon black grades differ from one another regarding their particle size, aggregate form and shape.

A wide variety of non-black fillers for rubbers exists. Today, the principal non-black fillers are silicas and calcium carbonates. Other major fillers are mica, talc, zinc oxide, magnesium carbonate, magnesium oxide, titanium oxide, barites and many others. Short fibres of aramid, carbon, glass, nylon or polyester, are also widely used in rubber compounds.

Fillers are added for economical or technical purposes. Some are incorporated as extenders and therefore to make the final product less expensive and others mainly to reinforce it. Consequently, fillers may be also classified into two categories: reinforcing and non-reinforcing.

3.1.3 Plasticizers

Commercial plasticizers or softeners are normally supplied in the form of low or high viscosity liquids and more rarely as solid products. They are generally incorporated for various aims [2]:

> ➢ as an extender to reduce the cost of the final product;
> ➢ as a processing aid to improve the workability of the compounded rubber during processing;
> ➢ as a modifier of certain vulcanizate properties.

About 90% of all plasticizers used for commercial purposes are recovered from petroleum. Generally, a large amount (above 20 phr) may act as an extender and a small (ca. 2-5 phr) as a processing aid.

3.1.4 Antidegradants

Elastomer-based products suffer irreversible changes to their required design properties during service. In particular, a loss in mechanical properties and alterations in surface aspect can occur.

These changes, brought about by a number of agents such as oxygen, ozone, heat, light, high energy radiation and high humidity, are collectively referred to as ageing.

In order to combat these changes additives, often collectively referred to as antidegradants or age resistors, are employed. Typical loading levels are of the order of 1-4 phr.

The most common antidegradants are the antioxidants, which protect the elastomer against oxidation, and the antiozonants, that retard or prevent the appearance of surface cracks caused by ozone. Age resistors may be divided into two main groups: staining and nonstaining. While the former are strong protective agents but discolour and stain to various degree, the latter are less effective but can be used in white and coloured rubber compounds.

3.1.5 Vulcanizing ingredients

Vulcanizing ingredients are those chemicals that are able to form cross-links between polymer chains when the compounded stock is heated to an appropriate temperature.

Elemental sulphur is the most widely used vulcanisation agent for crude rubbers that contain double bonds in their chains. However, the reaction of rubber with sulphur is slow even at high temperatures, in fact usually requires several hours. In order to increase the rate of vulcanization, it is necessary to add accelerators and activators. By adding accelerators, the vulcanization time can be cut to minutes or seconds and in most cases the physical properties of the final product are also improved. Activators are generally added in small amounts to increase the effectiveness of accelerators. Zinc oxide and stearic acid are the most commonly used activators.

Saturated crude rubbers cannot be cross-linked by sulphur because of the absence of double bonds in polymer chains. Consequently, they are usually vulcanized by organic

peroxides. Peroxides curing takes place via a free-radical mechanism and leads to carbon-carbon cross-links.

Other vulcanizing agents used for certain rubber kinds include, for instance, metal oxides, diamines, bisphenols and special resins.

3.1.6 Special purpose ingredients

Certain ingredients are added for specific purpose, but these ingredients are not normally required in the majority of the rubber compounds. Some of them are discussed below.

Pigments are substances added for imparting the desired colour to non-black rubbers. Pigments can be classified as inorganic or organic. Comparing the two, inorganic pigments are often dull and large amounts are needed to achieve a given intensity. However, they are stable to heat and light, insoluble and thus cannot bloom. Organic pigments produce bright colours but are more sensitive to heat and other chemicals.

Odorants are capable of masking the characteristic odour of some rubbers or imparting a pleasant scent. Vanillin and menthol are frequently used for this aim.

Antistatic agents are added to reduce the accumulation of dust or dirt on the surface of the elastomeric part during service, and also to minimize the possibility of sparking resulting from discharge of accumulated static electricity.

Flame retardants are substances added to inhibit or to stop the rubber combustion. In function of their nature, flame retardant systems can either act physically or chemically [6].

The combustion process can be retarded by physical action in different ways [7]:

➤ Cooling: endothermic decomposition of the flame retardant additive cools the material.

➤ Forming a protective layer: obstructing the flow of heat and oxygen to the polymer, and of fuel to the vapour phase.

➤ Dilution: release of water vapour or inert gases (CO_2, NH_3) may dilute the radicals in the flame so it goes out.

The most widely used fire retardant additive which acts physically is the aluminium tri-hydroxide (ATH). Its endothermic decomposition occurs between 180 and 200 °C and leads to the release of water, which dilutes the radicals in the flame, and the production of alumina, which forms a protective layer:

$$2Al(OH)_3 \rightarrow Al_2O_3 + 3H_2O \text{ (1050 kJ/kg)}$$
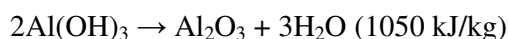
Flame retardancy by chemical action can occur in either the gaseous or the condensed phase [7]:

- ➢ Gas phase: the radical reactions of the flame can be interrupted by the incorporation of flame retardant additives that preferentially release specific radicals (e.g. Cl· and Br·) in the gas phase. These radicals can react with highly reactive species (such as H· and OH·) to form less reactive or even inert molecules. Consequently, the intensity of the exothermic reactions are marked decreased and the system cools down.

- ➢ Condensed phase: two types of chemical reactions are possible. First, the flame retardants accelerate the rupture of the polymer so it melts like a liquid and flows away from the flame. Alternatively, the flame retardant can cause the formation of a carbonized or vitreous layer at the polymer surface by chemical transformation of the degrading polymer chains.

3.2 Mixing methods

Rubber compounding is accomplished with two-roll mill (open mill) or internal mixer. The former consists of two adjacent, hardened-steel rolls set horizontally. The rolls rotate in opposite directions at different speed, in order to produce a friction or grinding action between them (Figure 3.1).
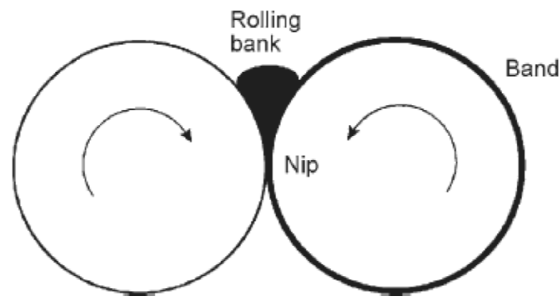

Fig. 3. 1 Schematic of a two-roll mill [3].

The mixing process involves masticating or breaking down the crude rubbers an even and smooth band is formed around the front roll. When the crude rubber becomes soft and plastic, the other ingredients are added. The two-roll mill is a mixing method entirely dependent on operator intervention. In fact, during the processing the powders drop into

the mill tray and the operators must to collect them and to add back to the mix. In addition, in order to favour a uniform dispersion of the ingredients, cutting and folding are continuously carried out.

The behaviour of a rubber compound on a two-roll mill depends on its flow characteristics and on the selected milling conditions. 'Good' behaviour comprises consistent banding round the working (front) roll during loading, an active rolling bank, with little or no stagnation and a band that does not sag and remains in full contact with the mill roll [3].

This mixing equipment is generally used for laboratory and low volume production. However, for the long time needed for filler incorporation, the dust hazard thus created and the poor ingredient dispersion achieved, it has been replaced with other devices. As this reason, nowadays it is mainly used as a second-stage mixing device, for adding vulcanizing agents and for completing the ingredient dispersion.

The internal mixer (Figure 3.2) is the mixing device mainly used in the rubber industry. Its dominance can be assigned to a several factors, among which the good filler dispersion achieved and the considerable reduction of the mixing time.
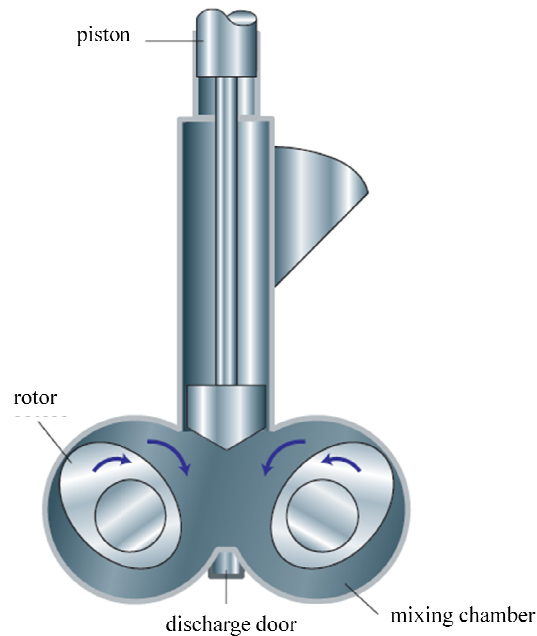

Fig. 3.2 Schematic of an internal mixer.

48

There are two primary internal mixers designs, intermeshing rotor and tangential (non-intermeshing) rotor, and many variations on these two themes [3]. Figures 3 (a) and (b) show cross-sections of examples of these two designs. The main features of both designs are the two contra-rotating rotors; the ram, which is raised to permit feeding and lowered and pressurised to hold the rubber compound in the active mixing region; the drop door, designed for rapid discharge of the batch; and the channels in the chamber walls, the rotors, the drop door and (sometimes) the ram for circulation of cooling water [3].
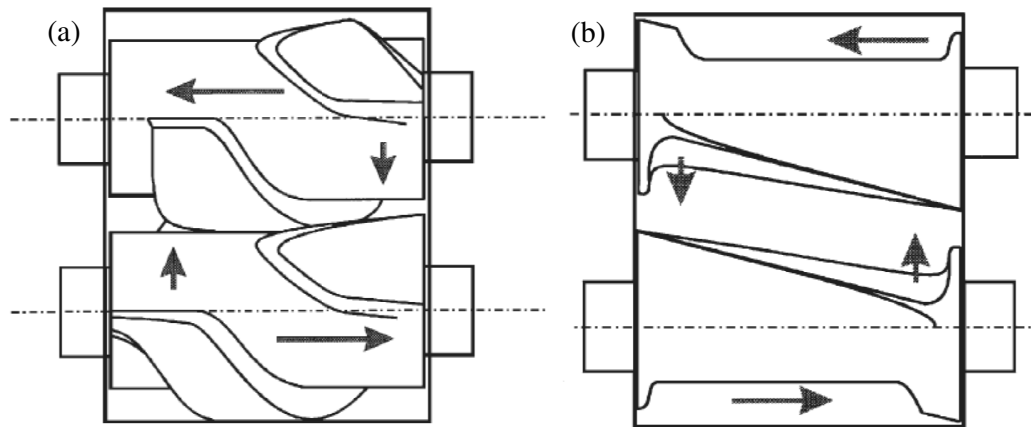

Fig. 3.3 (a) Intermeshing internal mixer rotors (b) tangential internal mixer rotors [3].

3.3 Forming operations

After the mixing, the forming and the vulcanizing operations follow; sometimes these could also coincide. With the forming step the crude compounds will retain the shape imposed on it because it is predominantly plastic. The processing machines mainly used for forming are the calenders and the extruders [2].

The calender is equipped with two or more internally heated or cooled rolls. The latter rotate in opposite directions. The calender is used essentially for producing rubbers sheets of different lengths and thickness.

Extruder is generally used to produce rubber tubes and weather-sealing strips. In this machine rubber compound is transferred along a cylinder by rotation screw. The green stock becomes hot and plastic as it moves to the exit end of the extruder, called die, with the desired shape and dimensions.

3.4 Vulcanization process

After the forming the green stock is converted into three-dimensional elastic network. This is accomplished by the vulcanization process, usually conducted under pressure at elevated temperature, in which the polymeric chains are chemically linked together. The process of vulcanization is depicted graphically in Figure 3.4.
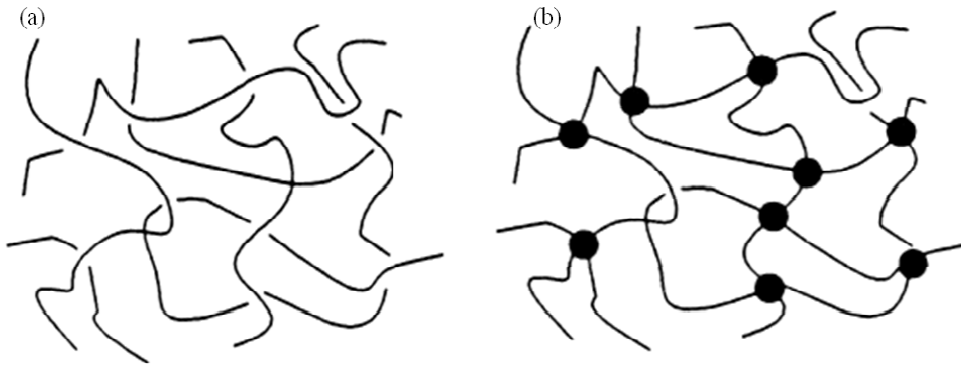

Fig. 3.4 Schematic of (a) raw rubber and (b) vulcanized rubber [8].

Physical properties of a vulcanized compound depend strongly on cross-link density (Figure 3.5). Modulus and hardness increase with increasing cross-link density, while the hysteresis decreases. Fracture properties, such as tear and tensile strength, pass through a maximum as cross-linking is risen.
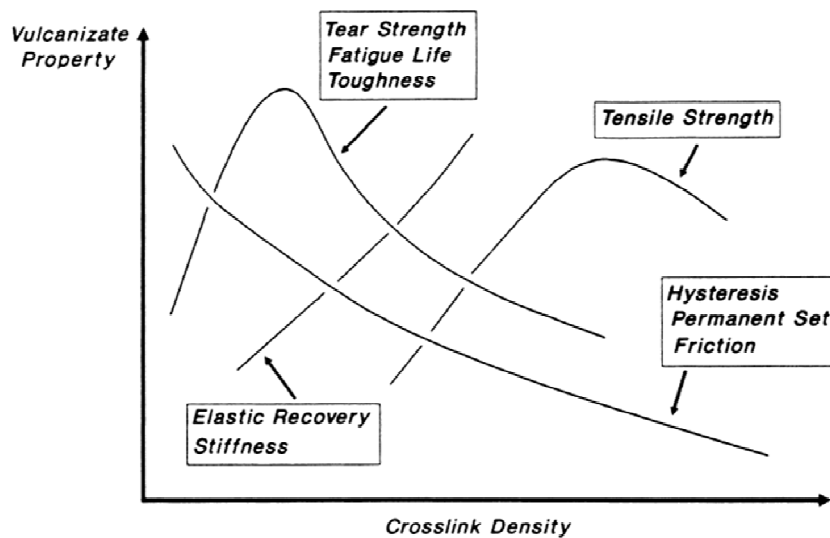

Fig. 3.5 Effects of cross-link density vulcanizate properties [8].

The kinetics of vulcanization are studied using rheometers that measure the torque variation as a function of time at a fixed temperature. Two different geometries existed for the rheometers (Figure 3.6): oscillating disc rheometer (ODR) and moving-die rheometer (MDR).
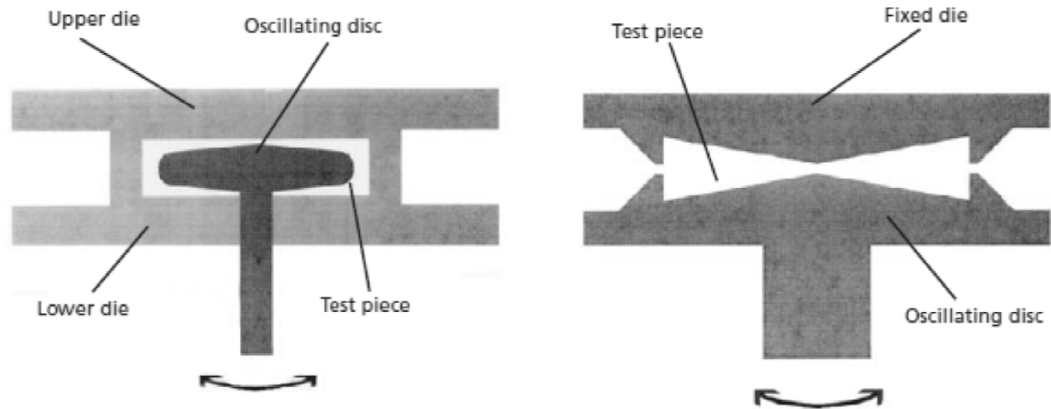

Fig. 3.6 Rheometer types: (a) oscillation disk and (b) moving die [3].

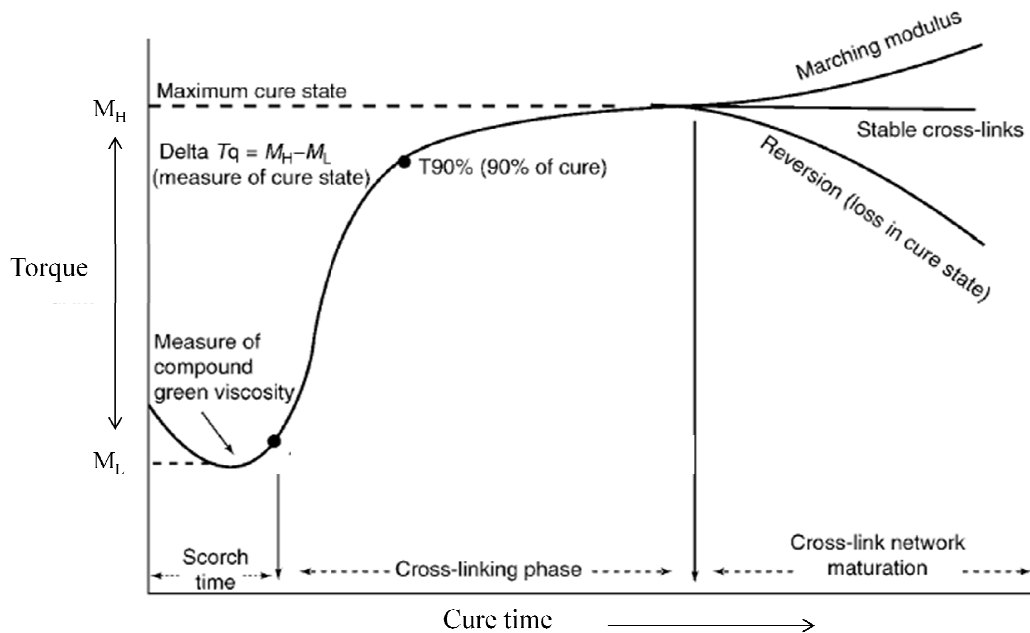A typical vulcanization curve obtained by using the rheometer is given in Figure 3.7.

Fig. 3. 7 Rheometer curve.

Several important information about the rate and the extend of the compound vulcanization can be derived from this curve. Initially, as the rubber is heated, the torque decreases until to reach a minimum value (M_L), strictly correlated to a decrease in the Mooney viscosity of the compound. Subsequently, the rubber begins to vulcanize and the torque rises and when it reaches a plateau a complete vulcanization and the formation of a stable network are carried out.

However, a chain scission may be occurring and, if this phenomenon becomes dominant, the torque passes through a maximum and finally decreases (reversion). On the other hand, some compounds show a slowly increasing torque at long cure time (marching modulus) [4].

Besides the M_L, a vulcanization curve permits to determine the maximum torque achieved and the optimum curing time (t_{90}), that is the time require to reach 90% of full cure. Generally, this is the state of cure at which the most physical properties achieve optimal results.

The curing ingredients are classified in two main groups: sulphur and non-sulphur vulcanizing agents.

3.4.1 Sulphur vulcanizing agents

Two forms of sulphur are used in industry for the vulcanization: soluble and insoluble. The molecular structure of soluble sulphur comprises an eight membered ring, crystalline in nature. Sometimes, in compounds containing high level of sulphur, a phenomenon called "sulphur bloom" is observed [4]. It appears as an off-white powdery coating on the surface of the uncured compound due to migration from the bulk compound when the limit of solubility is exceeded.

Consequently, to avoid the blooming insoluble sulphur is used. In fact, this is a crystalline, polymeric form of sulphur and is insoluble in solvents and elastomers. However, insoluble form of sulphur transforms in the soluble form above 120°C. Thus, the mixing temperature must be kept below 120°C.

Sulphur vulcanization occurs by the formation of polysulfide linkages between rubber chains (Figure 3.8). However, usually much of the sulphur is not involved in cross-links but there is the formation of dangling sulphur fragments and cyclic sulphides. As consequence, the network formed is unstable and has poor aging resistance.
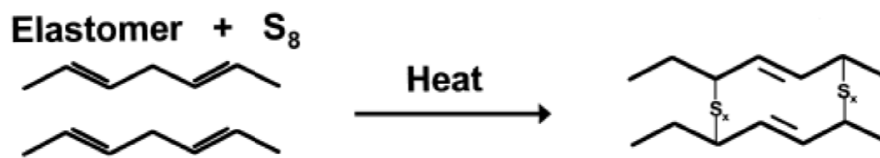
Fig. 3.8 Sulphur vulcanization.

To increase the rate and the effectiveness of the sulphur cross-linking, accelerators are normally added. These materials, known also as sulphur donors, are used to replace part of the elemental sulphur in order to produce vulcanizates with few sulphur atoms per cross-link (mono- and di-sulphidic linkages). These are organic chemicals and can be classified in five main groups: guanidines, thiazoles, dithiocarbamates, xanthates and thiurams.

Generally, delayed beginning of vulcanization is desirable peculiarity of rubber compounds. This permits forming operations to be accomplished before curing starts. Premature vulcanization is known as "scorch". The five accelerator groups have different effects on the curing process; consequently, a combination of them is usually employed to achieve the desired scorch resistance and cure rate.

The level and the kind of cross-links depend on: sulphur level, accelerator type, sulphur/accelerator ratio and cure time. High sulphur/accelerator ratio and long cure time increase the number of monosulphidic linkages, improving, as consequence, heat stability, set resistance and reversion resistance of the final vulcanized products. These properties derive to the greater stability of C-S bonds with respect to S-S bonds. On the other hand, compounds containing high number of polysulphidic linkages show better tensile strength and fatigue cracking resistance. This behaviour depends on the ability of S-S bonds to break reversibly.

3.4.2 Non-sulphur vulcanizing agents

The majority of rubber compounds are vulcanized using sulphur agents, however, there are some cases for which non-sulphur curing is necessary or preferable.

In the 1915 I. I. Ostromyslenski [9] disclosed that peroxides could be used as cross-linking agents for natural rubber. However, there was little interest in peroxide cross-

linking until the development of fully saturated ethylene-propylene copolymers in the early 1970s.

Peroxides decompose during vulcanization because of the increased temperature, forming free radicals which lead to the formation of carbon-carbon cross-links (Figure 3.9).
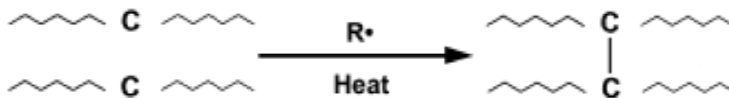

Fig. 3.9 Peroxidic vulcanization.

Several organic peroxides are available as curing agents, the choice depends on their stability, activity and cure temperature. Numerous advantages derive from the peroxide vulcanization, such as good aging resistance and low compression set; but also simple compound formulation and no discoloration of compounds. On the other hand, peroxides-initiated cure involves inferior mechanical properties, higher production cost, greater care in storage and processing.

Some elastomers, such as polychloroprene rubber, are vulcanized with metal oxides. The reaction mechanism occurs via allylic chlorines on the polymer chains. Generally, mixtures of ZnO and MgO are used.

Malaysian Rubber Producers Research Association (MRPRA) has developed a novel process of vulcanization based on urethanes [3]. The principal advantage of these chemicals lies in the high stability of the cross-links; however their use in the industry has found limited application because of lower scorch and high cost.

3.5 Applications of rubber compounds

In most applications of rubber products there are no alternative materials except other rubbers. Thank to their high deformability these materials can retain a memory of their original unstressed state and can return to their original dimensions when external forces are removed even after strains as high as 1000%. This ability to recover their original dimensions leads to a broad range of applications.

In most tyre compounds, the rubber is the largest ingredient in the formulation. It acts as a 'binder' into which the other ingredients are dispersed. Elastomers demonstrate a unique

set of materials properties, including viscoelastic characteristics and the ability to undergo extreme deformations.

The modern pneumatic tyre would be impossible without the use of elastomers.

While specialty rubber types are usually employed in specific tyre components, a generic formulation for a SBR rubber nanocomposite matrix might comprise (Table 3.2):

Table 3.2 Baseline formulation for SBR nanocomposite [5].

Ingredient	phr
Rubber	100
Carbon black	50
Oil	15
Stearic acid	1
Zinc oxide	5
Sulphur	2
Accelerators	2

Carbon black and silica are the fillers mainly used in the tyre production. Silica has greater reinforcing power, such as improving tear strength, abrasion resistance, age resistance and adhesion properties, compared to carbon black. However, the agglomeration nature of silica is generally believed to be responsible for considerable rolling resistance in tyre applications [5].

Another field of rubber compounds application is the footwear industry [3]. In some ways, tyres and shoe outsoles have very similar requirements in terms of wear resistance and traction, and compounds to meet these needs can be very similar. The differences are in the durability and in the types and number of surfaces each comes in contact with.

The choice of polymers, fillers and additives for producing a shoe is related to the need properties and requirements. For example, outsoles for running shoes need to provide good durability, good traction, and high rebound. The polymers of choice for running outsoles are natural rubber (NR) and polybutadiene (BR). Since one elastomer can rarely meet all performance requirements, rubber blends are usually prepared to achieve the desired balance of physical properties. In particular, very common are NR/BR blends which can achieved rebound values greater than 90%; sometimes SBR is also added.

On the other hand, safety shoes provide protection against severe work conditions and chemical contact [3]. A rubber frequently used for manufacturing safety shoes is polyacrylonitrile butadiene rubber. The advantage of this elastomer is the presence of two components which provide different properties. In particular, acrylonitrile provides resistance to oil and fuel, while the butadiene provides abrasion resistance and low temperature flexibility.

Another interesting sector where natural and synthetic elastomeric materials have a variety of applications is the construction industry [3]. For example, in building applications, rubber can help in the control or isolation of vibrations and noise generated from the building itself. The use of rubber materials in buildings, both for construction and decoration, continues to increase due to their advantages, such as soundproofing effects, anti-quake performance, easy fabrication and installation, sealing properties [3].

References

[1] http://www.lgm.gov.my/nrstat/T1.htm

[2] K. Nagdi, *Rubber as an Engineering Material: Guideline for Users*, Carl Hanser Verlag (1993).

[3] J.R. White and S.K. De, *Rubber Technologist's Handbook*, Rapra Technology (2001).

[4] B. Rodgers, *Rubber Compounding: Chemistry and Applications*, Marcel Dekker (2004).

[5] T. Sabu and S. Ranimol, *Rubber Nanocomposites: Preparation, Properties and Applications*, John Wiley & Sons (2010).

[6] F. Laoutid, L. Bonnaud, M. Alexandre, J.M. Lopez-Cuesta and Ph. Dubois, *Mater. Sci. Eng., R*, **63**, 100 (2009).

[7] T.R. Hull and B. K. Kandola, *Fire Retardancy of Polymers: New Strategies and Mechanisms*, Royal Society of Chemistry (2009).

[8] J.E. Mark, B. Erman and F.R. Eirich, *Science and Technology of Rubber*, Elsevier Academic Press (2005).

[9] I. I. Ostromysklenki, *J. Russ. Phys. Chem. Soc.*, **47**, 1467 (1915)

Chapter 4
Experimental

4.1 Materials

4.1.1 Raw rubbers

Three types of rubbers were used in this research activity and subsequently some information about these will be given.

Ethylene vinyl acetate (EVA) is a random copolymer consisting of ethylene and vinyl acetate (VA) as repeating units (Figure 4.1).
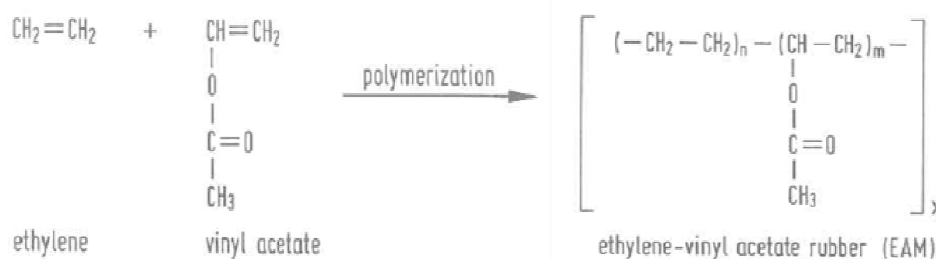

Fig. 4. 1 Synthesis of EVA copolymer [1].

EVA is considered one of the most important organic polymers, extensively used for wire and cable insulation, adhesives/paper coatings, component encapsulation and water proofing, corrosion protection, packaging of components [2, 3], and sound damping/sound barrier sheet.

The versatility of EVA, which permits its use in perhaps the broadest spectrum of applications of any synthetic polymeric material, derives from the possibility to vary the VA content in the copolymer. As this reason, nowadays EVA is available as plastic, thermoplastic elastomer and rubber depending on the vinyl acetate amount in the copolymer: 9–18% VA = plastic; 28–33% VA = thermoplastic elastomer; $\geq 45\%$ VA = rubber [4].

Vinyl acetate content has two fundamental effects which influence the properties of EVA copolymers [3]. The first effect is the interruption of the crystalline regions formed by

polyethylene segments. As consequence, by increasing the VA content the degree of crystallinity of a polyethylene can be progressively reduced. Generally, between 40 and 50 wt.% VA, the material becomes completely amorphous.

Some of the most important properties controlled in part by the degree of crystallinity are listed in Table 4.1 as a function of increasing vinyl acetate content (i.e. decreasing crystallinity).

Table 4.1 Changes in some physical properties of EVA as a function of decreased crystallinity due to increasing vinyl acetate content ($\downarrow$= decreases, $\uparrow$ = increases) [3].

Property	Behaviour
Stiffness modulus	$\downarrow$
Crystalline melting point/ softening point	$\downarrow$
Tensile yield strength	$\downarrow$
Chemical resistance	$\downarrow$
Impact strength	$\uparrow$
Gas permeability	$\uparrow$
Coefficient of friction	$\uparrow$

The second effect of vinyl acetate amount results from the polar nature of the acetoxy side chain; in fact by increasing the VA content a rising of the copolymer polarity is observed. Some properties that are influenced by the variation in the polarity are listed in Table 4.2.

Table 4.2 Changes in some physical properties of EVA related to increased polarity due to increasing vinyl acetate content ($\uparrow$ = increases) [3].

Property	Behaviour
Dielectric loss factor	$\uparrow$
Compatibility with polar resins and plasticizers	$\uparrow$
Specific adhesion	$\uparrow$
Printability	$\uparrow$

EVA copolymer with 70% VA used in this thesis was supplied by Bayer under the trade name Levapren HV 700 (Money viscosity, ML(1+4)@100°C 27±4).

Of the range of elastomers available to technologist, natural rubber (NR) (Figure 4.2) is among the most important, because it is the building block of most important rubber compounds used in products today. NR is a truly renewable resource obtained from the tree *Hevea brasiliensis* [5].
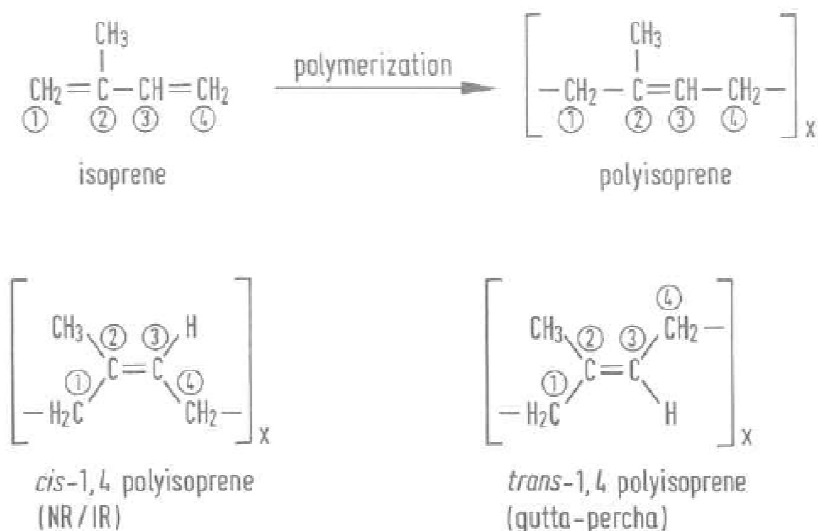

Fig. 4.2 Synthesis of natural rubber [1]

The physical properties of vulcanized natural rubber are dependent on several factors such as degree and type of crosslink, type and amount of fillers, degree of filler dispersion and presence of plasticizers. NR rubbers have high tensile strength, due to crystallization of the polymers chains which happens at high strains. Furthermore, this kind of rubber shows great resilience, low compression set, good electrical insulation and good resistance to abrasion, tear and fatigue. Being an unsaturated polymer, NR is highly susceptible to degradation by oxygen, ozone, radiation, heat and chemicals. The T_g of NR is about -70°C and the vulcanizate remains flexible at temperatures below to -55°C; however NR has the tendency to crystallize if it is stored for long periods at low temperatures.

Polybutadiene rubber is a homopolymer of 1,3-butadiene. The latter can be polymerized to produce a variety of isomers and only some of them are elastomers. 1,4 polymerized

BR can exist in cis or trans form depending on the orientation of the substituents across the enchained double bond (Figure 4.3). Each of these isomeric forms are different BR elastomers with unique physical, mechanical, and rheological properties. A mixture of these isomers on a single chain also leads to different elastomeric properties [6].
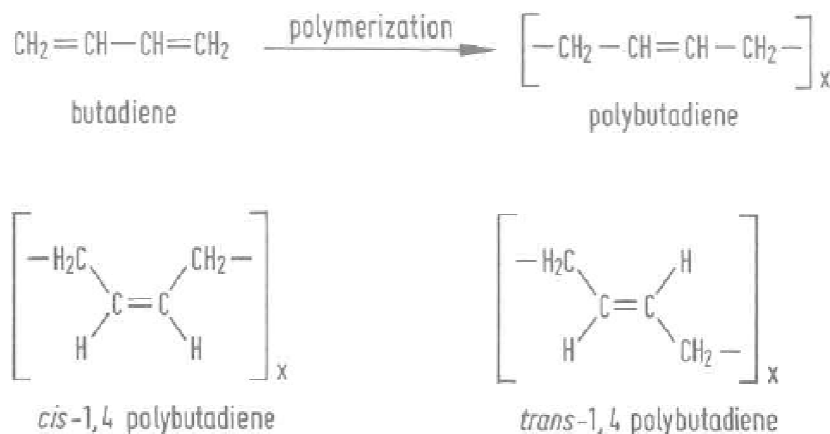

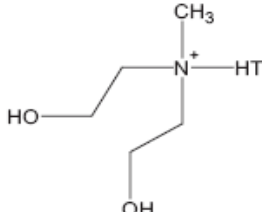**Fig. 4.3** Synthesis of polybutadiene rubber.

The vulcanizates of 100% BR have high abrasion resistance, the highest resilience of all known elastomers and, with the exception of silicone rubbers, the lowest glass transition temperature [7].
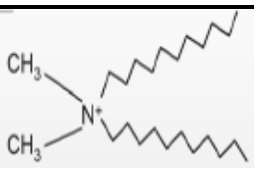
Natural rubber was supplied by Wurfbain Nordmann B.V. (The Netherlands) under the trade name SMR 10 CV60 (Money viscosity, ML(1+4)@100°C 60). Cis-1,4-polibutadiene rubber (Europrene NEOCIS BR40) was purchased from Polimeri Europa (Italy).
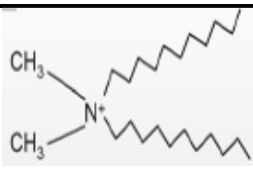
4.1.2 Nanoclays

Three types of montmorillonites, named as Cloisite Ca2+, Cloisite 30B and Cloisite 15A, were received from Southern Clay Products (USA). Montmorillonite Nanofil 15 were purchased by Süd-Chemie (Germany). The LDH clays called Perkalite LD and Perkalite F100, were offered free by Akzo Nobel (Italy). Some technical specification of nanoclays are listed in Tables 4.3.

Commercial name	Cloisite Ca^{2+}
Organic-modifier	None
Dry Particle Sizes	10% less than: 2 μm
	50% less than: 10 μm
	90% less than: 25 μm
Density	2.8 g/cm^3

Commercial name	Cloisite 30B
Organic-modifier	
	T is Tallow (~65% C18; ~30% C16; ~5% C14)
Dry Particle Sizes	10% less than: 2 μm
	50% less than: 6 μm
	90% less than: 13 μm
Density	1.98 g/cm^3

Commercial name	Cloisite 15A
Organic-modifier	
	T is Tallow (~65% C18; ~30% C16; ~5% C14)
Dry Particle Sizes	10% less than: 2 μm
	50% less than: 6 μm
	90% less than: 13 μm
Density	1.66 g/cm^3

Commercial name	Nanofil 15
Organic-modifier	T is Tallow (~65% C18; ~30% C16; ~5% C14)
Dry Particle Sizes	25 μm
Density	1.8 g/cm^3

Commercial name	Perkalite LD
Organic-modifier	None
Dry Particle Sizes	d_{99}< 25 μm d_{90}< 15 μm d_{50}< 10 μm
Density	2.1 g/cm^3

Commercial name	Perkalite F100
Organic-modifier	Hydrogenated fatty acid
Dry Particle Size	d_{99}< 20 μm d_{90}< 10 μm d_{50}< 5 μm
Density	1.4 g/cm^3

Table 4.3 Material specification of nanoclays used [8].

.

X-ray diffraction (XRD)

The diffraction patterns of tested nanoclays are shown in Figure 4.4.

XRD spectra were interpreted with respect to the position of the first order basal reflections (001) and (003), which depend on the distance between two adjacent sheets in the MMT and LDH crystal lattice, respectively.

The higher order reflections of the same (hkl) series (i.e. (002), (003) and so on for MMTs, or (006), (009) and so on for LDHs) are visible in some nanoclay spectra, such as C15, N15 and PF100. They indicate the presence of repeating crystal planes and symmetry in a specific crystallographic direction.
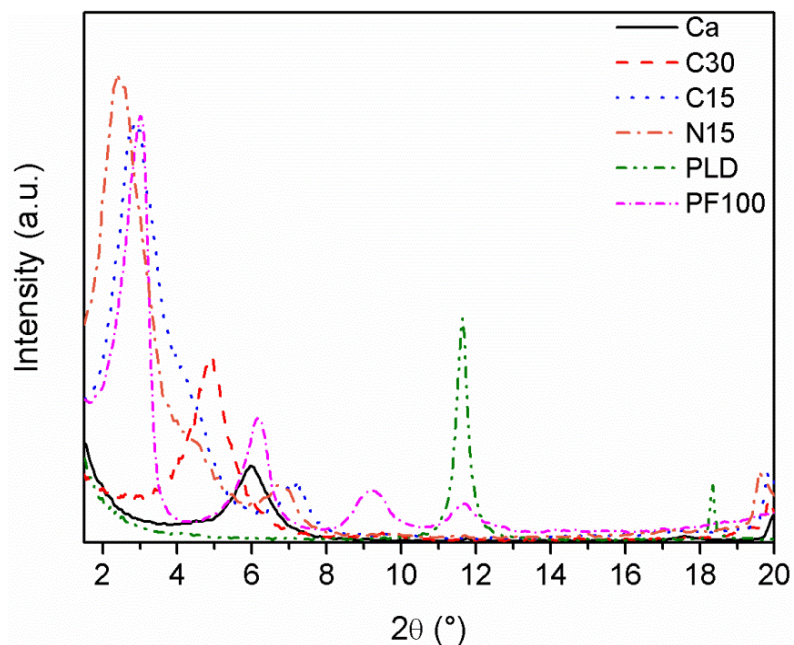
Fig. 4.4 XRD curves of nanoclays used.

The interlayer distance (d) of each clay was determined from the measured value of diffraction angle 2θ using Bragg's equation given by $\lambda = 2d \sin \theta$.

Table 4.3.lists 2θ angles and d-spacing of the different clays.

Table 4. 4 Nanoclay list with 2θ angle and interlayer distance.

Nanoclay	2θ (°)	d-spacing (nm)
Cloisite Ca^{2+}	5.99	1.48
Cloisite 30B	4.90	1.81
Cloisite 15A	2.89	3.01
Nanofil 15	2.64	3.35
Perkalite LD	11.68	0.76
Perkalite F100	3.03	2.92

Figure 4.4 and Table 4.3 demonstrate that the presence of organo modifiers increases the clay d-spacing.

Fourier Transform Infrared Spectroscopy (FT-IR)

The FT-IR spectra of Cloisite Ca^{2+}, Cloisite 30B, Cloisite 15A and Nanofil 15 are presented in Figure 4.5.
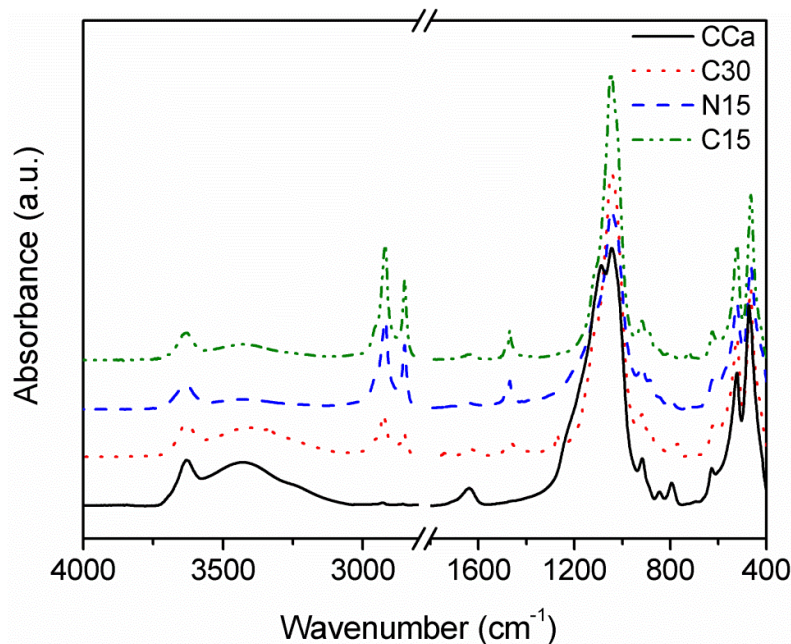

Fig. 4.5 FT-IR spectra of MMT nanoclays used.

All the clays show a sharp band around 3627 cm^{-1}, resulting from the OH stretching vibration of the silicate and a broad band between 3550-3100 cm^{-1}, characteristic of the stretching and deformation vibrations of the interlayer water. Infrared signal of adsorbed H_2O is visible also around 1635 cm^{-1} (bending vibrations). Additionally, the absorption pick at about 1040 cm^{-1} is ascribed to Si-O-Si stretching vibrations of clays. The other two absorption bands around 520 cm^{-1} and 465 cm^{-1} derive from Al-O stretching and Si-O bending vibrations of silicate. The organo-montmorillonites display some bands which are not exhibited by the pristine clay. These bands appear at 2920, 2850 and 1468 cm^{-1} and are attributed to the C–H vibrations of the methylene groups (asymmetric stretching, symmetric stretching and bending, respectively) from chemical structure of the organo-modifiers [9]. It is evident that the C15 and N15 spectra are identical.

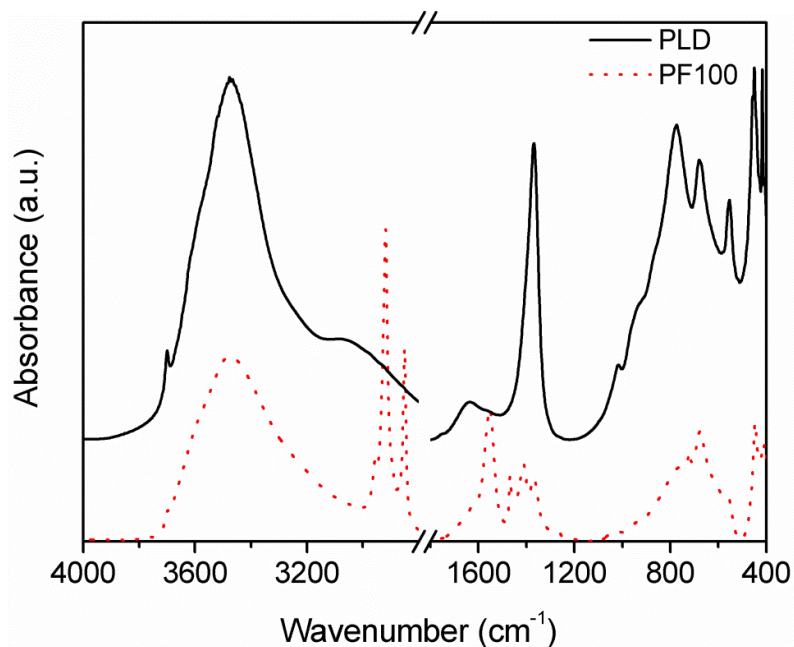The FT-IR spectra of LDH clays are shown in Figure 4.6.

Fig. 4.6 FT-IR spectra of LDH nanoclays used.

The CO_3^{2-} present in the interlayer region in LDH, in comparison to the free anions, shows shifting of the characteristic three vibration bands to lower values and also splitting of the bands. This is because of the fact that intercalation and also ionic interaction of the CO_3^{2-} ions with metal hydroxide layers impose steric hindrance on the normal vibration of the bonds. In most LDH clays, these characteristics bands are observed in the range 880-850 cm^{-1}, 1380-1350 cm^{-1} and 670-690 cm^{-1} [10].

In the range 3700-3200 cm^{-1} a broad band originates from the OH stretching of the metal hydroxide layer and interlayer water molecules is visible. A shoulder present around 3100 – 3000 cm^{-1} is caused by the interaction between the CO_3^{2-} and H_2O present in the interlayer region, which involves mostly hydrogen bonding. The presence of the interlayer water is also demonstrated by the band around 1600 cm^{-1}. The sharp bands around 780, 553 and 450-430 cm^{-1} are originated from various lattice vibrations associated with metal hydroxide sheets.

The PF100 clay displays two prominent vibrations at 2917 and 2950 cm^{-1}, corresponding to the antisymmetric and symmetric stretching modes of CH_2 groups of the hydrocarbon tail present in the organic modifier. The presence of characteristic vibration bands for CO_3^{2-} indicates that some ions exist still in the interlayer spaces. However, the absence of

the strong band at 1357 cm^{-1} indicates a significant decrease in the interlayer CO_3^{2-} amount.

The FT-IR spectrum shows also two strong characteristic bands at 1563 cm^{-1} and 1412 cm^{-1} respectively for the asymmetric and the symmetric stretching vibrations associated with the COO$^-$ group. The shoulder in the range 1600-1670 cm^{-1} is related to the bending vibration of the interlayer water. Finally, the broad band in the range 3200-3700 cm^{-1} and the peak around 445 cm^{-1} are mainly due to OH groups present in metal hydroxide layers [11].

Thermogravimetric analysis (TGA)

The thermal analysis of the clays is shown in Figure 4.7.Only the spectra of N15 is reported, C15 showed the same behaviour.
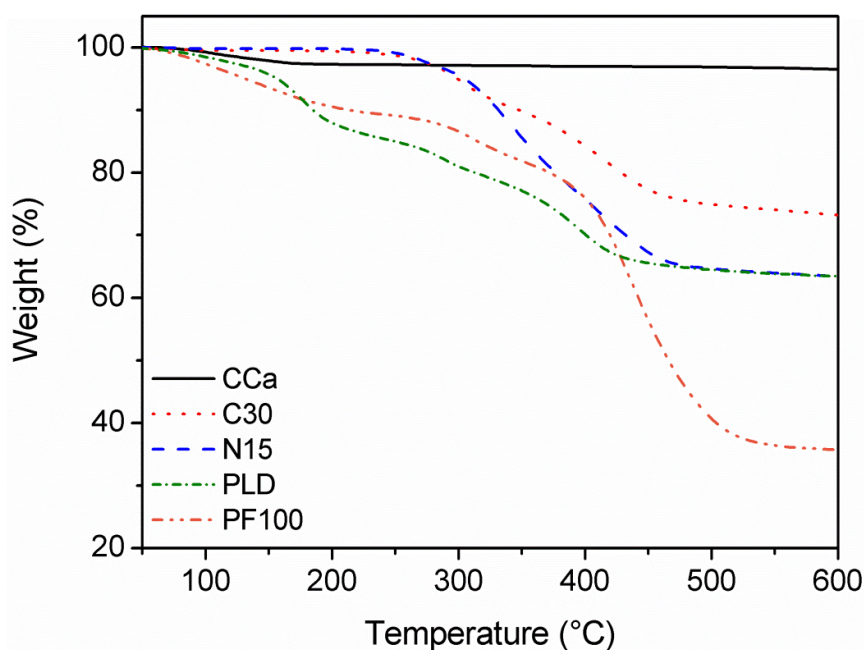

Fig. 4.7 TGA curves of nanoclays used in nitrogen atmosphere.

The weight loss at approximately 100 °C for CCa clay, is due to the loss of the hydration water. This loss is absent in the thermograms of C30 and N15: organophilic agent replaces the water molecules adsorbed on the clay surface, decreasing the amount of water on the surface of the filler. Organo-modified clays show a mass loss in the range from 250 to 400 °C due to the thermal degradation of the organophilic agents. A further

loss of weight occurs above 450 °C due to dehydroxylation of clays and to degradation of organic compounds of organophilic clays [9, 11].

In the thermal analysis of PLD clay two decomposition stages can be recognized. The first stage, up to 200°C, is due to the loss of interlayer water, while the second ones, between 200–500 °C, depends on the loss of interlayer carbonate and dehydroxylation of the metal hydroxide layer [12].

The latter generally occurs in two distinct steps with relation to Mg^{2+}/Al^{3+} ratio. In particular, these two steps become progressively noticeable as the ratio increases. The first of these two peaks is attributed to the partial loss of OH from the brucite-like layer and the second one to the complete loss of OH and carbonate ions.

The release of water molecules in PF100 clay starts al lower temperature compared to that in unmodified LDH. This phenomenon happens because in the unmodified clay interlayer water molecules remain in close interaction with the carbonate ions and the hydroxide sheets through hydrogen bonding. On the contrary, in the modified clay these interactions are largely reduced further to the decrease in the ions content in the interlayer region.

It is evident that the clay PF100 contains the highest amount of organic modifier.

Scanning electron microscopy (SEM)

Figure 3 displays SEM micrographs of used commercial layered silicates. All the clays have plate-like particle morphology. However more compacted aggregates are observed in Cloisite Ca^{2+} (Figure 4.9 (a)).
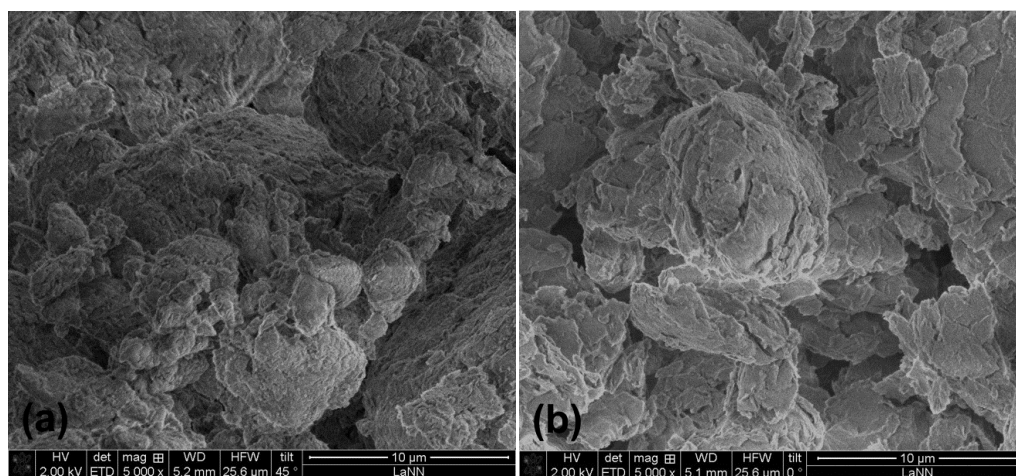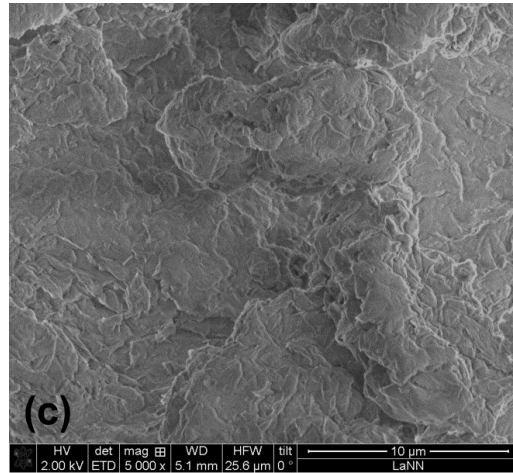
Fig. 4.8 SEM micrographs of: (a) Cloisite Ca^{2+}, (b) Cloisite C30B, (c) Nanofil 15.
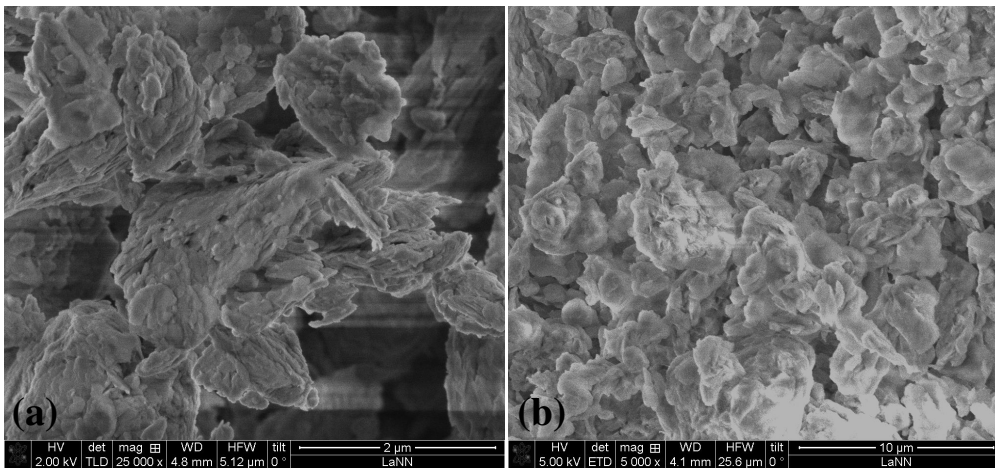

Fig. 4. 9 SEM micrographs of: (a) Perkalite LD (b) Perkalite F100.

In Figure 4.9 (a) the primary plate-like particles is clearly evident and seems characterized by hexagonal shapes. The treatment necessary to introduce the organic modify does not significantly changes the particle morphology, which keeps plate-like appearance (Figure 4.9 (b)).

4.1.2 Fire retardant additives

Aluminum tri-hydroxide

One of the most common fire retardant additive used in rubber compounds is aluminum tri-hydroxide (ATH). Aluminum tri-hydroxide decomposes endothermally between 180 - 200 °C with water release and the formation of alumina [13].

This reaction tend to occurs in two stages and the intermediate product formed is known as boehmite ''AlOOH''. The corresponding transition is less perceptible with decreasing ATH particle size. In fact, in Figure 4.10 for the ATH used, Martinal OL 107 LE, only a endothermic reaction is evident. The average particle size of this product is 1.6-1.9 µm [14]. The thermal degradation curve shows a residual mass around 70%.

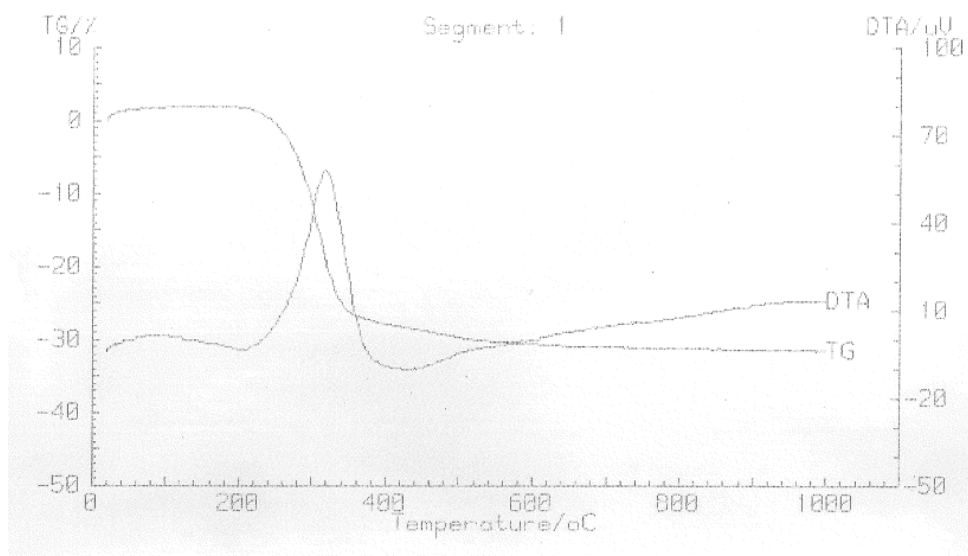**Fig. 4. 10** TGA and DTA curves of ATH in nitrogen atmosphere.

Zinc borate

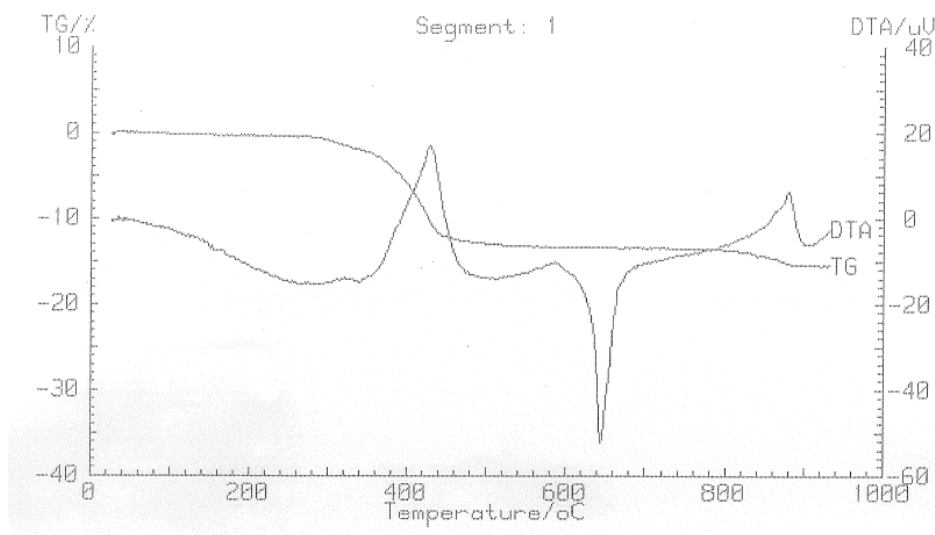Zinc borate is another fire retardant additive contained in the rubber formulations studied.

Fig. 4. 11 TGA and DTA curves of zinc borate in nitrogen atmosphere.

Its endothermic decomposition between 290 and 450 °C liberates water, boric acid and boron oxide (Figure 4.11). The latter formed softens at 350 °C and flows above 500 °C leading to the formation of a protective vitreous layer. This layer protects the polymer from heat and oxygen. The release of combustible gases is thus reduced [13].

Ceepree

The commercial products Ceepree (Chance and Hunt, UK) is based on diverse low-melting inorganic glasses, promoted as fire barrier for polymers [15].

When heated beyond its activation temperature of around 350°C, the lowest melting components in the Ceepree begin to melt. At higher temperatures, of around 750 – 850°C, components in the Ceepree formulation "devetrify", passing from a glassy state to a crystalline state. Figure 4.12 shows a very low weight loss in the TGA curve at 600°C. In the DTA analysis it evident an esothermic peak around 700°C probably due to the devetrifycation phenomenon.
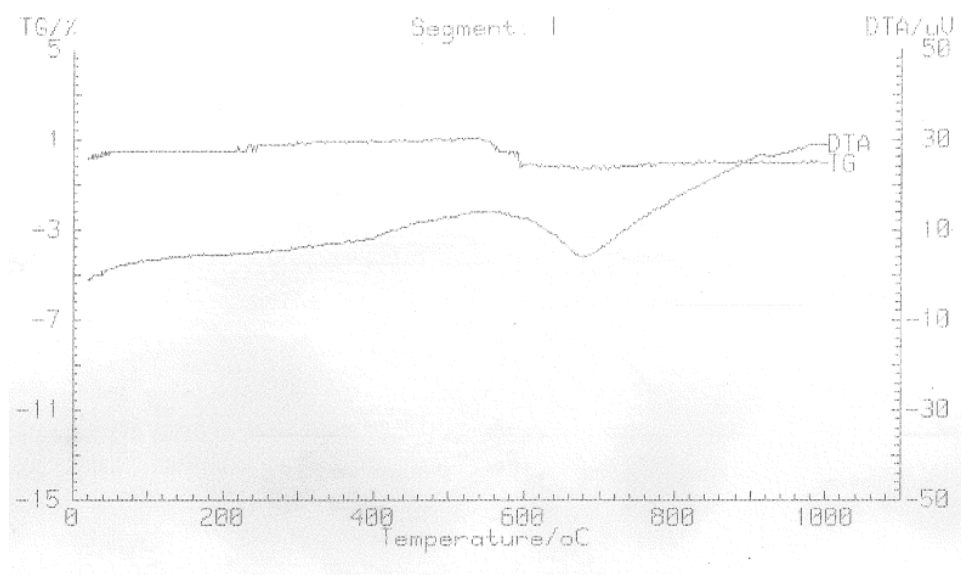

Fig. 4.12 TGA and DTA curves of Ceepree in air.

4.1.3 Conventional fillers

Carbon black N234 (Degussa) was used. Iodine adsorption number of this filler was 120 g/kg. Conventional silica ULTRASIL VN3 (Degussa) with a specific BET surface area of approximately 170 m^2/g was used in rubber compounds.

4.2 Compounding and sample preparation

The majority of the studied rubber compounds were prepared using a two-roll mill (see Chapter 3). The mixing process involved masticating or breaking down the crude rubber until an even and smooth band was formed around the front roll. When the crude rubber became soft and plastic the other ingredients, except the vulcanizing agents, were added in the rolling bank region. The space between the rolls was increased at intervals to maintain a constant bank. Powders that dropped into the mill tray were swept to the front by the operator and added back to the mix. During the mixing, the operator continuously cut and folded the compound sheet in order to obtain an uniform dispersion of the ingredients in the rubber mix. The last step was the addition and the incorporation of the vulcanizing agents. Finally, the rubber compounds were vulcanized in an electrically heated hydraulic using a temperature and a time prefixed.

A temperature of 150 °C was used for the sulphur-cured compounds while 160 °C was chosen for the peroxidic-cured ones. After the vulcanization a sheet of 200x200 mm with about 2 mm of thickness was obtained.

Some compounds were prepared by using the Brabender mixer at the Nanotechnology Centre CIVEN in Marghera-Venezia. The Brabender is torque rheometer for Laboratory-scale production of samples.

4.3 Characterization techniques

Rubber compounds were vulcanized by using the following experimental techniques.

4.3.1 Fourier Transform Infrared Spectroscopy (FT-IR)

Infrared spectra of the nanoclays were obtained from KBr pellets at room temperature using a Jasco 620 Spectrometer from 400 to 4500 cm^{-1}, with 2 cm^{-1} resolution.

4.3.2 Scanning electron microscopy (SEM)

The clay powders were investigated by using a dual beam FEI Nova 600 scanning electron microscopy.

4.3.3 Cure characteristics

The kinetic of vulcanization was studied with a Rheometer MDR 2000 from Alpha Technologies at 185°C, according to ASTM D 2084-01. The measure of the torque

variation as a function of time at a fixed temperature permits to determine the vulcanization times, t_2 (scorch time) and t_{90} (optimum cure time), as well as the maximum and minimum values of the torque, M_H and M_L, respectively.

Differential scanning calorimetry (DSC) measurements were carried out using a TA instruments DSC Q200 at a heating rate of 10°C/min under nitrogen atmosphere.

4.3.4 Thermal analysis (TGA/DTA)

The thermal stability of rubber compounds was determined with a Netzsch TGA 209C thermogravimetric analyzer in air or in nitrogen atmosphere at a heating rate of 10°C/min.

4.3.5 X-ray diffraction (XRD)

X-ray diffraction analysis were conducted using a Bruker AXS D8 Advance X-ray diffractometer (Bruker, Germany), using a CuK$_\alpha$ radiation (0.15418 nm). Peak positions in XRD patterns were used to derive the basal spacing (d) of the clays according to Bragg's equation, defined as $\lambda = 2d \sin \theta$.

The same amount of nanocomposite was used in the different measurements; therefore the diffraction peaks intensity are comparable

4.3.6 Mechanical properties

Tensile test

The tensile mechanical properties were measured with a universal tensile testing machine at room temperature at a crosshead speed of 500 mm/min. Tensile strength, elongation at break and 300% modulus were determined from the stress-strain curves. This latter is defined as the tensile strength observed at an elongation 300% [7].

Dumbbell-shaped samples were cut from the vulcanized sheets according to ASTM D412–93.

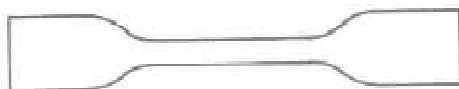Tensile test specimen are displayed in Figure 4.13.

Fig. 4.13 Tensile test piece.

Tear test

Angle test samples (Figure 4.14), type die C, were cut from the rubber sheets according to ASTM D624–9.

The test involves measuring the force required to completely tear the sample. The tearing force was applied by means of a tensile testing machine at a speed of 500 mm/min [7].

Fig. 4.14 Tear test piece.

Hardness

Hardness it is defined as the resistance of the surface to penetration by an indentor of specified dimensions under specified load. The hardness was quoted in Shore hardness degrees. The Shore hardness testers are called durometers, types A and D. The first, suitable for soft rubbers, was used for the compound characterization.

4.3.7 Abrasion and rebound resilience

Abrasion resistance is defined as the resistance of a rubber compound to wearing away by contact with a moving abrasive surface. Abrasion resistance in the terms of volumetric loss of a cylindrical sample was estimated according to DIN 53516 [7].

The rebound resilience was measured following the procedure described in ASTM D 2632. The test method verify the ability of an elastomers to return quickly to its original shape after a temporary deflection.
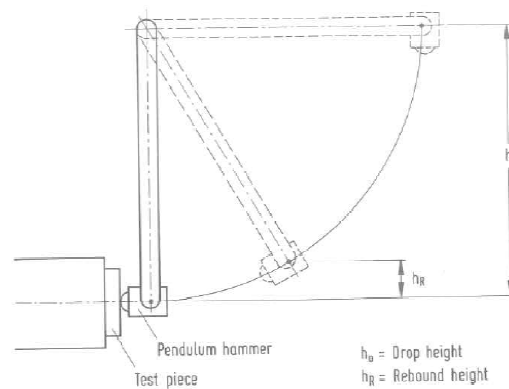

Fig. 4.15 Rebound resilience apparatus

During the test a falling pendulum hammer impacts a standard piece of rubber compound (Figure 4.15). The pendulum is free to rebound after the impact. The ratio of the rebound height to the drop height, expressed as a percentage, is equal to rebound resilience of the compound testes [7].

4.3.8 Fire resistance

Fire resistant test were carried out at "Politecnico di Torino, sede di Alessandria".

Limited Oxygen Index: LOI

The value of the LOI is defined as the minimal amount of oxygen $[O_2]$ in the oxygen/nitrogen mixture $[O_2/N_2]$ needed to maintain flame combustion of the material for 3 minutes or consumes a length of 5 cm of the sample, with the sample placed in a vertical position (the top of the test sample is inflamed with a burner) [13].

According to ISO 4589, the LOI is measured on 80x6.5x3 mm^3 specimens placed vertically at the centre of a glass chimney (Figure 4.16).

As air contains 21% oxygen, materials with an LOI below 21 are classified as ''combustible'' whereas those with an LOI above 21 are classified as ''self-extinguishing''. Consequently, the higher the LOI the better the flame retardant property [13].
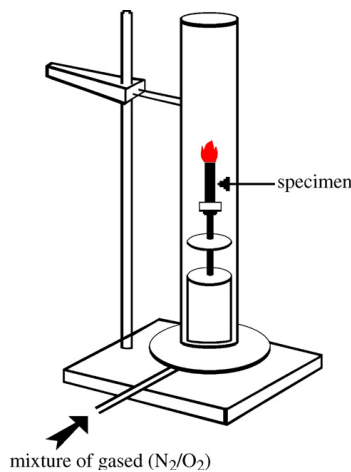

Fig. 4.16 Experimental set-up for LOI measurement [13].

Cone Calorimeter

The cone calorimeter (Figure 4.17) uses a truncated conical heater element to irradiate test specimens at heat fluxes from 10 to 100 kW/m^2, thereby simulating a range of fire intensities [16].

Cone calorimeter tests were carried out by using a 35 kW/m^2 incident heat flux. For each compound three samples, of dimensions 100x100x2 mm^3, were tested.

The cone calorimeter technique provides detailed information about ignition behaviour, heat release and smoke evolution during sustained combustion. One of the key parameter determined with the cone calorimeter is the heat release rate (HRR), expressed in kW/m^2 defined as the quantity of heat released per unit of time and surface area. The Peak of Heat Release Rate, (pHRR) taken as the peak value of the heat release rate vs. time curve, and considered to be the variable that best expresses the maximum intensity of a fire, indicating the rate and extent of fire spread.

In addition, the cone calorimeter test also enables characterization of the time to ignition (TTI), quantities of CO and CO2, total smoke released (TSR) and a lot of others.
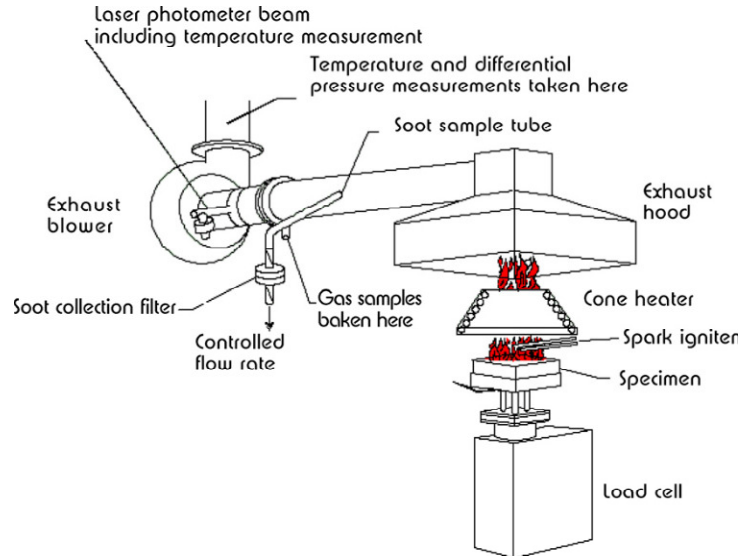

Fig. 4.17 Experimental set-up for a cone calorimetry measurement [13]

It is important to underline that while the LOI is widely used to evaluate the flame retardancy of materials, especially for screening flame retarded formulations of polymers, the cone calorimeter provides a wealth of information on the combustion behaviour [17].

4.3.9 Swelling

The swelling properties of the vulcanizates were investigated by setting the samples in toluene. The cured test pieces were weighted in the dry condition and immersed in the solvent for 72 hours at room temperature. Then, the samples were removed from the toluene, their surfaces wiped, and weighted again. The degree of swelling and the crosslink density was calculated by using appropriate relations reported afterwards.

The degree of swelling was calculated by using the relation [18]:

$$Q(\%) = \frac{m - m_s}{m} \times 100$$

where m and m_s are the masses of the sample before and after swelling.

The crosslink density, V_e per unit volume is defined [19] as the number of elastically effective chains totally included in a perfect network, and is given by the equation:

$$V_e = \frac{\rho_r N_A}{M_C}$$

where ρ_r is the rubber density, N_A is the Avogadro's number, and M_C is the average molecular weight between cross-links.

According to Flory-Rehner theory [20], for a perfect network:

$$M_C = -V_1 \rho_r \frac{(\phi_r^{1/3} - \frac{\phi_r}{2})}{[\ln(1 - \phi_r) + \phi_r + \chi\phi_r^2)}$$

where V_1 is the molar volume of the solvent, ρ_r the rubber density, ϕ_r the volume fraction of rubber in the swollen gel and χ is the Flory-Huggins interaction parameter between solvent and rubber.

References

[1] K. Nagdi, *Rubber as an Engineering Material: Guideline for Users*, Carl Hanser Verlag (1993).

[2] J.J. George and A.K. Bhowmick, *Nanoscale Res. Lett.*, **4**, 655 (2009).

[3] A.M. Henderson, *IEEE Electr. Insul. Mag.*, **9**, 30 (1993).

[4] M. Pramanik, S.K. Srivastava, B.K. Samantaray and A.K. Bhowmick, *J. Mater. Sci. Lett.*, **20**, 1377 (2001).

[5] B. Rodgers, *Rubber Compounding: Chemistry and Applications*, Marcel Dekker (2004).

[6] J.R. White and S.K. De, *Rubber Technologist's Handbook*, Rapra Technology (2001).

[7] K. Nagdi, *Rubber as an Engineering Material: Guideline for Users*, Carl Hanser Verlag (1993).

[8] Data sheets of Cloisite Ca2+, Cloisite 30B, Cloisite C15A, Nanofil 15, Perkalite LD, Perkalite F100.

[9] J.M. Cervantes-Uc, J.V. Cauich-Rodriguez, J. Vazquez-Torres, L.F. Garfias-Mesias and D.R. Paul, *Thermochim. Acta*, **457**, 92 (2007).

[10] F. Cavani, F. Trifiro, and A. Vaccari, *Catal. Today*, **11**, 173 (1991).

[11] S.P.S. Ribeiro, L.R.M. Estevão and R.S.V. Nascimento, *Sci. Technol. Adv. Mater.* **9**, 024408 (2008).

[12] E. Kanezaki, *Mater. Res. Bull.*, **33**, (1998).

[13] F. Laoutid, L. Bonnaud, M. Alexandre, J.M. Lopez-Cuesta and Ph. Dubois, *Mater. Sci. Eng. R*, **63**, 100 (2009).

[14] Data sheets of aluminium tri-hydroxide.

[15] Data sheets of Cepree.

[16] M.S. Cross, P.A. Cusack, P.R. Hornsby, *Polymer Degradation and Stability*, **79**, 309 (2003).

[17] J. Chuanmei and C. Xilei, *Iran. Polym. J.*, **18**, 723 (2009).

[18] S.J. Park and K.S. Cho, *J. Colloid Interface Sci.*, **267**, 86 (2003).

[19] S.E. Gwaily, M.M. Badawy, H.H. Hassan and M. Madani, *Polym. Test.*, **22**, 3 (2003).

[20] P.J. Flory, *J. Chem. Phys.*, **18**, 108 (1950).

Chapter 5

Flame retardancy of ethylene vinyl acetate-based rubber compounds

5.1 Introduction

Ethylene vinyl acetate copolymer (EVA) is widely used in many fields, particularly in cable industry. Unfortunately, due to its chemical compositions, this polymer is easily flammable, and because of this, its flame retardancy is widely studied.

The main approach used up to now to impart flame retardant properties to this class of polymeric materials has been the incorporation of additives. The most effective fire retardant (FR) additives commonly used in polymers are halogen-based materials. However, these systems are known to be a source of corrosive, obscuring and toxic smoke during combustion [1].

Consequently, driven by environmental and safety considerations, research and development turns towards halogen-free FR formulations. The most common additives alternative to halogen-based materials are metallic hydroxides, such as aluminium (ATH) or magnesium hydroxides (MH). The latter decompose endothermally and release water at a temperature around at which the polymer decomposes, no evolution of smoke and corrosive gas is observed [2]. Zinc borate is another fire retardant additive frequently used in polymeric matrices. In several studies it has been mentioned as smoke and afterglow suppressant, corrosion inhibitor, anti-tracking agent and, sometimes, as synergic agent [1].

In recent years, fillers with at least one dimension in the nanometric range have been increasingly used to improve the flame retardancy of polymers. Their effects include [3]:

- reinforcing organic char as a barrier layer;
- providing a catalytic surface to promote char-forming reactions;
- enhancing the structural rigidity of the polymer;
- changing the melt-flow properties of the polymer close to its ignition temperature; and
- providing intimate contact between a fire retardant and the host polymer.

The interest in these nanomaterials is also due to the possibility to use low amounts (0-10 phr) in the polymeric compounds, contrary to the common additives, such as the metallic hydroxides, which must be added at high loadings (60-70 phr).

A considerable number of research has been devoted to flame retardancy improvement of ethylene vinyl acetate copolymers. Bourbigot et al. [4] used zinc borates as a synergic agents in EVA-ATH and EVA-MH formulations. They demonstrated that the heat release rate of the compounds are strongly reduced in comparison with the virgin polymer. In addition, an increase in the ignition time and a reduction in the volume of smoke production are achieved in the formulations with the zinc borate (Figures 5.1 (a) and (b)).
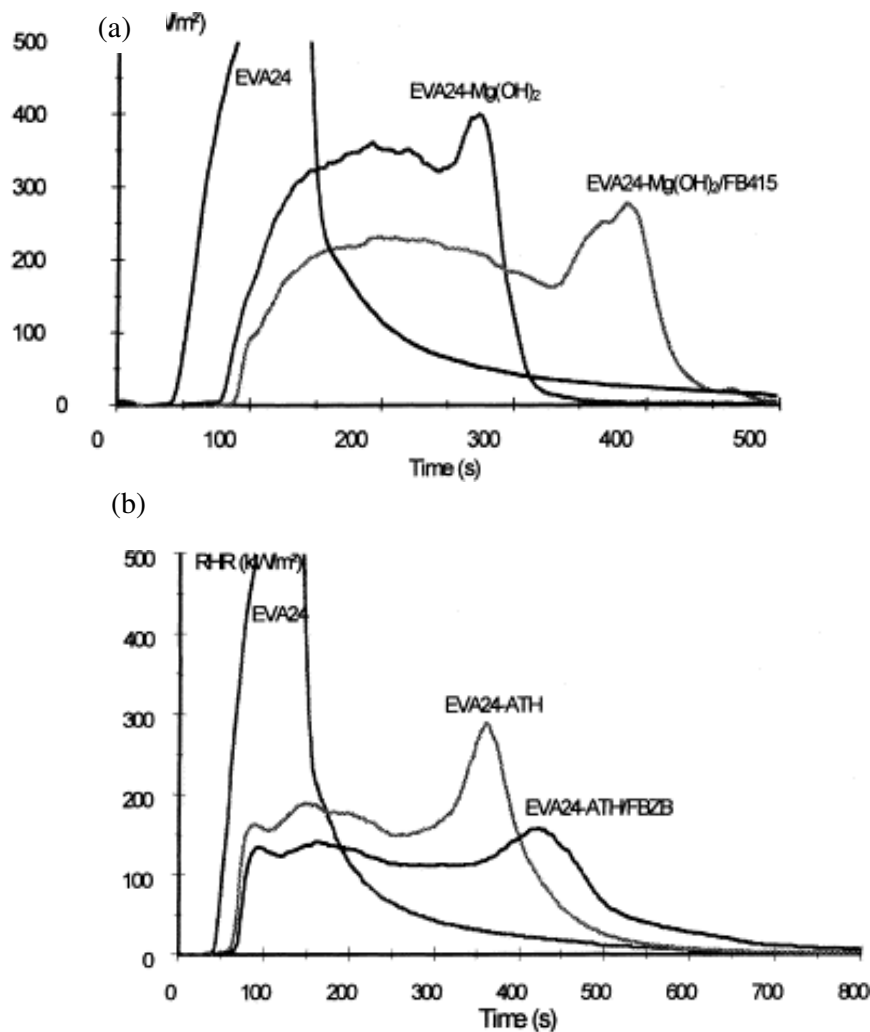

Fig. 5.1 HRR values versus time of the formulations: (a) EVA24-Mg(OH)$_2$ and EVA24-Mg(OH)$_2$/FB415 and (b) EVA24-ATH and EVA24-ATH/FB415, in comparison with the virgin EVA24 [4].

Bugajny et al. [5] investigated new intumescent materials based on ethylene-vinyl acetate copolymers, with different amounts of vinyl acetate. The fire retardant additive used was a commercial product, containing an acid source, a carbon source and a blowing agent. The results demonstrated that the incorporation of the additive at 30 wt. % in the polymer reduces the flammability of EVA and provides good fire retardant properties by development of an intumescent coating.
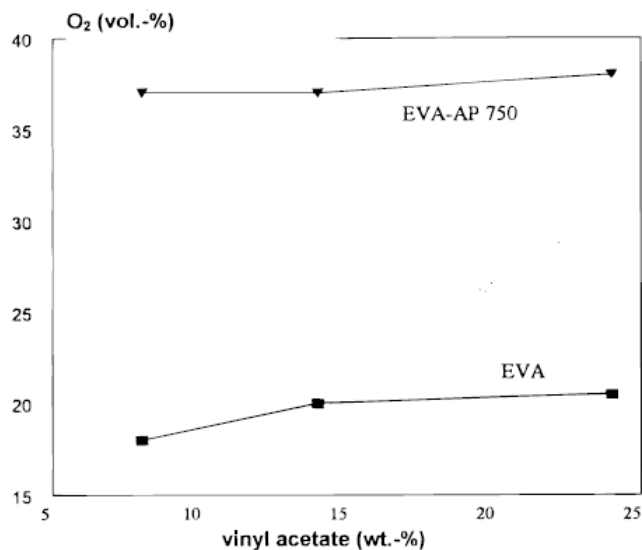

Fig. 5.2 LOI versus vinyl acetate content [5].

Table 5.1 UL-94 rating of virgin EVA and EVA-AP750 [5].

	EVA	EVA − AP 750
EVA 8%	Failed	V-0
EVA 14%	Failed	V-0
EVA 24%	Failed	V-0

The combustion behaviour of EVA copolymer filled with nanoclays was presented by several authors. Zanetti et al. [6], for example, demonstrated that depending on the clay used, it is possible to produce a microcomposite which burns in the same way as pure EVA or a nanocomposite whose heat release is reduced by 70-80%. This result is due to the formation of a protective charred ceramic surface layer as a result of reassembly of the clay platelets and catalyzed charring of the polymer.

However, the most part of the studies about the flame retardancy of EVA concerns the ethylene-vinyl acetate copolymers with a low VA content (e.g. 5-8-19-24 wt.%) while the researches deal with the fire resistance properties of EVA rubber (up to 50 wt.%) are really poor.

A study on the flame retardancy of EVA with 70 wt. % vinyl acetate content were accomplished. Regarding the best fire resistant formulation achieved by "IVG Colbachini" as reference, an in-depth analysis of the effectiveness of commercial different fire retardant products in EVA-rubber matrix were carried out.

5.2 EVA-based fire retardant formulations

EVA-based fire retardant formulations were compounded by using two roll mills. All the compounds contained carbon black and silica powders as reinforcing fillers. Zinc oxide, stearin and peroxide were also added to rubber compounds. The mix of fire retardant additives in the standard formulation of "IVG Colbachini" was constituted by aluminium hydroxide, zinc borate and 10 phr of nanoclay N15. Some different fire retardant commercial products were added to the standard formulation and the compounds were tested.

First of all a preliminary characterization of the sample EVAFRN15 was conducted. In particular a morphological characterization by using XRD of the compounds produced with Banbury mixer and two rolls mill was carried out. Figure 5.3 shows the XRD diffractograms detected for the samples produced.
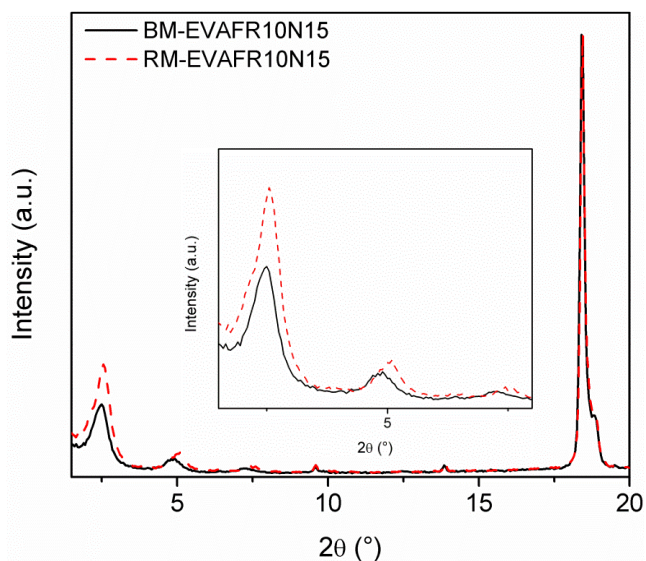

Fig. 5.3 XRD patterns of the vulcanized compounds.

It is clear that the platelets carry out an intercalation condition in both the compounds. In fact, while the N15 d-spacing is around 3.35 nm, it increases of 0.20 nm and of 0.11 nm in BM-sample and in RM-sample, respectively. Contrary to what was expected, no a significant difference in the intercalation degree were observed between the two production methods . This probably depends on EVA rubber features, in fact it is very tacky and generally it sticks to rolls or to rotors not achieving a good mixing condition.

However, normalizing the diffractograms to the ATH peak appearing around 18.45°, it can be noted that the diffraction peak intensity of the BM-sample is lower than the one of RM-sample. Concerning that the nanoclay content is the same in both compounds, it is probable that a part of the platelets in the BM-sample are exfoliated.

In addition the high intensity of the (001) diffraction peak and the presence of second order reflections indicate that the platelets of the clay achieved a well-ordered disposition. In fact, generally low intensity, broad band and no higher order reflections are signs of a strong intercalation.

Both the samples were subjected to a preliminary homemade fire test. Some stripes, obtained from the rubber vulcanized sheets, were exposed to a small Bunsen flame in vertical position for a prefixed time. The extinction time, the amount and the density of the smoke, and finally the residual char were observed.
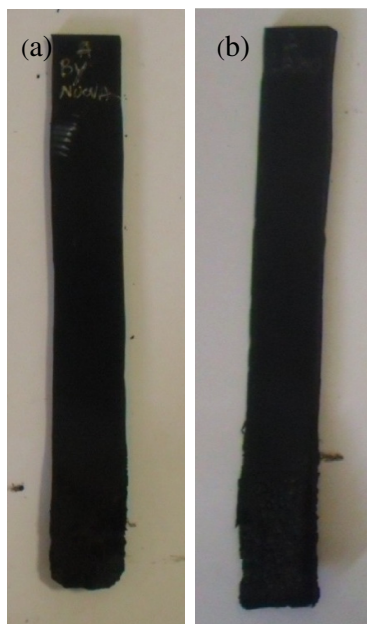

Fig. 5.4 Burned stripes of (a) Banbury mixed compound, (b) two-roll mill mixed compound.

Figures 5.4 (a) and (b) show the burned stripes. The burned part is longer in the RM-produced sample, in addition the extinction time was higher. No significant difference was observed in the smoke developed. Banbury mixer permits to achieve a better dispersion of the fillers in the rubbery matrix.

One of the first experiments carried out concerned the substitution of the O-MMT Nanofil 15 with the O-LDH Perkalite F100, which was presented in literature as an efficient fire retardant additive.

Figure 5.5 shows the XRD curves. Both clays have a higher d-spacing thanks to the precence of the organo-modifiers. This probably permits an easy accomodation of rubber chains and clay intercalation is achieved.

However, significant differences are evident observing the diffractograms. In particular, the sample EVAFR10PF100 shows a very reduced intensity band at 2θ lower than EVAFR10N15. Regarding this result it is possible to suppose that a part of PF100 platelets is exfoliated. This behaviour could be related to the chemical nature of its organo-modifier. In fact, the high polarity of the latter probably increases the affinity between the clay and the matrix and originates strong interactions with the carboxyl groups belonging to EVA.
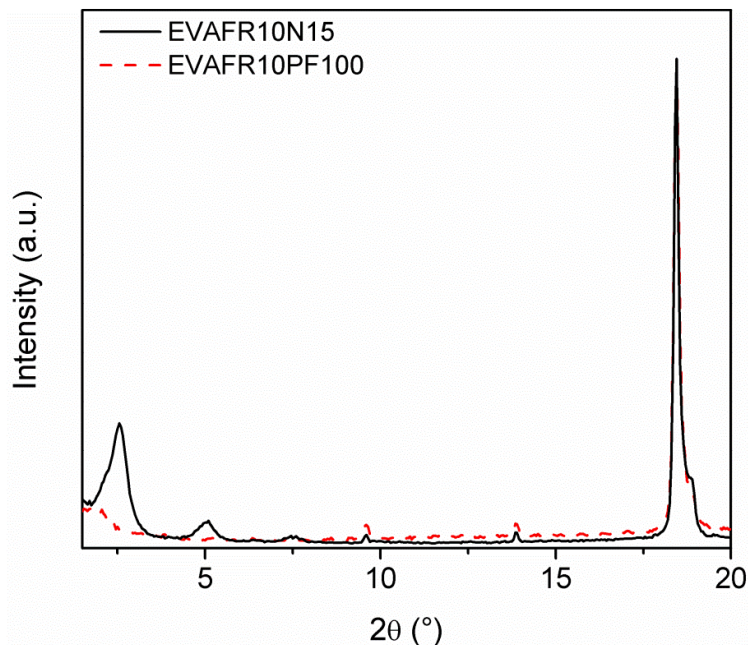

Fig. 5.5 XRD patterns of the vulcanized compounds.

Fig. 5.6 Burned stripe of PF100-filled compound.

Despite the good nanoclay dispersion carried out, the fire test performed on the sample stripes demonstrated that the compound filled with PF100 has a lower flame retardancy property (Figure 5.6). This is probably related to the organic-modifier amount, in fact Figure 4.7 .in Chapter 4 shows that PF100 contains 63 wt% of surfactant while N15 only 36 wt.%. Consequently, the number of platelets, which contribue to flame retardancy, is very low and their effectiveness is poor.

Concerning the numerous research articles showing the improvement of fire retardancy of ethylene vinyl acetate with low VA content by using intumescent additives [6-8], the rubber compound was filled with 50 phr of a commercial intumescent product, BUDIT 3167. The sample did not contain aluminium hydroxide as the BUDIT producer suggested. Also in this case a stripe of vulcanized compound was burned. The desire was to carry out a fire test for 1 minute lasted only 40 seconds due to the increase of the flame developed from the BUDIT-filled sample. After removing the Bunsen flame no auto-extinction phenomenon was observed but an intense flame was noted so it was decided to put it out.

Figures 5.7 (a) and (b) show the burned stripes. The reference sample EVAFR10N15 maintains its shape and a compact char is formed on the surface. On the contrary, in the

BUDIT-filled sample, the burned part is more extended and deformed. Regarding these results, it is clear that the intumescent product BUDIT is not able to substitute the ATH.
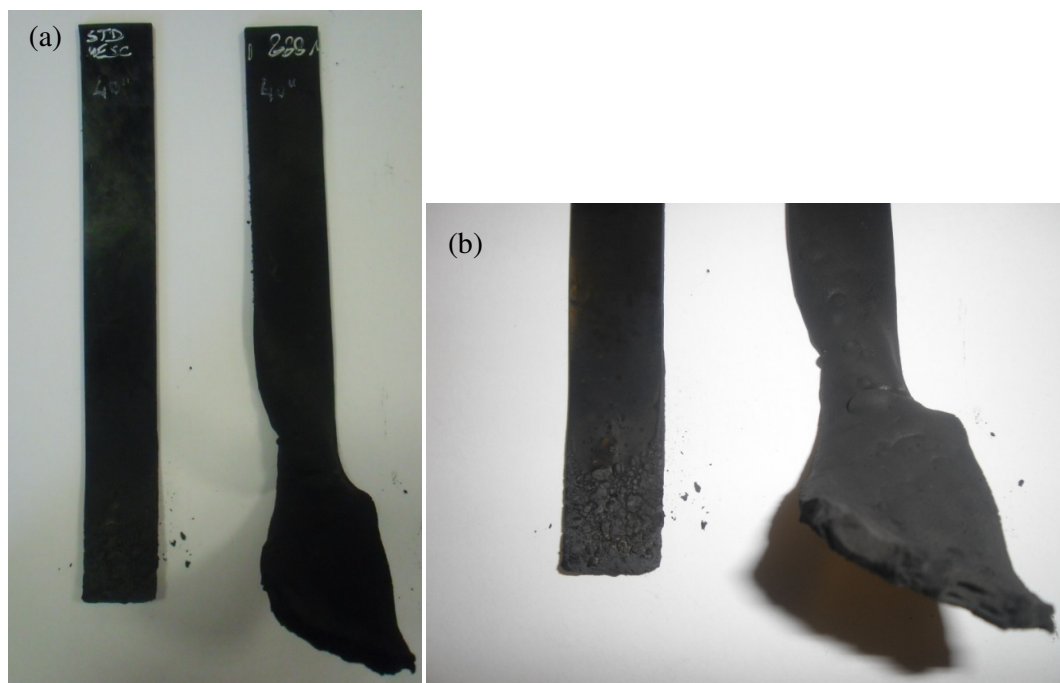

Fig. 5.7 Burned stripes of the vulcanized compounds (b) zoom.

Consequently another EVA-based compound was prepared replacing 20 phr of ATH with 20 phr of intumescent additive. Figure 5.8 shows the burned stripe.

Fig. 5.8 Burned stripe of vulcanized compound.

Several research articles demonstrated that the addition of low amounts of intumescent products in thermoplastics and thermosets causes significant improvement in flame retardancy. Unfortunately previous results showed that for rubber compounds the effectiveness of the additive is lower.

In addition an economical evaluation has to be carried out. In fact, while the cost of ATH is less than 1 euro/kg, an intumescent product, such as BUTID 3167, has a cost of around 5 or more euro/kg. It is obvious that the use of these kinds of products for industrial production would be justify only if the fire retardant properties are significantly improved.

Regarding the state of art, it is clear that the flame retardancy improvement can be achieved forming a protective layer onto sample surface during the combustion. Consequently, it was decided to introduce in the rubber compound soda-lime glass powders available in the laboratory as glass cullet. The idea was that these powders would have provide a more integral layer, acting as an agent to merge and strengthen the rubber compound/char during the combustion.

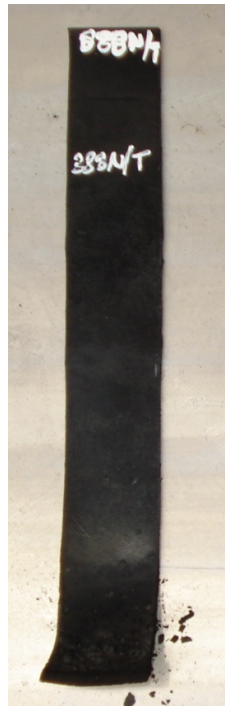Soda-lime powders available, added 30 phr, had a dimension minor 150 μm.

Fig. 5.9 Burned stripe of vulcanized compound.

Figure 5.9 shows the burned stripe. No significant differences were observed between this sample and the standard sample. It was supposed that the effect of powder glass was not detectable because of the presence of other charring additives. Hence, these powders where then added to a chloroprene rubber-based compound without the presence of any further fire retardant additive.

Figures 5.10 (a) and (b) show the stripes with and without glass powders.

Fig. 5.10 Burned stripes of cloroprene-based compounds without (a) and with (b) glass powders.

Figures 5.10 demonstrate that glass powders optimize the protection layer; in fact, a limited deformation on the burned part is observed in the soda-lime-filled sample.

An in-depth commercial research revealed the existence of a product based on diverse low-melting inorganic glasses promoted as flame retardant for organic polymers. This product, called Ceepree, is a very thin almost white powder.

Two EVAFR10N15 formulations containing in addition 15 phr (EVAFR10N1515Ce) and 30 phr (EVAFR10N1530Ce) of Ceepree were prepared. Vulcanized EVA without fire retardant additives and the reference sample EVAFR10N15 were also compounded.
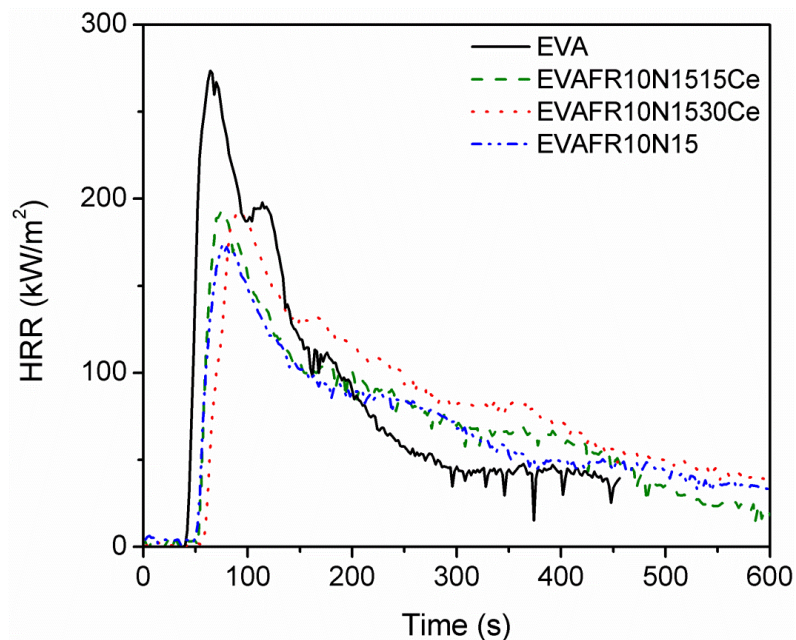
Fig. 5.11 HRR values versus time.

Cone calorimeter investigations can be used as a universal method to compare and evaluate the behaviour of rubber compounds in a fire scenario. Figure 5.11 presents HRR curves for EVA, EVAFRN15 and compounds containing Ceepree.

Unlike to thermoplastics and thermosets whose fire retardant properties can be evaluated on the unfilled matrix, a rubbery matrix does not permit this. In fact, to obtain a rubber sheet necessary to produce the samples for the characterization, the curing process is required.

A very sharp peak is evident in all the curves which is the typical behaviour of the non-charring material [9]. However, the samples EVAFR10N15, EVAFR10N1515Ce and EVAFR10N1530Ce show a significant increase in the time to ignition (TTI), respectively of 11, 14 and 20 seconds (Table 5.2). The TTI is determined visually and it is defined as the period required for the entire surface of the sample to burn with a sustained luminous flame. It is obvious that an operator error could be committed. The peak in the HRR curve is defined as the peak heat release rate (pHRR), which is the variable that best expresses the maximum intensity of a fire, indicating the rate and extent of fire spread. As expected, the addition of the fire retardant additives reduces the pHRR values in respect to the one of the EVA vulcanized sample. However, the behaviour is not the same shown for the TTI parameter. In particular, the sample EVAFR10N15 shows the lowest pHRR. On the other hand, Ceepree seems to increase the intensity of fire. This phenomenon could be

due to the way of action of Ceepree. In fact, at higher temperatures the components in the Ceepree formulation pass from a glassy state to a crystalline state. The heat release increase observed in the sample-filled with Ceepree could be caused by the exothermic reaction of crystallization, which is evident in the DTA curve in Figure 4.12 in Chapter 4. The samples with the fire retardant additives display, after the pHRR, a decrease in HRR less steep than the EVA compound and they show an extension in HRR with prolonged burning before flame out probably due to a char formation.

Another important parameter is the time to peak heat release (TTP) which is indicated in Table 5.2. The fire retardant additives induces an increase in TTP of or higher than 14 seconds. This result is very significant because TTP can be related to the time that people have in a fire scenario to escape before the fire achieves maximum intensity.

Other parameters determined with the cone calorimeter are summarized in Table 5.2. Total smoke released (TSR) and specific extinction area (SEA), a measure of smoke obscuration averaged over the entire test period, are halved in the sample EVAFR10N15. No significant difference are observed after the Ceepree addition.

The effect on the smoke developed during the combustion is mainly due to the zinc borate additive which acts as smoke suppressor.

Table 5.2 Measured parameters in the cone calorimeter test.

Sample	TTI (s)	TTP (s)	pHRR (kW/m^2)	TSR (m^2/m^2)	SEA (m^2/kg)
EVA	48	64	273.4	658.7	424.7
EVAFR10N15	59	78	175	295.4	166.6
EVAFR10N1515Ce	62	81	191.3	280.8	150.9
EVAFR10N1530Ce	68	87	193.1	331.1	177.05

Figures 5.12 (a), (b), (c) and (d) show the residues of the burned samples. Figures 5.12 demonstrate that the sample without fire retardant additives produces a fragmentary residue after burning. The other samples exhibit fire residual surfaces with a more integral structure, however a lot of cracks and openings are evident. Obviously a homogeneous residue with structural integrity is crucial for providing the most effective protective layer. Unfortunately this result is very difficult to carry out using rubber as matrix, even if it is strongly filled with fire retardant additives.

In fact, several research articles concerning the flame retardancy of thermoplastics and thermoset resins show more compact char residues using very low amounts of fire retardant additives.
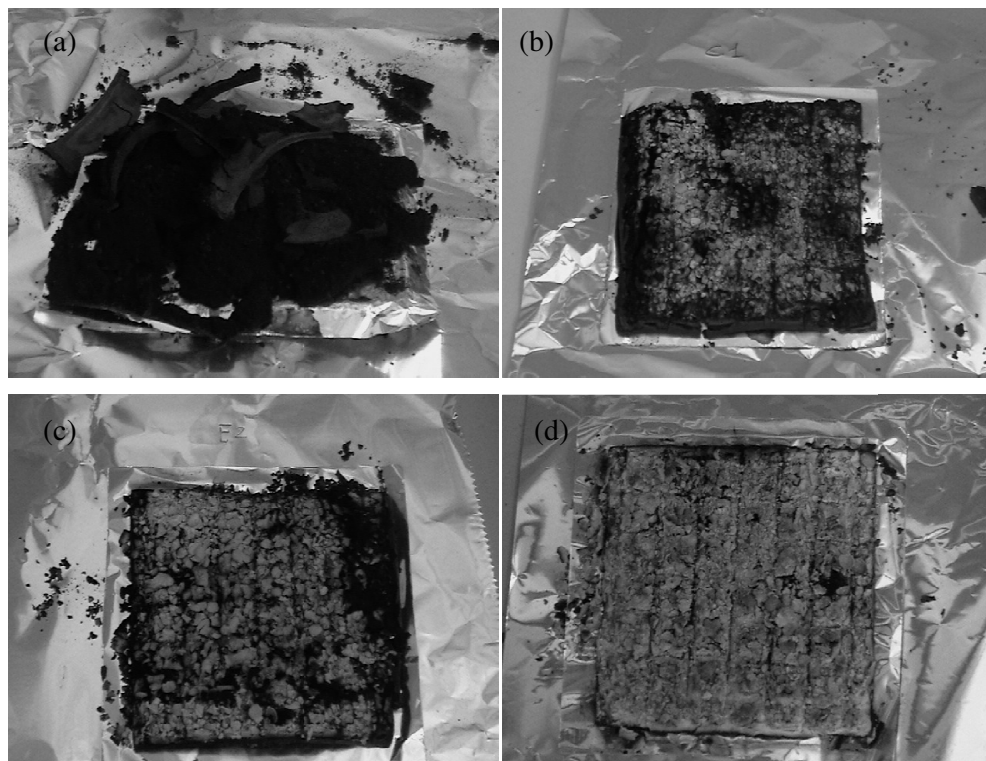

Fig. 5.12 Cone calorimeter residues for: (a) EVA, (b) EVAFR10N15, (c) EVAFR10N1515Ce, (d) EVAFR10N1530Ce.

The values for flammability in terms of reaction to small fire, characterized by LOI, are summarized in Table 5.3

The addition of ATH, zinc borate and nanoclays in the EVA compounds provokes an increase in the LOI value to 30.6 from 24.3 of original EVA sample without any fire retardant additive.

The self-extinguishing behaviour of the compound is not improved by the Ceepree loading, in fact the LOI value is similar to one found for EVAFR10N15.

Table 5.3 LOI results for vulcanized compounds**.**

Compound	LOI (vol.%)
EVA	24.3
EVAFR10N15	30.6
EVAFR10N1515Ce	30.1
EVAFR10N1530Ce	30.6

Regarding the results obtained by the cone calorimeter and the LOI is clear that the Ceepree additive does not provoke an improvement in the fire retardant properties of the EVA-based compounds studied.

An in-depth study about the compatibility between ethylene vinyl acetate with 70 VA content and different nanoclays were carried out.

Ethylene vinyl acetate rubber was compounded with five kinds of nanoclays at different concentration (1, 5, 10 phr). The compounds were prepared with the melt blending technique using a Brabender mixer. The sample code of the ethylene vinyl acetate compounds are given in Table 5.4, where the clay and its amount are also indicated.

Table 5.4 Rubber compounds tested.

Sample code	Filler	Phr
EVA70	/	/
EVA1CCa	CCa	1
EVA5CCa	CCa	5
EVA10CCa	CCa	10
EVA1CC30	C30	1
EVA5CC30	C30	5
EVA10CC30	C30	10
EVA1N15	N15	1
EVA5N15	N15	5
EVA10N15	N15	10
EVA1PLD	PLD	1
EVA5PLD	PLD	5
EVA10 PLD	PLD	10
EVA1PF100	PF100	1
EVA5 PF100	PF100	5
EVA10 PF100	PF100	10

XRD analysis

The morphology of the rubber compounds was investigated using X-ray diffraction. The diffractograms of the compounds containing MMT are shown in Figure 5.13 (a) while the ones containing LDH are in Figure 5.13 (b).

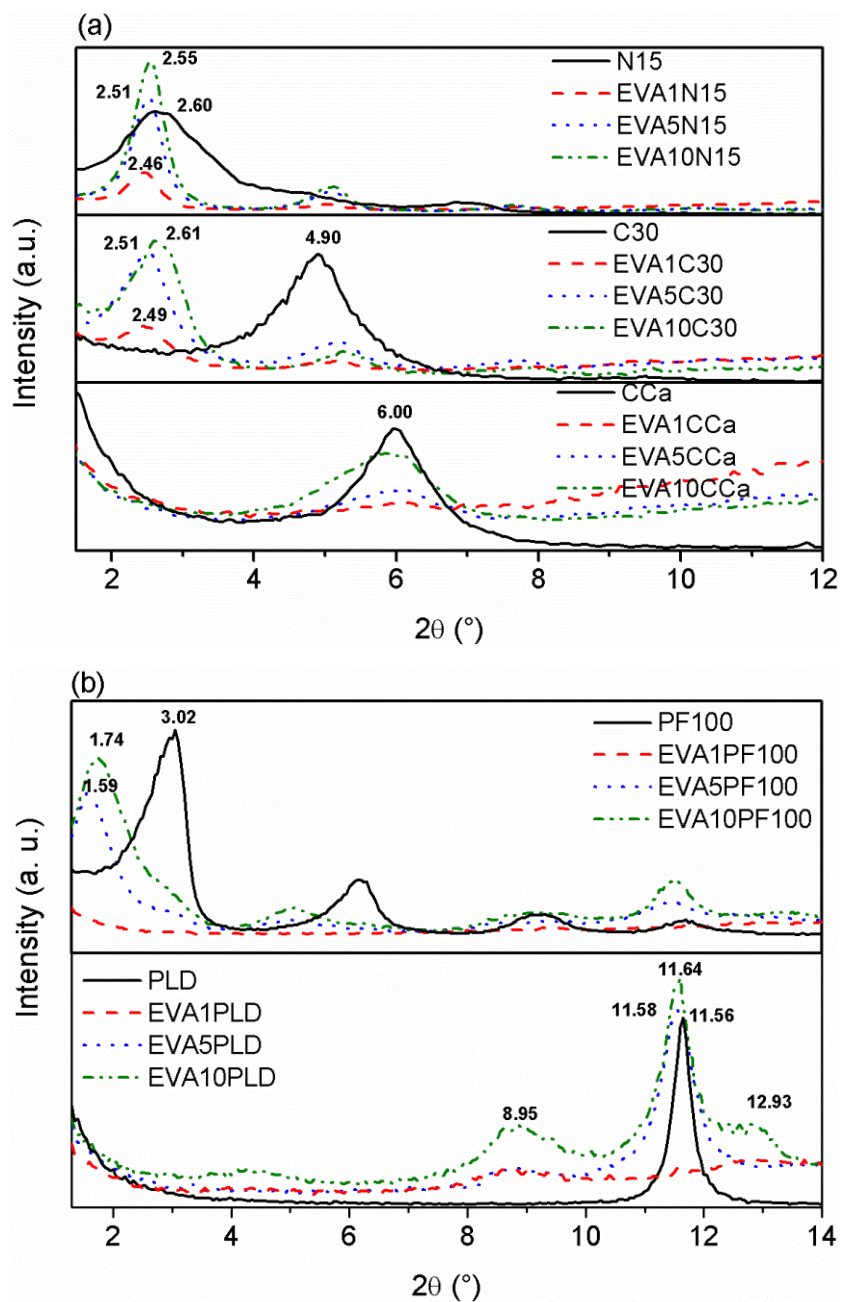The scans of the nanoclays are also reported as references.

Fig. 5.13 XRD patterns of rubber compounds filled with (a) MMT clays, (b) LDH clays.

Looking at Figure 5.13 (a) can be observed that the low interlayer distance of CCa clay does not permit an accommodation of the polymeric chains into the gallery spaces. In fact, a broad band around the 2θ angle of the clay is visible and it becomes more intense increasing the filler content.

With the loading of Cloisite 30B a different result is obtained instead of using the Cloisite Ca^{2+}. A condition of intercalation is achieved: the original peak of the pure nanoclay disappears and new peaks are observed at lower 2θ angles. The highest interlayer spacing shift is displayed for the EVA1C30 sample, in fact it changes from 1.8 nm to about 3.6 nm, while a small reduction in the gallery space is obtained increasing the filler content.

The compounds loaded with Nanofil 15 also show an increase in the distance between the layers, however the Δd (d-spacing $_{composite}$-d-spacing $_{filler}$) are smaller than those obtained for EVA/C30 samples.

The presence of the (002) reflections in the XRD pattern of both O-MMTs indicates an incomplete randomization of the platelets during the mixing [10]. However, the poor broadening of the (001) diffraction peak in the sample-filled with N15 suggests that a lower degree of platelet disorder is achieved than in the sample-filled with C30.

The different behaviour between C30 and N15 can be explained by the interplay of entropic and enthalpic factors that happen during the polymer melt intercalation [11] and by the unlike affinity that C30 and N15 shows for the EVA matrix. As reported by Vaia et al. [11], during mixing, the entropy decrease associated with polymer confinement between the silicate layers is compensated by the increased conformational freedom of the tethered ammonium cations as the layers separate. However, the total entropy change is generally small and the intercalation process depends on the total enthalpy. The latter is strictly related to the interaction that the polymeric chains develop with the ammonium cations and with the silicate layers. For organo-modified silicates, the enthalpy can play a favourable role maximizing the polymer-silicate interactions or minimizing the ones between the polymer and the surfactant. These concepts can help to explain the XRD results of EVA/clay compounds. The biggest initial interlayer distance of Nanofil 15 allows an easy intercalation of EVA chains [12]. However, the higher hydrophobic nature of the ammonium cations into the layers leads to weak interaction between the matrix and silicate. Consequently, an enhancement in the degree of intercalation is difficult to achieve [13].

On the other hand, the surfactant in the Cloisite 30B contains two hydroxyethyl groups which probably originate strong polar interaction with the carboxyl groups belonging to

EVA. These interactions drive the significant intercalation and probably exfoliation which has been observed in the XRD data [13].

In the diffractogram of the sample EVA1PLD (Figure 5.13 (b)) any peak is visible around the 2θ angle of the pure clay but a broad band appears close to 2θ = 8.76°. This result permits to affirm that the nanoclay is intercalated.

The sample EVA1PF100 (Figure 5.13 (b)) seems to be an exfoliated composite in fact any peak is present in the scan. However, increasing the amount of the clay an intercalation condition is achieved and the intercalation of the PF100 becomes more difficult with the rising of the nanoclay amount. In addition, the samples EVA5PF100 and EVA10PF100 show a broad band around 2θ = 11.5° which could be due to a deintercalation phenomenon (see the peak of PLD clay). However in the scan of the pure PF100 a band appears in this region and it could be due to unmodified powder.

Mechanical properties

The tensile properties of EVA70 and EVA/clay vulcanizates are plotted in Figure 5.14.
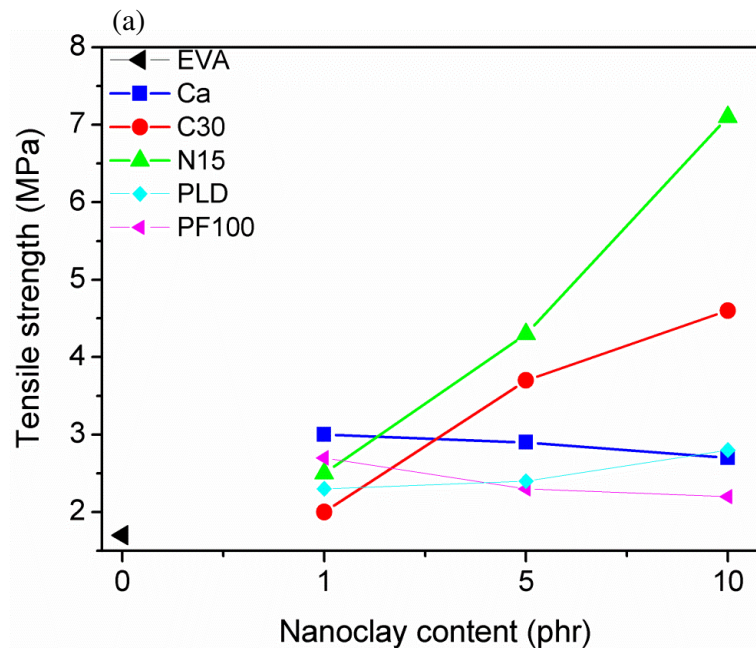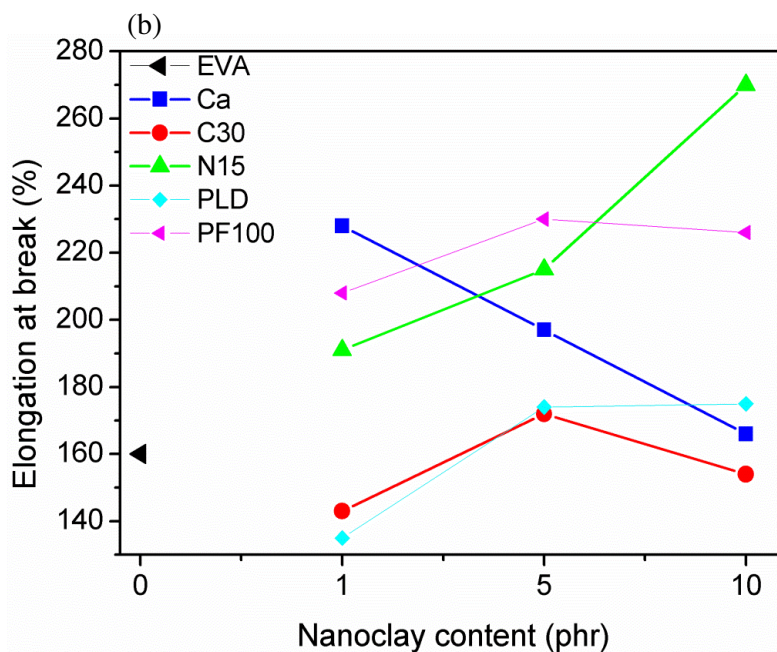
Fig. 5.14 Tensile strength (a) and elongation at break (b) of rubber compounds.

The tensile strength (Figure 5.14 (a)) shows an increment in all the samples containing 1 phr nanoclay in respect to pure vulcanized EVA.

A different behaviour is shown by the EVA filled with pristine MMT and with organo-MMTs when the nanoclay content is raised to 5 and 10 phr. In fact, the tensile strength values decrease by using Cloisite Ca^{2+} while an increase is observed by adding the other two nanoclays. These results corroborate X-ray diffraction analysis..

LDH clays show a poor effect on tensile strength, in particular no significant changes are observed increasing the clay amount.

The strength depends on the dispersion of clays in the elastomeric matrix and on the intensity of the interactions between the fillers and the rubber chains. Observing XRD results and mechanical characterization it is possible to presume poor interaction between LDH clays and EVA matrix and platelets agglomeration presence.

More complex is the effect of nanoclays on the elongation at break (Figure 5.14 (b)). An increased value is observed for EVA1CCa sample while the higher amounts of this filler induce a reduction in the data. EVA/C30 vulcanizates show an increasing-decreasing trend. The lowering of the elongation at break values indicates the increase of the EVA matrix stiffness with the clay addition.

The samples loaded with Nanofil 15 display an enhancement of elongation at break values with increasing filler content. Tensile strength improvement, related to a rising in the elongation at break, is a rather unexpected phenomenon for rubber/organoclay nanocomposites. Nevertheless, it was observed in other rubber compounds and it was explained by a synergistic effect of platelet orientation and chain slippage [14].

PLD clay shows an increasing trend for the elongationt break. However the values found are lower than the ones obtained for the PF100-filled samples. This result indicates that the PLD has a stronger effect in the matrix stiffness increase in respect to the organo-modified LDH clay. The different behaviour is probably due to the higher content of surfactant in the PF100.

Thermogravimetric analysis

The thermal degradation of ethylene vinyl acetate takes place in two steps (Figure 5.15).

In the first, between 300 and 400°C the loss of acetic acid (deacetylation) with the formation of carbon-carbon double bonds in the chain backbone occurs. The second degradation step, between 400 and 500°C, involves the oxidation and the volatilization of the remaining partially unsaturated polyethylene polymer. Figure 5.15 shows that the vulcanization of the rubber provokes an improvement in the material thermal stability, increasing the both degradation temperatures of about 5 °. This is due to the crosslinking formation between rubber chains.
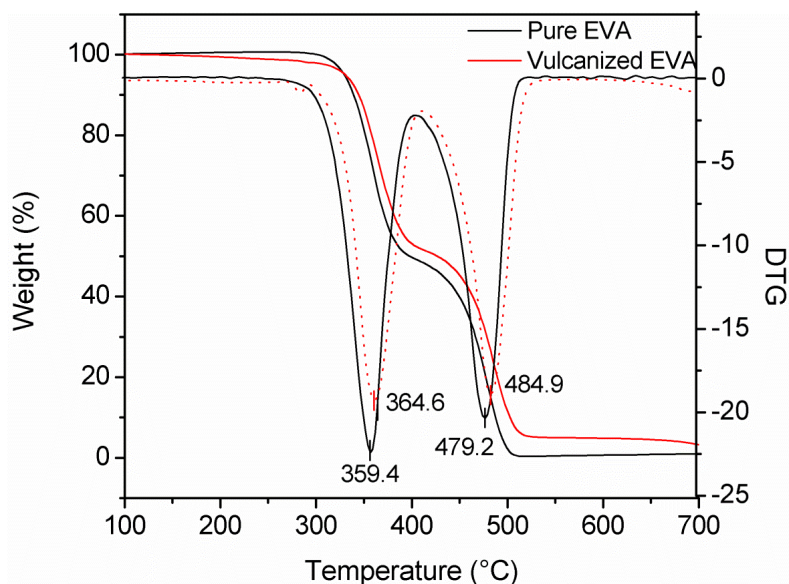

Fig. 5. 15 Mass loss and derivative mass loss of unvulcanized and vulcanized EVA70 under N_2.

Thermogravimetric analysis was carried out to study how the degradation behaviour of EVA changes adding the fillers, since it is well-know that clays affect the thermal stability of polymeric materials. The results are displayed in Table 5.5.

No great variations are observed on the first step of degradation when the clays are incorporated in EVA. However, in some formulations the loss of acetic acid is accelerated as a function of clay loading, possibly due to the catalytic effect of the acidic sites of the clay and of the thermal decomposition of the organo-modifier [2].

The second degradation step takes place at a higher temperature with respect to EVA without clay loading. However, no significant difference is observed for the three different amounts of CCa while the degradation temperature increases with the rise of organo-clay content.

In particular, a significant enhancement on the thermal stability is achieved for the EVA10C30B sample, whose second peak decomposition temperature shows an increase of 9.4°C . This result is probably due to the greater compatibility shown by Cloisite 30 rather than by Nanofil 15 for EVA matrix.

Also the addition of LDH clays accelerates the deacetylation process. The second step degradation temperature increases with 10 phr of the clays, the lower filler content do not provoke significant differences in respect to vulcanized EVA.

Table 5.5 Thermogravimetric data for the vulcanizates.

Sample	$T_{50\%}$ (°C)[a]	T_{Max1} (°C)[b]	T_{Max2} (°C)[b]
EVA70	425	364.6	484.9
EVA1CCa	422.9	361.7	487.5
EVA5CCa	440.6	363.4	487.3
EVA10CCa	444.8	362.5	488.9
EVA1C30	428.9	364.0	486.2
EVA5C30	434.0	363.4	490.5
EVA10C30	438.2	362.6	494.3
EVA1N15	433.5	364.0	485.5
EVA5N15	433.2	364.0	489.4
EVA10N15	438.2	362.4	490.2
EVA1PLD	432.4	359.4	484.3
EVA5PLD	437.8	361.5	483.9
EVA10 PLD	449.0	365.0	489.6
EVA1PF100	427.9	360.4	483.6
EVA5 PF100	430.3	359.3	483.9
EVA10 PF100	431.0	359.7	487.4

[a] $T_{50\%}$, temperature at which 50% of weight loss occurs

[b] T_{Max}, temperature at which the TGA curves shows the maximum slope.

Regarding previous results, EVA rubber compound was prepared replacing Nanofil 15 with Cloisite 30.

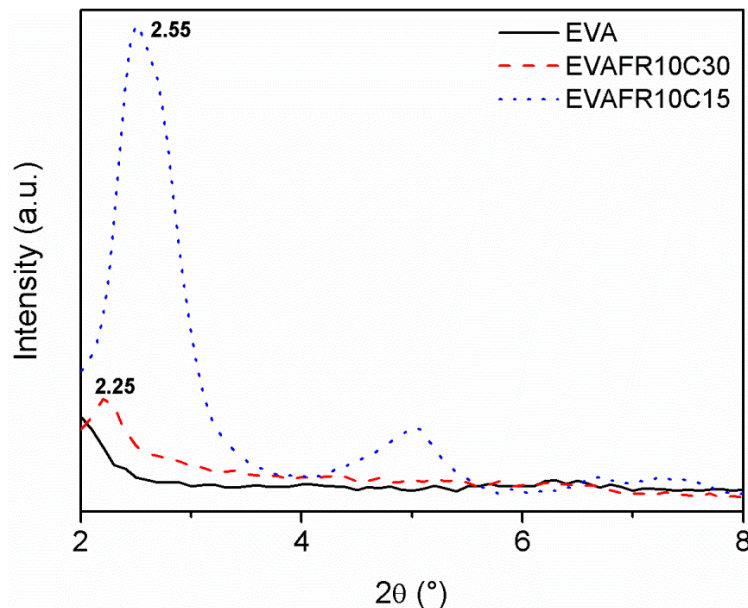First of all, a morphological analysis was carried out (Figure 5.16).

Fig. 5.16 XRD patterns of rubber compounds.

A higher intercalation condition is observed for the C30-filled sample, confirming the stronger compatibility of this clay compared to N15 for EVA rubber, probably due to the presence of two hydroxyethyl polar groups. In addition the higher intensity of N15-loaded sample and the presence of second order reflections suggest that while the N15 platelets carry out a well-ordered disposition, the C30 ones achieve a randomization.

Another method to evaluate the compatibility between a rubber matrix and a nanoclays is the curing characterization of the sample carried out by using a moving die rheometer. The results obtained are summarized in Table 5.6. The increase in the minimum torque (M_L) after the addition of the fire retardant additives indicates a worsening in the processability of the compound. This phenomenon is due to a change in the viscosity of the compound.

The values in Table 5.6 corroborate the results obtained with XRD analysis. In fact it is well-known that the maximum torque and the torque value depend on the extent of crosslinking created and on the reinforcement induced by the filler particles. A significant increase is observed in these two parameters after the addition of the fire retardant fillers.

Furthermore, higher values are obtained by using Cloisite 30B clay. This result probably means that a more crosslinked rubber compound is realized in the presence of Cloisite 30B. Therefore, a better interaction between the elastomeric matrix and the C30 is expected in respect to Nanofil 15.

Table 5.6 Minimum torque, maximum torque and delta torque of rubber compounds.

Sample	M_L (dNm)	M_H (dNm)	ΔM (dNm)
EVA	0.27	10.09	9.82
EVAFR10N15	0.70	17.83	17.13
EVAFR10C30	1.82	22.10	20.28

Fire resistant properties of the compound EVAFR10C30 were characterized by using cone calorimeter.

Figure 5.17 shows HRR curves of the sample EVAFR10C30 but also the ones of EVA and EVAFR10N15 are displayed as references.

The compound loaded with the nanoclay Cloisite 30B shows an increase in the TTI of about 9 seconds in respect to the EVA sample, as for the sample EVAFR10N15.
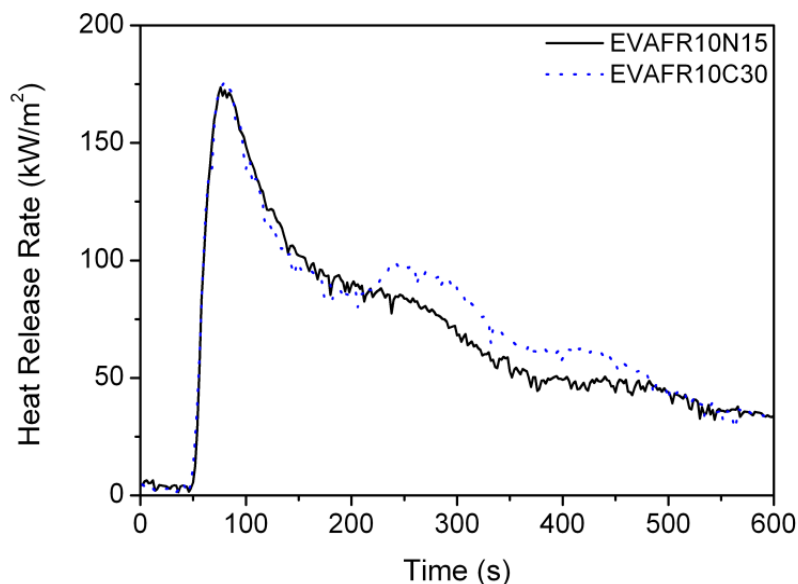

Fig. 5.17 HRR curve of the EVA-based fire retardant formulations.

Fire retardant additive-filled samples display a sharp peak but also two shoulders are evident for time higher than 200 seconds. The latter are probably related to the release of the volatiles trapped in the foamed structure formed during combustion [15]. The lower intensity of these shoulders in EVAFR10N15 is probably due to a more gradual release of the heat and the volatiles produced during combustion.

Table 5.7 summarizes some parameters obtained with cone calorimeter test and the LOI test result. While cone calorimeter does not show significant differences between the compound containing Nanofil 15 and the one filled with Cloisite 30B, LOI test displays interesting results. In fact using Cloisite 30B instead of Nanofil 15 in the EVA compound the LOI value increase to 32.4 from 30.6. This result highlights an improvement in the flame retardancy of the material.

Table 5.7 Measured parameters in the cone calorimeter test.

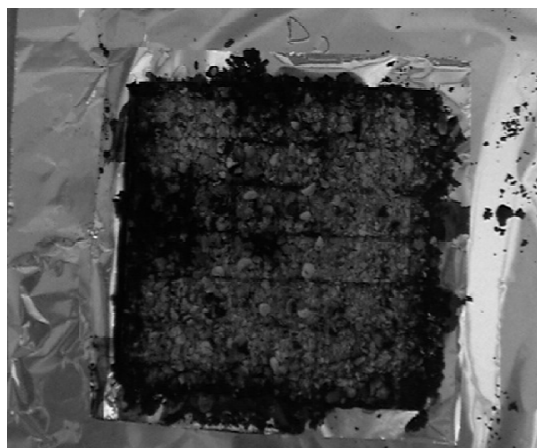| *Sample*	*TTI* *(s)*	*TTP* *(s)*	*pHRR* *(kW/m^2)*	*TSR* *(m^2/m^2)*	*SEA* *(m^2/kg)*	*LOI*
EVAFR10C30	58.5	79	177.48	289.55	155.315	32.4

Fig. 5.18 Cone calorimeter residues for EVAFR10C30.

Figure 5.18 shows the residue of the sample EVAFR10C30 after cone calorimeter test. Another sample containing 20 phr of Nanofil 15 was compounded. Table 5.7 demonstrates that no significant differences in combustion behaviour were found by using cone calorimeter. On the contrary the increase in the nanoclay content improves the flame

retardancy. However, the LOI value determined is very similar to the one obtained for the C30-filled sample which contains less nanoclays.

This result is a further demonstration of the higher compatibility between C30 and the rubber matrix. When nanoclays platelets are stronger intercalated or totally exfoliated the interfacial area increases enormously. This permits to obtain a great improvement in physical and mechanical properties of a compound using small clay amounts.

Mechanical characterization is necessary to define if the rubber compounds respect the minimum requirements indicates in the material standard specifications. The latter, in fact, dictate the tests to be made and lay down the allowable limits of the property data.

It is obvious that the reinforcing fillers acting in all the compounds studied are silica and carbon black. The addition of the fire retardant additives provokes a reduction in the tensile strength and an increase in the elongation at break with a different extent. The most effect in the tensile properties is attributed to ATH, which is added with an amount higher than 50 phr (Figures 5.20 (a) and (b)).
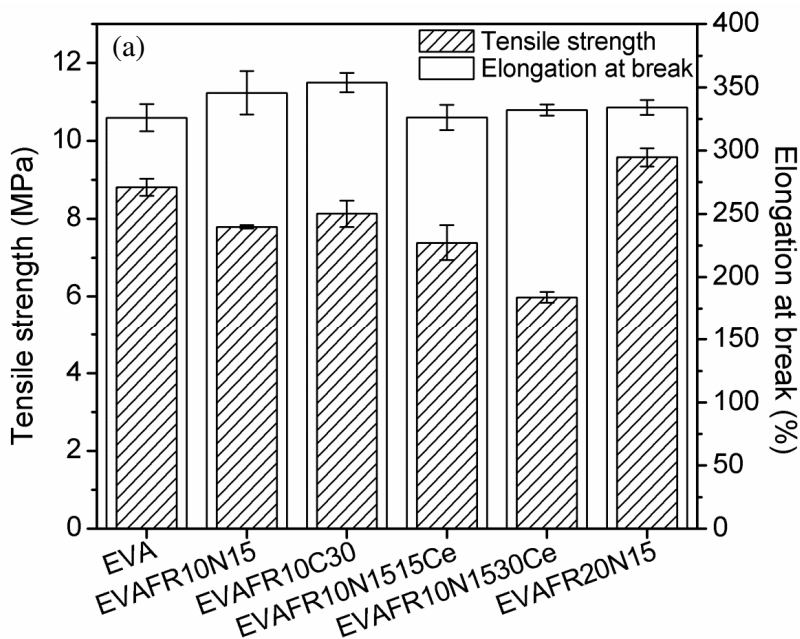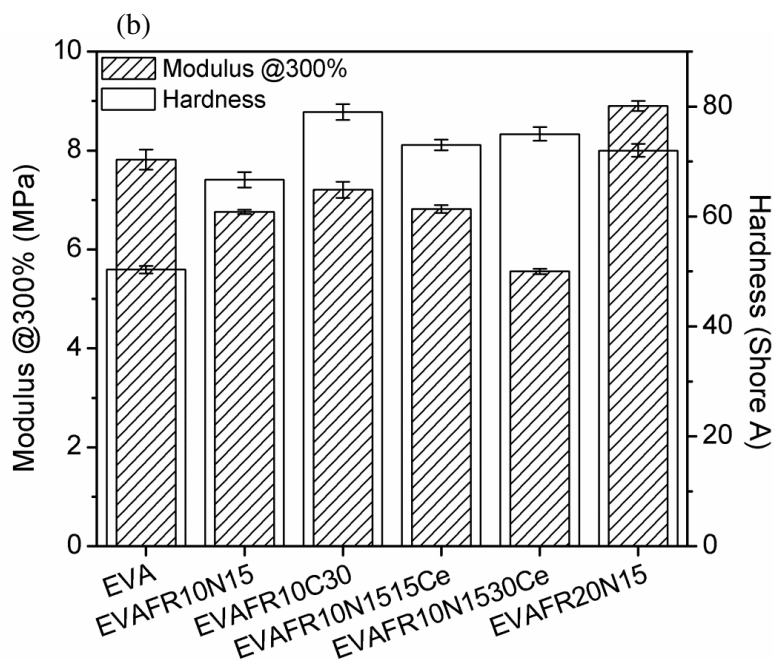
Fig. 5. 19 (a) Tensile strength and elongation at break, (b) modulus @300% and hardness of rubber compounds.

Very interesting are the results obtained with the addition of the nanoclays. In particular, the tensile performance corroborates the results obtained with the other characterizations. In fact, the sample EVAFR10C30 shows higher tensile strength, modulus at 300% and elongation at break. This result is probably to the higher affinity between rubber matrix and nanoclay which results in a better dispersion of the platelets. However, it is possible to observe the action as reinforcing filler of the N15 when the clay content is double. A significant increase is obtained in the tensile strength and in the modulus at 300%.

The further addition of Ceepree in the sample EVAFR10N15 causes a detrimental of the mechanical performance. This additive seems to stiff strongly the compound, in fact the elongation at break is reduced while the hardness increases.

References

[1] F. Carpentier, S. Bourbigot, M. Le Bras, R. Delobel and M. Foulon, *Polym. Degrad. Stab.*, **69**, 83 (2000).

[2] F. Laoutid, L. Bonnaud, M. Alexendre, J.M. Lopez-Cuesta and P. Dubois, *Mater. Sci. Eng., R*, **63**, 100 (2009).

[3] T.R. Hull and B. K. Kandola, *Fire Retardancy of Polymers: New Strategies and Mechanisms*, Royal Society of Chemistry (2009).

[4] S. Bourbigot, M. Le Bras, R. Leeuwendal, K.K. Shen and D. Schubert, *Polym. Degrad. Stab.*, **64**, 419 (1999).

[5] M. Bugajny, S. Bourbigot, M. Le Bras and R. Delobel, *Polym. Int.*, **48**, 264 (1999).

[6] M Zanetti, T. Kashiwagi, L. Falqui and G. Camino, *Chem. Mater.*, **14**, 881 (2002).

[7] M. Le Bras, S. Bourbigot and B. Revel, *J. Mater. Sci.*, **34**, 5777 (1999).

[8] A. Riva, G. Camino, L. Fomperie and P. Amigouët, *Polym. Degrad. Stab.*, **82**, 341 (2003).

[9] G.M. Wu, B. Schartel, M. Kleemeier and A. Hartwing, *Polym. Eng. Sci.* (2011).

[10] D.S. Chaudhary, R. Prasad, R.K. Gupta and S.N. Bhattacharya, *Thermoc. Acta*, **433**, 187 (2005).

[11] R.A. Vaia and E.P. Giannelis, *Macromolecules,* **30**, 7990 (1997).

[12] C.H. Jeon, S.H. Ryu and Y.W. Chang, *Polym. Int.*, **52**, 153 (2003).

[13] X. Li and C.S. Ha, *J. Appl. Polym. Sci.*, **87**, 1901 (2003).

[14] Y.P. Wu, Y. Ma, Y.Q. Wang and L.Q. Zhang, *Macromol. Mater. Eng.*, **289**, 890 (2004).

[15] L. Haurie, A. Fernandez, J. Velasco, J. Chimenos, J. Lopezcuesta and F. Espiell, *Polym. Degrad. Stab.*, **94**, 1082 (2007).

Chapter 6

Nanoclays vs. conventional fillers in natural rubber/ polybutadiene compounds

6.1 Introduction

In recent years, natural rubber and polybutadiene rubber/clay nanocomposites, prepared by melt blending, have been subject of research. The attention of the authors has been often focalized on the mechanical properties of the compound.

Varghese et al. studied composites based on natural rubber, containing organophilic and pristine layered silicates of natural and synthetic origin. The property improvements due to the fillers were ranked as follows: organophilic clays > pristine synthetic layered silicate > pristine natural clay. This behaviour was attributed to partial intercalation of the organophilic clay by NR on the basis of XRD and TEM results and to the high aspect ratio of the fluorohectorite. Therefore, the addition of organoclays resulted in better mechanical performance [1].

The effect of organoclays with different modifier concentration on the vulcanization behaviour and mechanical properties of BR compound was investigated by Kim et al [2].

A remarkable increase of the mechanical properties was observed for the BR/O-MMT hybrids compared with BR/pristine MMT compound. In addition, the rebound resilience and abrasion resistance is also improved remarkably.

The nanoclays are nowadays considered as new "white" fillers which can replace the conventional fillers for rubbers: carbon black and silica. Consequently, in a great number of articles the mechanical properties of NR filled with nanoclays were compared to those of compounds containing carbon black or silica.

Natural rubber was compounded with organo-modified montmorillonite by Teh et al. [3]. For comparison purposes, rubber compounds containing carbon black and precipitated silica were also prepared. The results showed that the improvement of tensile strength, elongation at break (Figure 6.1) for OMMT/rubber compound were significantly higher compared with carbon black and silica filled vulcanizates.

The better reinforcement efficiency of organoclay was attributed to the strong interaction between organoclay and NR. The smaller particle size provided a larger surface area for the interaction between the filler and rubber matrix.
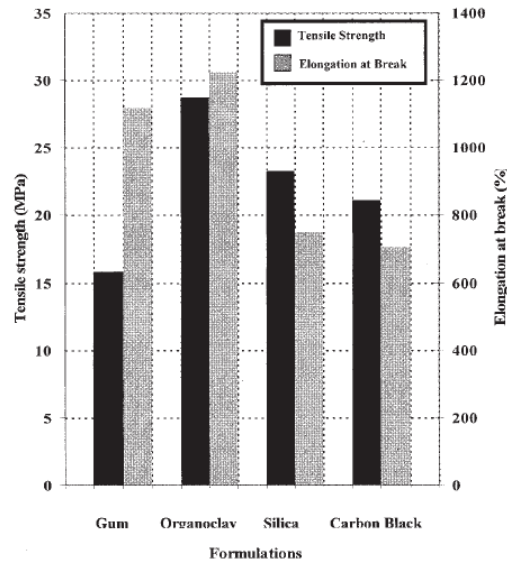

Fig. 6.1 Tensile strength and elongation at break of NR gum, organoclay, silica, and carbon black filled vulcanizates [3].

Carli et al. [4] prepared and analysed different natural rubber nanocomposites varying the content of organoclay Cloisite C15 (2, 4, 8 phr). For comparative purposes, a sample with 50 phr of silica was also studied. The RCNs showed a general increase in mechanical properties when increasing the OC content (Figure 6.2).
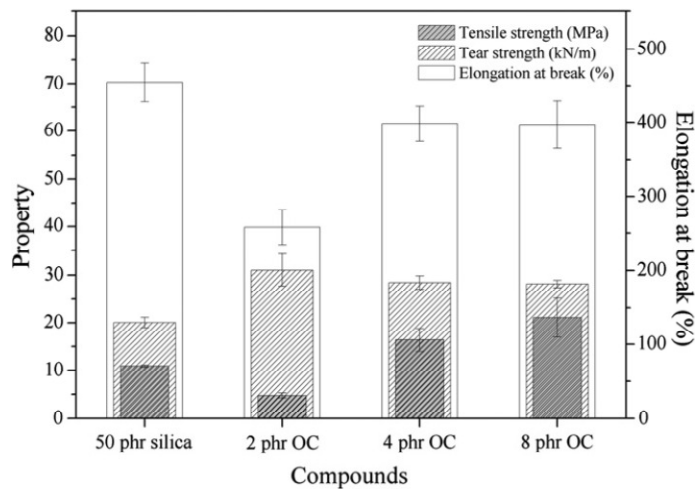

Fig. 6.2 Mechanical properties of the natural rubber compounds [4].

This results was explained with a strong interaction between the clay interface and the elastomeric matrix. In particular, it was supposed that the side surface of the layers can bond to the rubber chains in two dimensions, giving the composites better tensile performance and slowing failure during deformation [5].

Despite the increasing interest on natural rubber and polybutadiene rubber filled with nanoclays, the reports on NR/BR blend nanocomposites are not so many. As this reason, we focalized our attention on this argument.

6.2 NRBR/nanoclay compounds: preliminary tests

Natural rubber/polybutadiene rubber blends filled with 3 phr of different kinds of nanoclays were compounded by using a laboratory size open two roll mixing mill.

Table 6.1 summarizes the compounds produced.

Table 6.1 Rubber compounds tested.

Sample
NRBR
NRBR3CCa
NRBR3C30
NRBR3C15
NRBR3PLD
NRBR3PF100

6.2.1 Curing characteristics

First of all cure characterization of the unvulcanized compounds were carried out by using a moving die rheometer, which measures the torque variation as a function of time at a fixed temperature.

Table 6. 2 Minimum torque, maximum torque and delta torque of rubber compounds.

Sample	M_L (dNm)	M_H (dNm)	ΔM (dNm)
NRBR	0.29	5.83	5.54
NRBR3CCa	0.31	4.45	4.14
NRBR3C30	0.40	6.65	6.25
NRBR3C15A	0.43	8.35	7.92
NRBR3PLD	0.58	4.32	3.74
NRBR3PF100	0.47	4.48	4.01

The maximum and minimum values of the torque, M_H and M_L, respectively and the delta torque ΔM ($\Delta M = M_H\text{-}M_L$), deduced from this measure, are listed in Table 6.2.

It is possible to observe an increase in the M_L value for all the rubber/clay compounds. Since this parameter is often correlated to the Mooney viscosity of the compound, its rising indicates a worsening in the processability of the rubber mix.

The maximum torque and the delta torque ($\Delta M = M_H\text{-}M_L$) depend on the extent of crosslinking between the rubber chains and on the reinforcement induced by the filler particles.

A decrease in the M_H and ΔM values is observed for the rubber compounds with CCa, PLD and PF100 clays. This result suggests a poor interaction at the filler-matrix interphase probably due to a limited affinity between the rubber and the clays. A conventional composite at the microscale level is probably obtained using these nanofillers.

On the other hand, the compounds with the organo-montmorillonites show higher torque values with respect to the pure NR/BR blend. Regarding these results, it can suppose that the final compound becomes more crosslinked in the presence of Cloisite 30B and Closite 15A, probably for a better interaction between these last two clays and the elastomeric matrix.

The optimum cure time t_{90} and cure rate index CRI, determined by the rheometric curves, are summarized in Table 6.3.

Table 6.3 Optimum cure time and cure rate index of rubber compounds.

Sample	t_{90} (min)	CRI (min^{-1})
NRBR	1.31	217
NRBR3CCa	2.12	161
NRBR3C30	1.23	232
NRBR3C15	0.93	256
NRBR3PLD	1.13	454
NRBR3PF100	1.38	303

A decrease in t_{90} and CRI is observed by using the Cloisite Ca^{2+}. This result does not surprise because it is well-known that pristine montmorillonite can absorbs the curatives

inducing its partial inactivation. This effect obviously leads to slow curing process resulting in a higher optimum cure time (given by t_{90}) in the filled compounds [6].

On the contrary, the OMMTs seem to behave as a accelerant agents for the elastomeric matrix curing, in fact the cure times are reduced. To explain this phenomenon previous literature has suggested the formation of a zinc-containing intermediate complex, in which sulphur and ammonium modifiers of MMTs participate, having catalytic activity on the rubber vulcanization reaction [7]. If this assumption is true, the large torque difference and the faster vulcanization rate of NRBR3C15 than NRBR3C30 are probably due to higher modifier concentration, 125 mequiv/100g and 90 mequiv/100g respectively.

The rubber compounds with Perkalite LD and Perkalite F100 show very high values of CRI. To explain this particular behaviour, it can suppose that a catalytic effect in the curing process is played also by the anion clays.

As reported elsewhere [8], the -OH groups, placed in the layer surface of LDH, enter in a kind of ''coordination complex'' with the zinc ions, such complex could be responsible for the observed acceleration of the curing process. In fact, in organo-modified clay PF100, where the presence of the anion makes the –OH groups less available to enter into the ''coordination complex'', the acceleration process is less pronounced.

6.2.2 DSC analysis

The vulcanization process can be also studied by differential scanning calorimetry (DSC). Carrying out a DSC measure from 0°C to about 200°C, an exothermic peak is visible in the thermogram (Figure 6.3). This peak is due to the occurring of the curing reaction. DSC analysis corroborates the results obtained by moving die rheometer, showing that the vulcanization temperatures depending on the nanoclay used in the rubber compound. In particular, while the vulcanization of the NRBR3CCa sample takes place at the highest temperature, the others compounds show a lower vulcanization temperature in respect to the pure NRBR blend. This result confirms what has been claimed previously.

It is very interesting to note that the organic modifiers of the clays bring opposite effects on the vulcanization process: while the cationic surfactant in MMT accelerates the curing reaction, the anionic one in LDH slows it down.
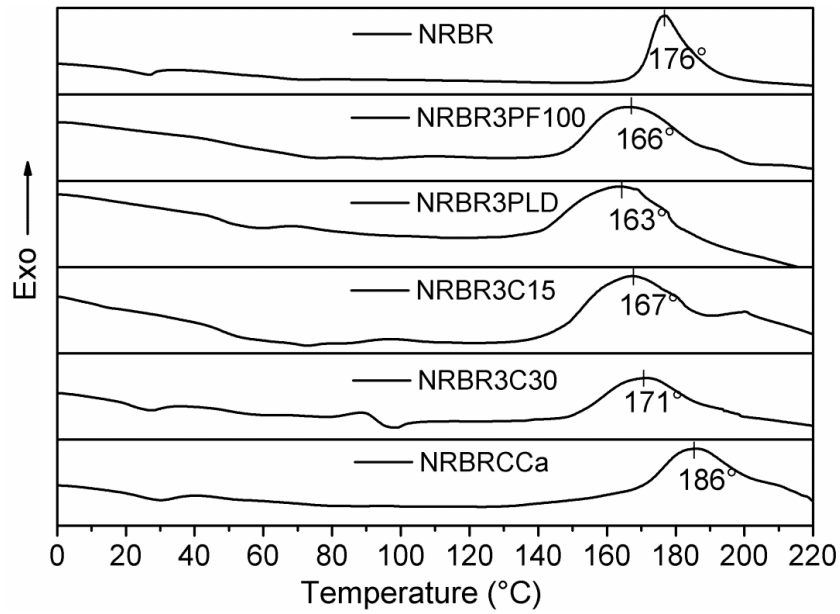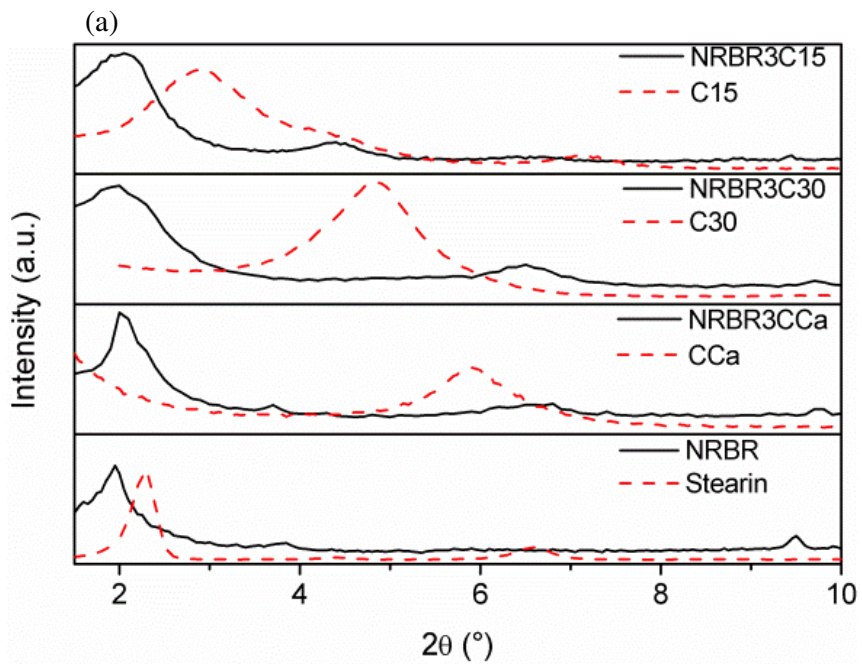
Fig. 6.3 DSC thermograms of uncured rubber compounds.

6.2.3 XRD analysis

XRD spectra of the compounds are shown in Figure 6.4. The curve of unfilled NRBR blend and stearin are also reported as references.
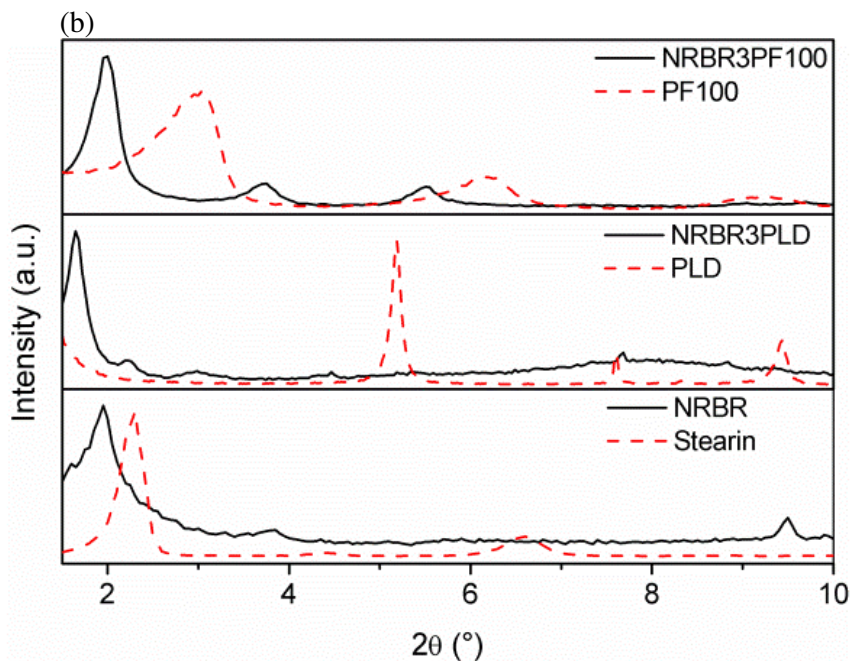
Fig. 6.4 XRD patterns of NRBR blends filled with (a) MMT clays, (b) LDH clays.

The analysis of the spectra resulted complex because of the presence of the diffraction peaks of the stearin. These appeared in the same 2θ range of (001) and (003) reflections of the nanoclays. Consequently, the diffraction peaks are probably a combination of the two peaks. However, all the clays are probably intercalated, in fact the reflections of the pure clays are not visible. In addition some fillers, such as C15 and PF100, show clearly the higher reflection orders, indicating an order disposition of the platelets in the matrix.

Despite all the clays seem to achieve a good intercalation condition, the other characterizations will evidence significant differences in the final properties of the compounds

6.2.4 Mechanical properties

The tensile strengths obtained for the rubber/clay compounds (Figure 6.5 (a)) appear significantly dependent to the nanoclay used. In fact, the tensile strength of CCa, PLD and PF100 filled compounds decreases with respect to the pure NR/BR blend while it increases when the organo-montmorillonites are added. The effect of filler loading in a rubber compound is strictly related to the dispersion degree achieved by the clay.

While the tensile strength is not always improved depending on the nanoclay used, the elongation at break of all the samples undergoes a decrease (Figure 6.5 (a)). Lower elongation at break values with higher modulus at 300% and hardness indicate an increase in the stiffness of the elastomeric matrix (Figure 6.5 (b)).
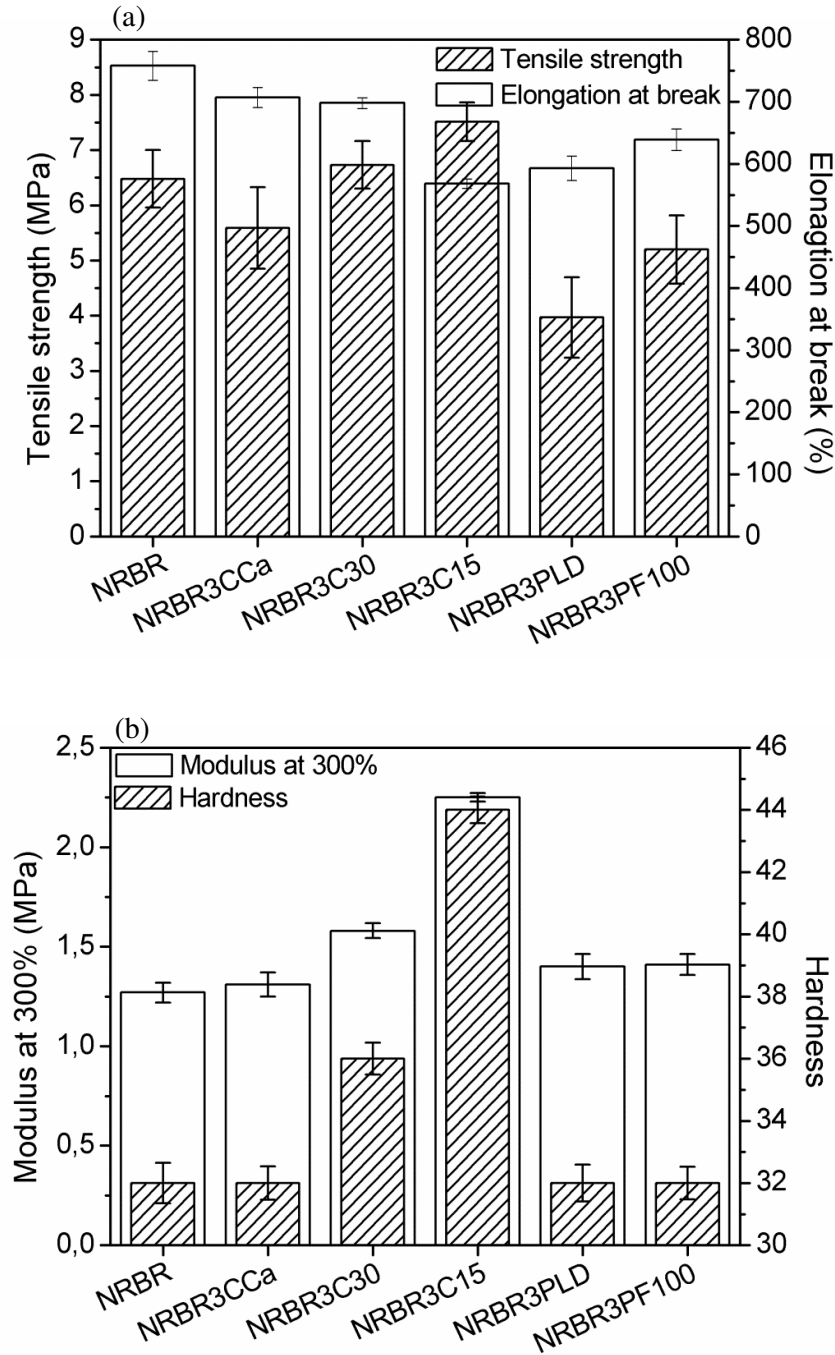

Fig. 6.5 (a) Tensile strength and elongation at break (b) modulus at 300% and hardness of rubber compounds.

6.2.5 Abrasion resistance and rebound resilience

Abrasion resistance is defined as the resistance of a rubber compound to wearing by contact with a moving abrasive surface, and is dependent on the resistance of rubber to fracture and tearing. An higher abrasion resistance corresponds to a poor volume loss. An improved abrasion resistance is obtained adding to NRBR blend the organo-modified montmorillonites (Figure 6.6). On the contrary, with the pristine MMT and LDHs the volume loss is higher in respect to the pure NRBR blend (Figure 6.6). In addition, the unfilled NRBR blend and the NRBR compound filled with CCa, PLD and PF100 show very high error bars. This is a sign of a not homogeneous dispersion of the clays in the rubbery matrix.

It was reported [9] that crosslink density, hardness, modulus, and friction coefficient of the vulcanizate are important factors controlling the abrasion resistance. To be more precise the enhancement of the abrasion resistance is obtained when crosslinking density, hardness and modulus are high, and the friction coefficient is low. These parameters are also strictly related to the dispersion degree of the clay in the elastomeric matrix [10].
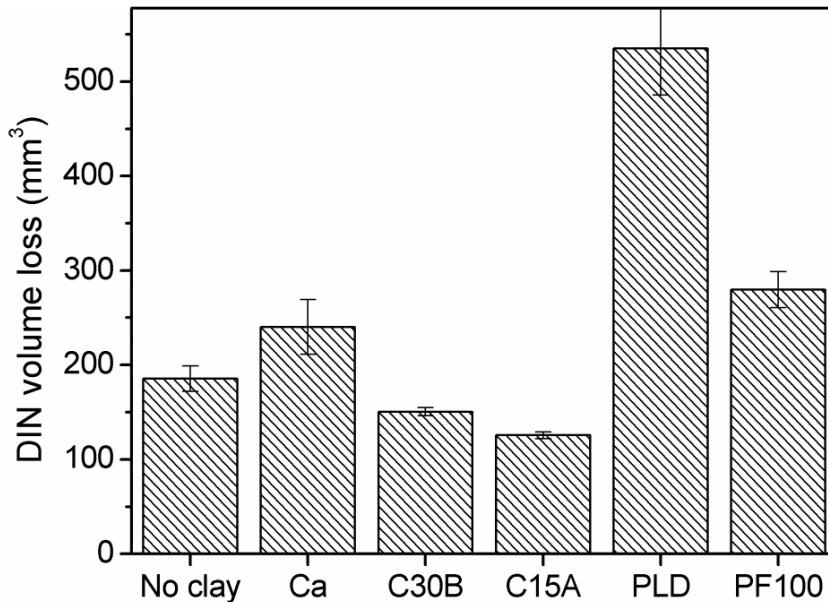

Fig. 6.6 Abrasion resistance of the rubber compounds.

Abraded surfaces of the samples were examined with optical microscope (Figure 6.7). Greater roughness of the surfaces corresponds to poor abrasion resistance. Organo-montmonillonite blends show an abraded surface less rough than those of the others compounds.
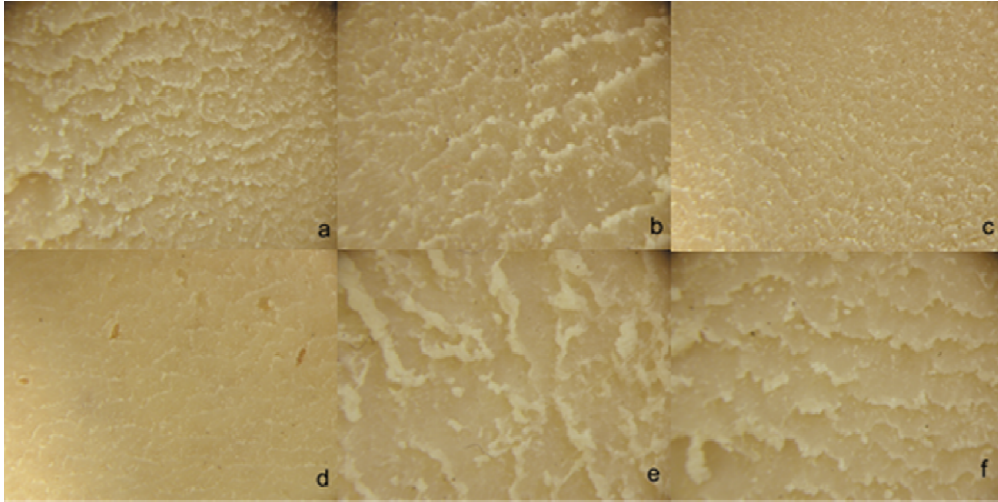

Fig. 6.7 Optical images of abraded surface of (a) NRBR, (b) NRBR3CCa, (c) NRBR3C30, (d) NRBR3C15, (d) NRBR3PLD (e) NRBR3PF100 compounds.

The rebound resilience can be considered a measure of the ability of the material to recover quickly its original shape after a temporary deformation.
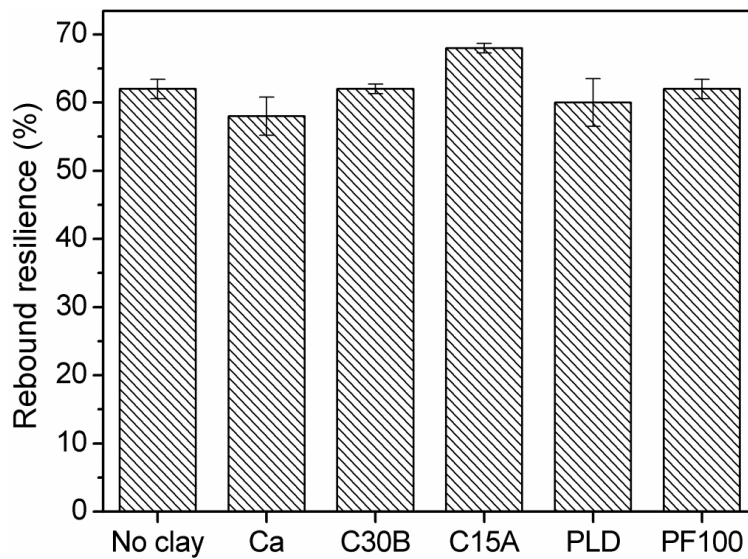

Fig. 6.8 Rebound resilience of the rubber compounds.

It is important to note that the elastic characteristics of the elastomeric matrix are increased in presence of Cloisite 15A while are maintained similar or worsened with the other clays (Figure 6.8).

Concerning the results in tensile properties, abrasion resistance and rebound resilience it is possible to conclude that the organo-MMT Cloisite 15A has the better distribution in the NR/BR blend. This is probably related to the strong hydrophobic character of the clay that permits a high compatibility with the apolar NR/BR matrix.

6.2.6 Swelling properties

The degree of swelling and the crosslink density of the compounds are listed in Table 6.4 The swelling percentage is the measurement of the degree of cross-linking, reduction in swelling indicates increase in cross-link density. The experimental results demonstrate that the cross-link densities are strongly increased with the addition of the organo-montmorillonites, indicating the good compatibility between the clays and the matrix. On the contrary, the unmodified clays show a cross-linking density similar to the pure NR/BR blend. Poor dispersion of the clays in the blend and agglomerate presence are supposed. The crosslink density of the samples is in agreement with the tensile modulus trend.

Table 6.4 Degree of swelling and crosslink density of the rubber compounds.

Sample	Q (%)	$V_e \times 10^{19}$ (m^{-3})
NRBR	444	1.94
NRBR3CCa	403	2.15
NRBR3C30	358	2.74
NRBR3C15	304	3.62
NRBR3PLD	438	1.94
NRBR3PF100	382	2.53

6.2.7 TGA analysis

The thermal degradation of NR/BR blend takes place in two steps (Figure 6.9). First, the decomposition of the NR matrix occurs between 280°C and 410°C. The second step is attributed to the BR phase degradation and it is observed in the range 410-520°C.
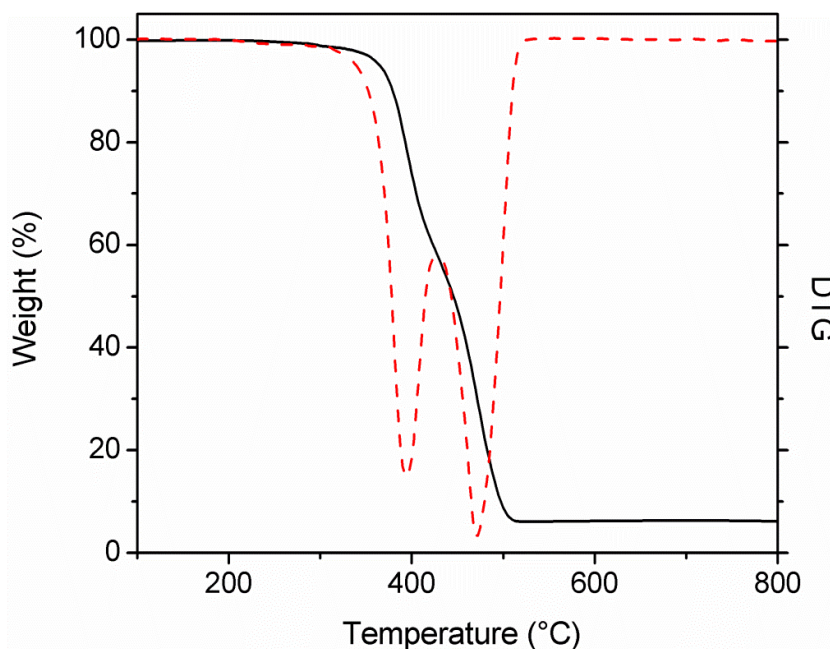
Fig. 6.9 TGA curve of pure NRBR blend.

The addition of clays lowers the temperature of the first decomposition peak, probably owing to a poor dispersion of the fillers in the NR phase (Table 6.9).

Only O-MMTs increase the temperature of the second thermal degradation. The improvement is equal to 4.4°C and 5.2°C for Cloisite 30B and Cloisite 15A, respectively. This result is in agreement with a good compatibility of these nanoclays with the BR matrix. It was demonstrated that in a nonpolar rubber blend, such as NRBR, the governing factor for the distribution of the nanofillers was the viscosity of the individual phases. In this case, BR showed a lower viscosity than NR (40 vs. 60), which probably eased chain diffusion into the clays [11].

Table 6.5 Degradation temperatures of rubber compounds.

Sample	T_{max1} (°C)	T_{max2} (°C)
NRBR	394.1	470.8
NRBR3CCa	391.6	468.8
NRBR3C30	392.2	475.2
NRBR3C15	392.4	476.0
NRBR3PLD	391.9	465.1
NRBR3PF100	393.3	466.3

The increase of thermal stability of nanocomposites is generally attributed to the barrier effect that hinders the diffusion of small molecules generated during thermal decomposition [4].

6.3 NRBR/organo-montmorillonite compounds

Concerning the results obtained until now it is clear that the OMMTs permit to achieve better mechanical properties. An in-depth study about NRBR blends loaded with OMMTs was carried out.

The optimum curing time at a specific vulcanization temperature is commonly determined automatically by a rheomether. It can lasts from few minutes to several dozens of minutes, depending on rubber compound features. The compound vulcanization lasts for the optimum curing time previous determined.

Unfortunately the rheometer available in "IVG Colbachini" is used to control the industrial production, so the measure lasts 3 minutes and occurs at 185°C to accelerate the quality control phase. The only variation possible is the change of the temperature. Consequently, to determine the optimum curing temperature, a series of rubber sheets vulcanized for different times at 150°C was produced starting from the same compound Table 6.6 summarizes the samples compounded and characterized.

Table 6.6 Rubber compounds tested.

Sample	1.5 phr	3 phr	10 phr	C30	C15
NRBR1.5C30	X			X	
NRBR1.5C15	X				X
NRBR3C30		X		X	
NRBR3C15		X			X
NRBR10C15			X		X

6.3.1 Curing characteristics

Figures 6.10 (a) and (b) show the vulcanization curves obtained for the samples NRBR3C30 and NRBR3C15 detected at 150°C for 3 minutes.
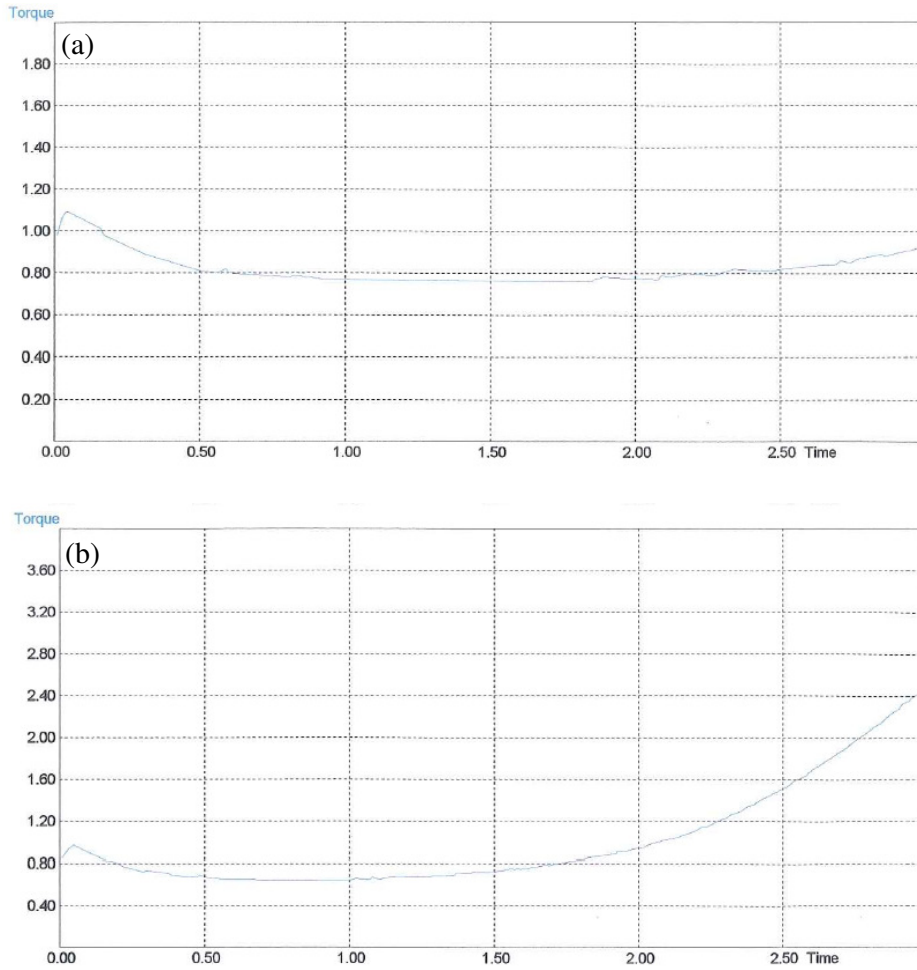
Fig. 6.10 Rheometric curves of (a) NRBR1.5C30 and (b) NRBR1.5C15.

It is evident that the optimum of vulcanization was not achieved, in fact the curves are not similar to the one shown in Figure 3.7 in Chapter 3. Particularly, no changes in the torque are observed in NRBR3C30 and little increase is noted for NRBR3C15 after 2 minutes. These results demonstrate that this treatment is not sufficient to carried out a complete rubber vulcanization.

The same behaviour was observed for the samples filled with 1.5 phr of organoclays at 150°C.

On the contrary, executing the test at 185°C, the vulcanization curve shows a strong increase in the torque (Figure 6.11) due to an increase in the crosslink density. In addition, a reversion behaviour is observed. This means that a thermal treatment at 185°C for 3 minutes leads to a chain scission in the rubber compound.
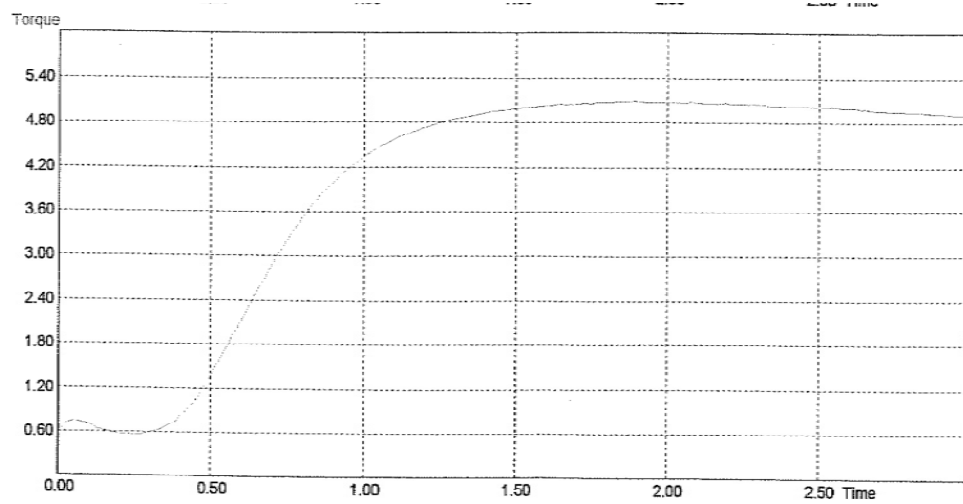
Fig. 6.11 Rheometric curve of NRBR3C15.

Increasing the C15 content up to 10 phr, a smaller increase in the M_L is observed but the reversion becomes more evident (Figure 6.12).
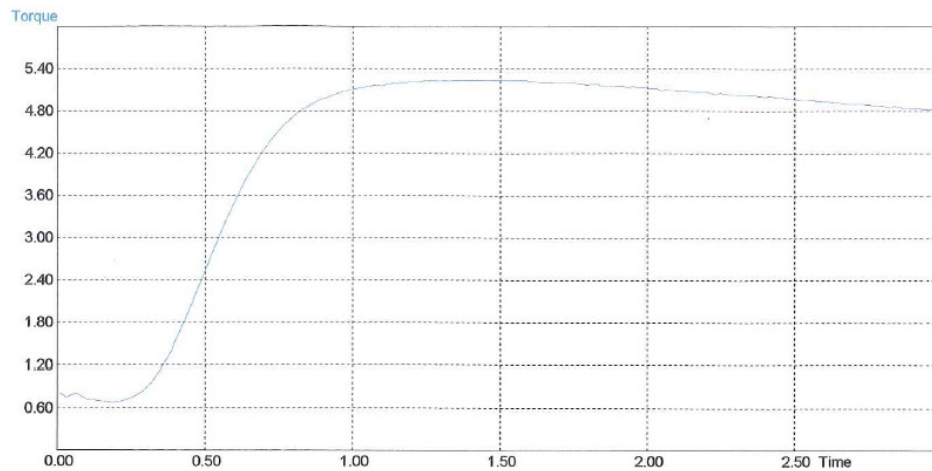

Fig. 6.12 Rheometric curve of NRBR10C15.

These results demonstrate that each vulcanization temperature has a corresponding optimum curing time.

6.3.2 XRD analysis

Vulcanized samples were characterized by using X-ray diffraction. As previous indicated the analysis was complex for the presence of stearin diffraction peaks.
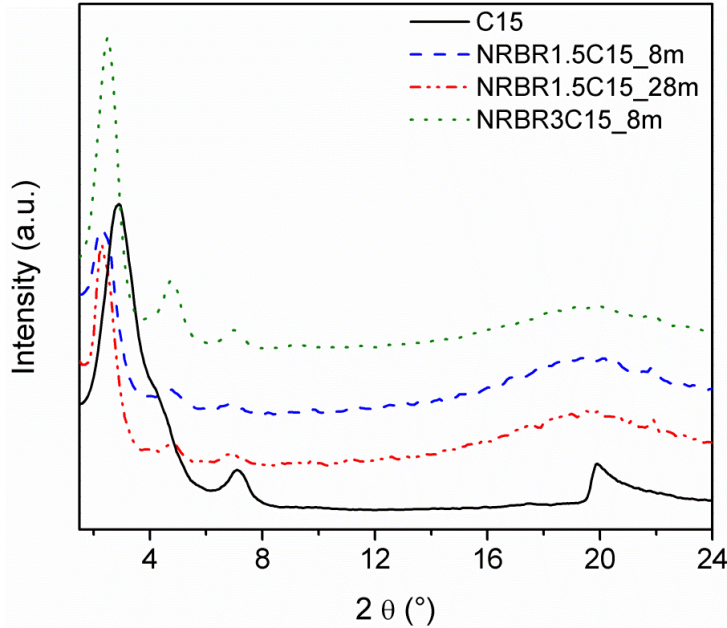

Fig. 6.13 XRD patterns of rubber compounds.

Figure 6.13 shows the spectra of the samples filled with 1.5 phr of C15 for the shorter and the longer vulcanization time. An intercalation condition is probably achieved in these compounds, in fact the C15 (001) reflection, detected at $2\theta = 2.89°$, is not displayed. On the contrary a diffraction peak is shown around $2\theta = 2.29°$, indicating an increase in the d-spacing of the nanoclays. As previous explained, this peak could be due to an overlap of both stearin and C15 reflections.

Comparing the diffractograms in Figure 6.13 and Figure 6.4 a difference in the intercalation degree achieved can be noted. In fact in the Figure 6.4 the clay d-spacing obtained after the mixing is higher ($2\theta = 2.04°$). This result demonstrates that the two-roll mill is a compounding method which does not provide reproducible performance. The curing time seems to not cause deintercalation phenomena, contrary to other authors reported [12, 13].

Higher order reflections are present in Figure 6.13 and they become more evident increasing the nanoclay content. This means that the platelets achieved an ordered

disposition into the rubber matrix. Filling the sample with 3 phr of C15 the d-spacing decreases. The dispersion of the clay becomes more difficult.

It is well-known that stearic acid, contained in the used stearin, acts as an activator in sulphur curing. During the course of the vulcanization, the steari acid dissolves zinc oxide and forms a kind of zinc organic complex, which is an cure activator. Several authors supposed that ester linkages are formed with the acidic silanol groups at the edge of the silicate layers and the carboxylic groups of stearic acid. This interaction can provoke the migration of the zinc organic complex inside the clay galleries by causing rubber crosslinking here, and consequently inducing better clay dispersion via layers separation or delamination/exfoliation. This phenomenon probably occurs with C15 nanoclay.

For the C30-filled samples a mix of intercalation and deintercalation phenomena is probable (Figure 6.14).
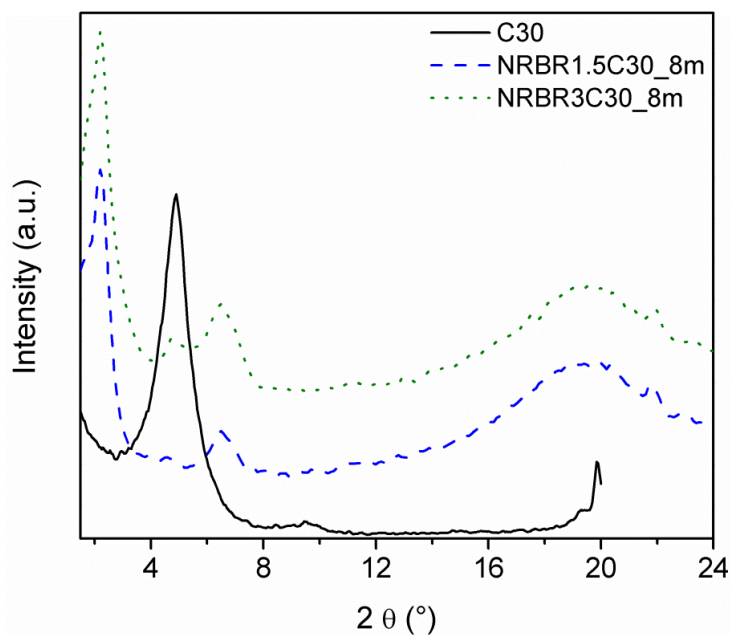

Fig. 6.14 XRD patterns of rubber compounds.

In fact, 1.5 and 3 phr loaded compounds show a peak around $2\theta = 2.20°$. This is the same range where the diffraction peak of pure stearin appears, in addition this band is also present in the XRD curves of silica and carbon black-loaded samples. The peak around $2\theta = 6.50°$ could derive mainly from the extraction of the organic modifier and not to the stearin because its intensity increases with the rising of clay content. In addition, pure

stearin shows diffraction peaks at 2θ = 6.60° and 2θ = 21.58°and the former displays a lower intensity in respect to the latter. Consequently, the reflections around 2θ = 6.50° to be attributed to stearin would have an intensity reduced than the bands which appears around 2θ = 21.80°. However, a clay intercalation can also be supposed because of the presence of the little band around 2θ = 4.80 which could be the second order reflection of the clay.

6.3.3 Mechanical properties

Tensile test results in function of curing time, in terms of tensile strength, elongation at break and modulus at 300%, are summarized in Figures 6.15 (a) and (b).

Figures 6.15 (a) and (b) show the data obtained for 1.5 phr OMMT-filled samples. It is clear that mechanical properties change with vulcanization time. In particular, the sample NRBR1.5C15 displays an increasing trend in tensile performance up to around 18 minutes (Figure 6.15 (b)). For curing time longer than 18 minutes the properties make worse, a reversion phenomenon can be supposed.

The sample NRBR1.5C30 shows the best mechanical properties between 23 and 28 minutes (Figure 6.15 (a)). The optimum curing time is probably in this range. In addition, these results confirm the action of the organo-modifiers as catalytic agents for the vulcanization. In fact, C15-filled sample shows a optimum curing time lower than C30-filled sample, this is probably related to the higher modifier concentration of C15.
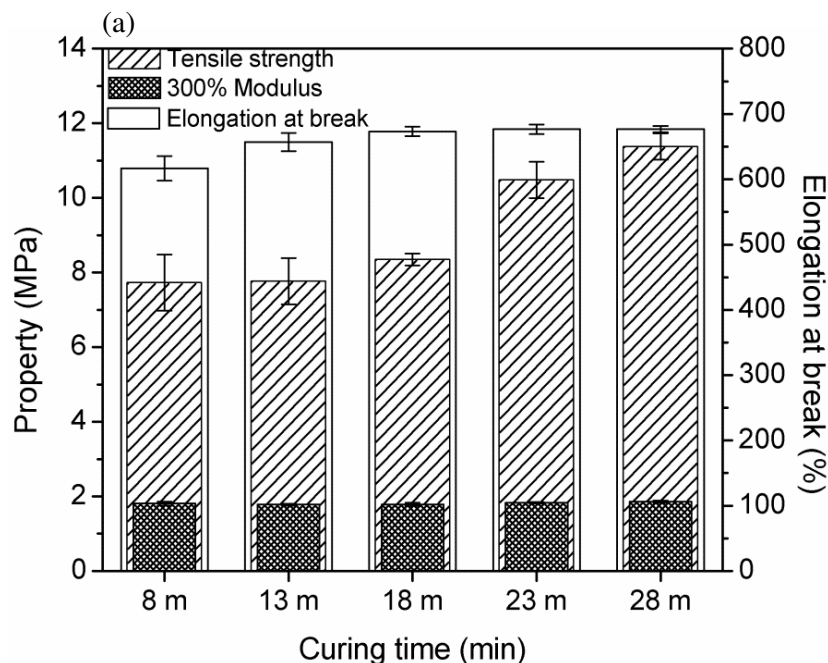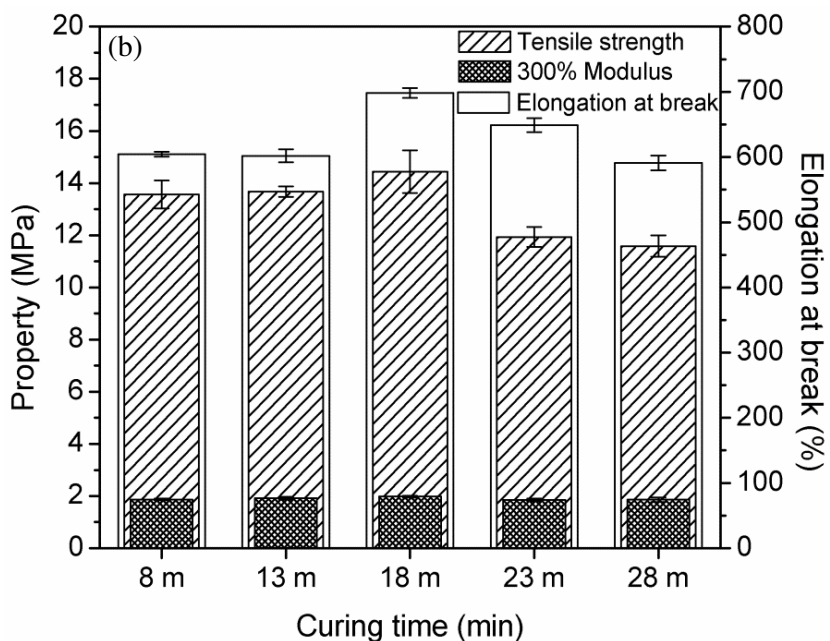
Fig. 6.15 Mechanical properties of rubber compounds filled with (a) 1.5 phr of C30, (b) 1.5 phr of C15 at different curing time.

Concerning the tensile performance displayed by the two rubber compounds at the optimum curing time, it is possible to observed that Cloisite 15A gives better mechanical performance. This clay acts as reinforcing agent increasing the tensile strength. At the same time the higher modulus at 300% indicate stronger interactions developed between the clay and the rubber matrix.

The tensile performance obtained for the samples filled with 3 phr of nanoclays are shown in Figures 6.16. As expected the optimum curing time is reduced increasing the OMMT content.
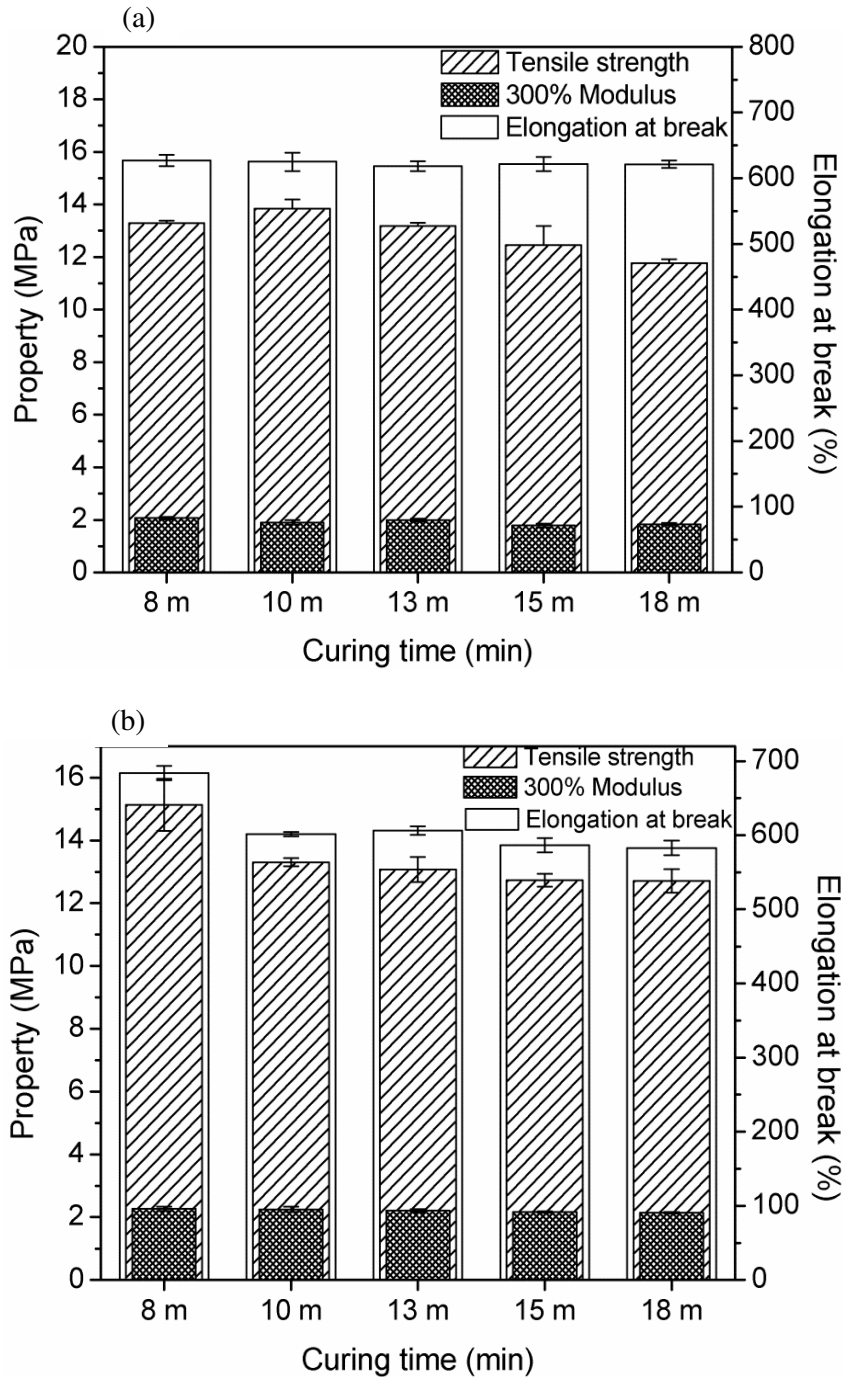
Fig. 6.16 Mechanical properties of rubber compounds filled with (a) 3 phr of C30, (b) 3 phr of C15 at different curing time.

Doubling the nanoclay amount an increase in the tensile strength and in the modulus at 300% is obtained. However, a decrease in the elongation at break is noted for the sample loaded with C30, considering 10 minutes as optimum curing time. This is probably due to

a poor dispersion of this clay in the matrix and to aggregation phenomena. No significant variations in elongation at break were observed for C15-filled sample.
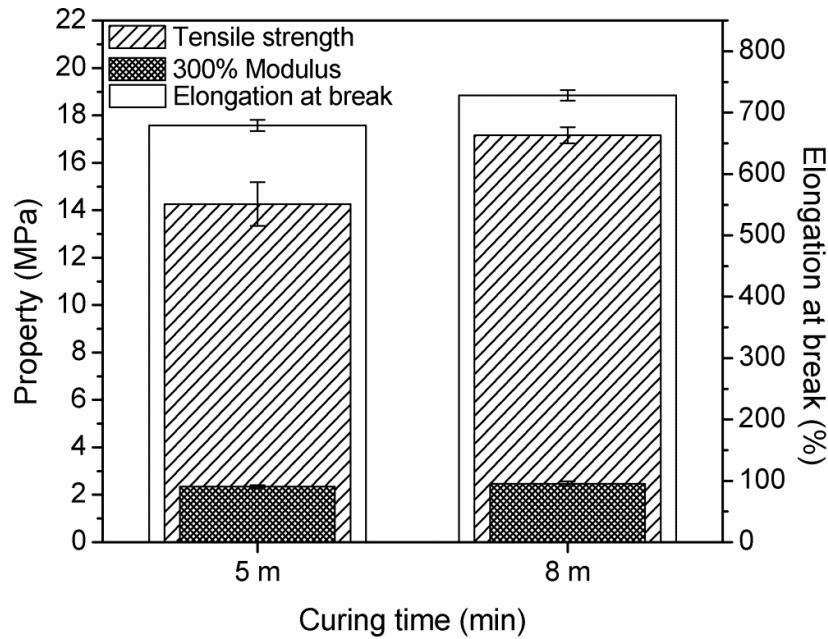

Fig. 6.17 Mechanical properties of rubber compounds filled with 10 phr of C15 at different curing time.

Figure 6.17 shows the tensile performance obtained for 10 phr C15-filled samples. Regarding the previous results only two curing times were considered. Better mechanical properties were observed after 8 minutes of vulcanization as for the 3 phr filled sample. Since large minute ranges were considered it is possible that 8 minutes is not the optimum curing time for these samples.

An improvement in the tensile strength, modulus at 300% and elongation at break is noted adding 10 phr C15. Tensile strength improvement, related to a rising in the elongation at break, is a phenomenon already observed for rubber/organoclay nanocomposites.

Tear strength data are indicated in Figures 6.18 (a), (b) and (c). These results are agree with the tensile test values.
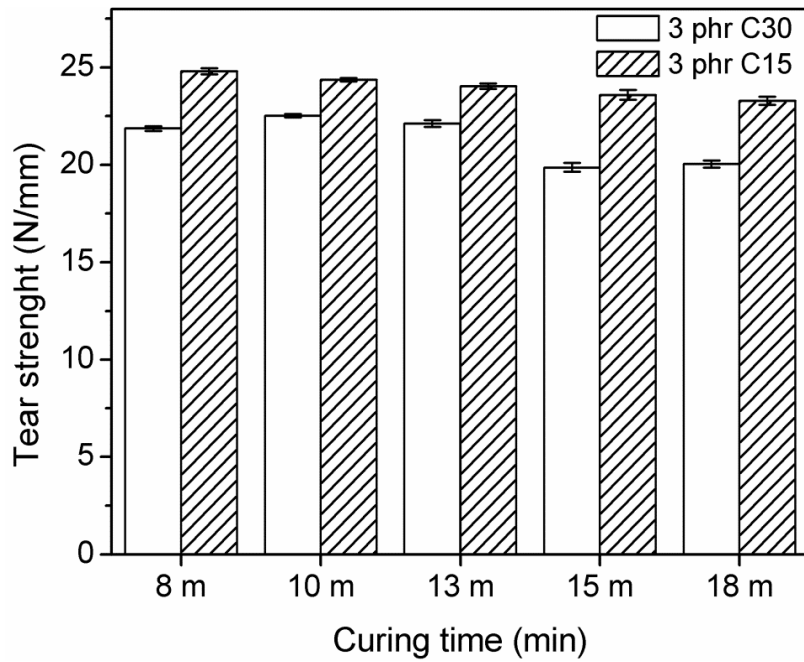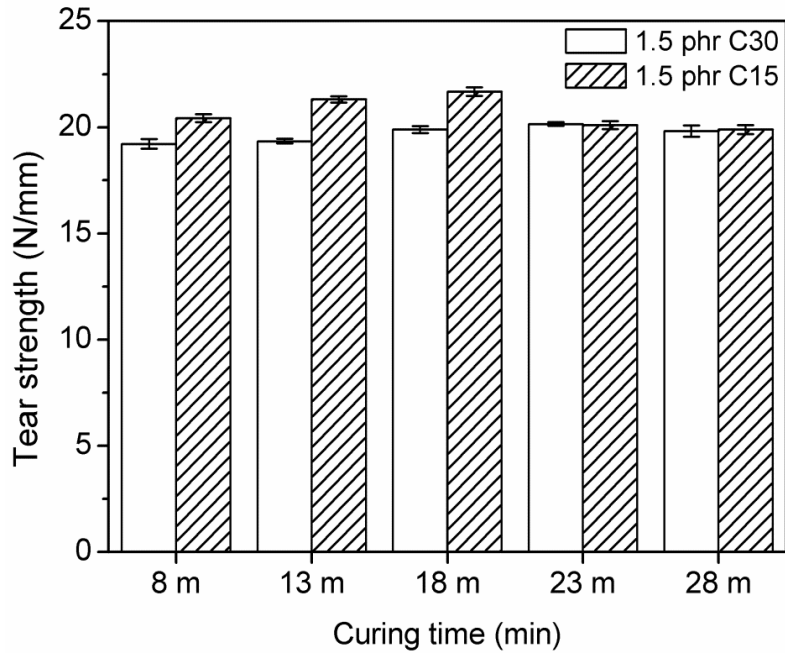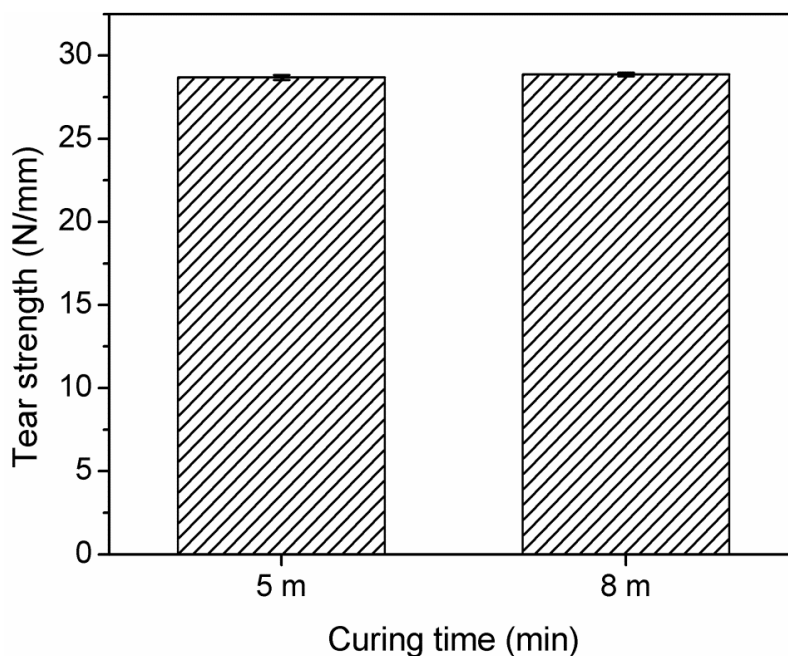
Fig. 6.18 Tear strength of rubber compounds filled with OMMTs (a) 1.5 phr , (b) 3 phr (c) 10 phr at different curing time.

6.4 NRBR/conventional filler compounds

For comparison purposes, rubber compounds loaded with the conventional fillers, carbon black (CB) and silica (S), were prepared. Until now, several works have proposed studies on mechanical properties of rubber filled with carbon black, silica and nanoclays. Generally, filler loadings higher than 10 phr are used for CB and S, while the clay concentrations do not exceed this value.

NRBR blends filled with 1.5, 3 and 10 phr of CB and S were compounded by using two roll mill and vulcanized at 150°C for different times. A sample filled with 30 phr of filler were obtained only by using CB, with silica it was impossible to produce a compound.

6.4.1 Curing characteristics

As the nanoclays, CB and S influence the curing process. In particular, CB acts as catalysts and accelerates the vulcanization reaction, while the acidic nature of silica provokes filler an absorption of accelerators retarding the vulcanization process. However, their effect on optimum cure time is less pronounced with respect to the organoclays.

Table 6.7 Minimum torque, maximum torque and delta torque of rubber compounds**.**

Sample	M_L (dNm)	M_H (dNm)	ΔM (dNm)
NRBR1.5S	0.60	4.93	4.33
NRBR3S	0.62	4.90	4.30
NRBR10S	1.06	3.99	2.93
NRBR1.5CB	0.53	4.50	3.97
NRBR3CB	0.59	5.44	4.85
NRBR10CB	0.81	5.99	5.18
NRBR30CB	1.25	9.48	8.23

The minimum torque shows an increase with increasing filler content (Table 6.7). This means that the processability of the compounds becomes a little more difficult, in particular for the sample NRBR10S which presents the higher M_L value. The increase could be due to the agglomeration of the powders in the rubber matrix.

An opposite trend is observed in M_H and ΔM when silica or carbon black loading rises in the compound (Table 6.7). Particularly, decreasing for the silica-filled samples and increasing for the carbon black-filled ones is noted. It was reported that fillers, such as silica, reduce ΔM values due to interaction of the polar –OH groups with the accelerator molecules [14]. On the contrary, the ΔM increase in the CB filled compounds is attributed to the strong physico–chemical interactions which involve a number of various reactive groups on the carbon black surface as well as the mechanical anchorage of the rubber chains inside the carbon black structure [14].

As expected, t_{90} and CRI increase or decrease for higher amount of silica and carbon black, respectively (Table 6.8).

Table 6.8 Optimum cure time and cure rate index of rubber compounds.

Compound	t_{90} (min)	CRI (min^{-1})
NRBR1.5S	1.85	152
NRBR3S	1.83	152
NRBR10S	2.22	208
NRBR1.5CB	1.93	166
NRBR3CB	1.57	164
NRBR10CB	1.69	153
NRBR30CB	1.32	149

6.4.2 Mechanical properties

The tensile properties of the silica-filled vulcanizates are present in Table 6.9.

Table 6.9 Mechanical properties of silica-filled compounds at different curing time.

	1.5 phr		3 phr	
	20 min	30 min	20 mins	30 min
Tensile strength (MPa)	> 11.70	> 10.98	> 11.28	> 11.08
Elongation at break (%)	> 693	> 710	> 770	> 768
Modulus at 300% (MPa)	1.61	1.58	1.42	1.39

The samples tested show no significant differences varying of the curing time, this means that the effect of the silica in the vulcanization is less pronounced in respect to nanoclays for low filler contents.With low loadings of silica the rubber compound keeps a high elasticity. In fact, all the samples tested do not achieve the break, consequently the maximum values obtained for the tensile strength and the elongation % were considered.

The results demonstrate that silica has a lower reinforcing effect with respect to OMMTs, in fact lower tensile strength were obtained at the same loadings. On the contrary very high elongation at break were achieved, this means that the matrix was not strongly stiff by silica. The lower modulus obtained is probably related to the common aggregation phenomena of silica.

Increasing the silica content up to 10 phr, the retardant effect of silica on the vulcanization process is observed and 40 minutes of thermal treatment were used (Table 6.10). The tensile strength and the 300% modulus reduce significantly when silica loading is high. This effect is due to aggregation phenomena and decrease in crosslink density. As a consequence, a rise in the elongation break is observed because of this rubber matrix is less stiff in respect to the 1.5 and 3 phr filled matrices.

Table 6.10 Mechanical properties of 10 phr silica-filled compounds.

Tensile strength (MPa)	> 7.83
Elongation at break (%)	> 850
Modulus at 300% (MPa)	> 0.99

It is well-known that for its high polarity silica achieves a good dispersion, and consequently improves the properties, when it is added in polar rubber. In non-polar

rubbers, such as NRBR blend, silica shows a great tendency to aggregate if no surface treatments are carried out.

Figures 6.19 (a) and (b) show the mechanical properties of the compounds filled with low amounts of CB. It is interesting to note that the properties depend on the curing time. In particular, increasing the amount of CB the optimum curing time is shorter due to the catalytic action of the filler.
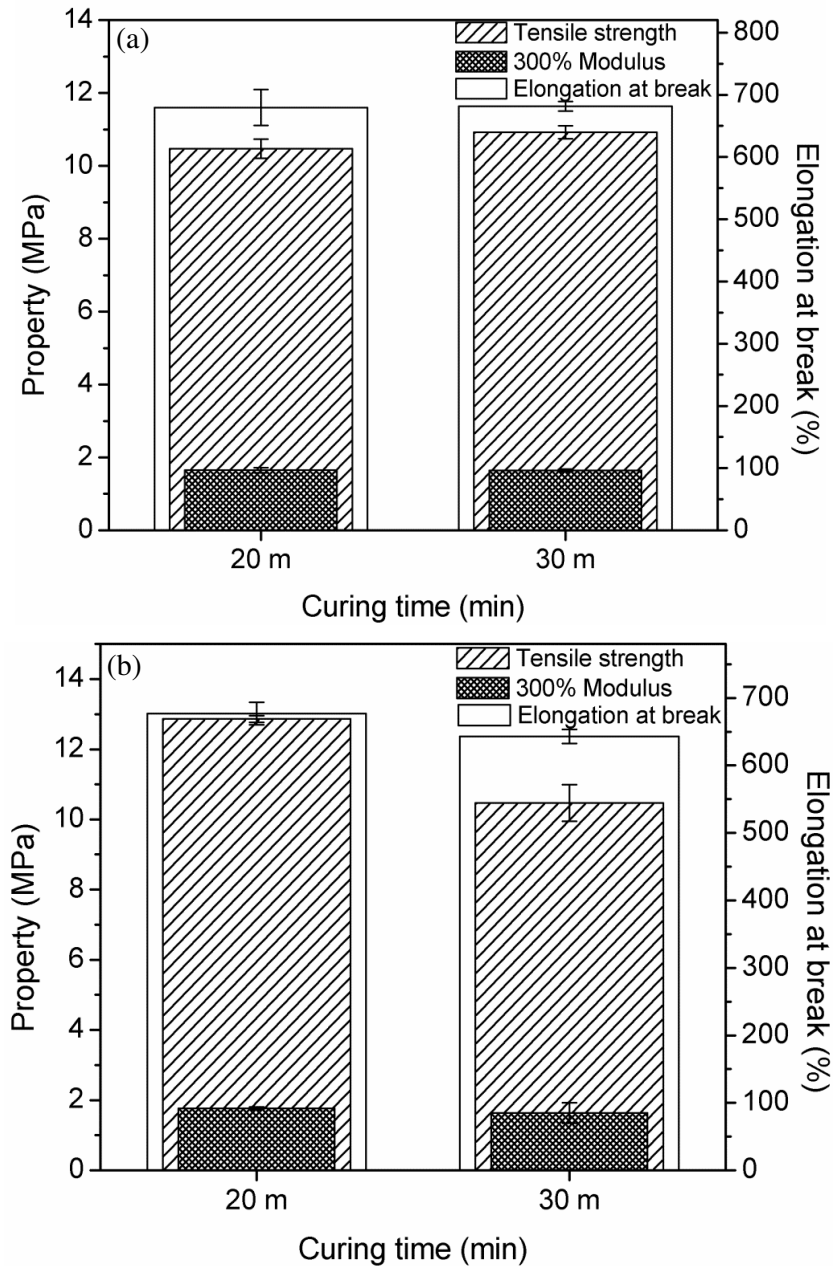

Fig. 6.19 Mechanical properties of rubber compounds filled with (a) 1.5phr, (b) 3 phr CB at different curing time.

Figure 6.20 summarizes the tensile properties obtained for the CB-filled samples at the optimum curing time. It is clear that 1.5 phr is a too low amount to improve the mechanical properties. In fact the tensile strength it is similar to the one of 1.5 phr-silica-filled sample, this means that no significant reinforcing effect is carried out by carbon black.

The increase of CB content provokes an improvement in the tensile strength and in the modulus at 300% at the expense of the elongation at break, which strongly decreases. The increase in the values of modulus at 300% is due to the strong interactions developed between the filler and the rubber matrix. The increase in crosslink density, demonstrated by the high modulus at 300%, on the other hand is responsible for the significant decrease of the elongation at break. In fact, a stiffening of the matrix is achieved.
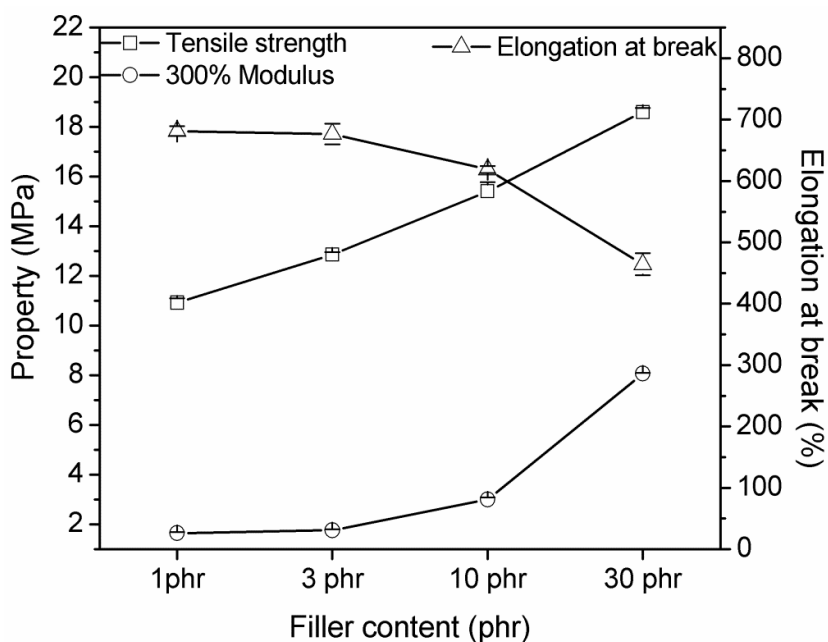

Fig. 6.20 Mechanical properties of CB-filled compounds vs. carbon black content.

Comparing tensile results obtained for CB-filled samples with the ones obtained for C15-filled samples, it can be noted that the latter show overall better mechanical performance, at the same level loading. However, the improvement obtained using an OMMT in respect to CB is not so evident as reported in several other scientific works [3, 15, 16]. This is probably due to the mixing method used for the compound productions, which does not permit strong filler dispersion and reproducibility.

The different results obtained using CB or C15 as filler in the NRBR blend is mainly due to the interaction mechanism developed between filler and matrix. In particular, carbon black forms strong covalent bonds with rubber chains but these are restricted in zone at filler/rubber interface. These interactions limit the movement of rubber chains and consequently the entanglements slippage is reduced. This interaction mechanism justifies the mechanical performance showed by compounds highly loaded with CB, which display an increase in the tensile strength but the detriment of the elastic characteristics.

On the other hand, nanoclays exhibit physical absorption with the rubber matrix consequently the mobility of the rubber chains is higher than in carbon black loaded compounds. In addition, nanoclays have a high aspect ratio, so if the exfoliation condition is achieved a small amount of nanoclays is enough to interact with the total mass rubber [17].

Figure 6.21 displays the tear strength of various vulcanizates filled with silica. 1.5 and 3 phr filled samples show similar values for the tear strength. Increasing silica amount up to 10 phr the tear strength decreases as observed for tensile strength.
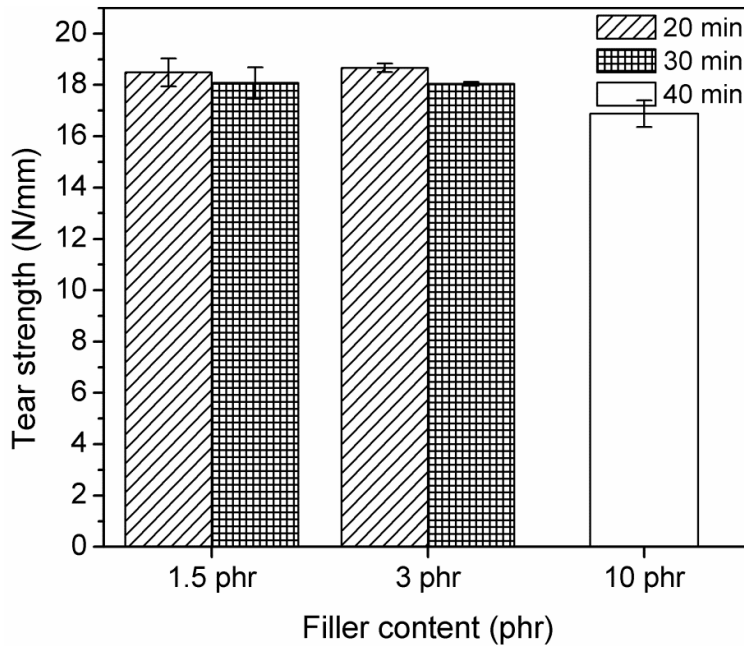

Fig. 6.21 Tear strength of silica filled compounds.

On the other hand, using the CB an increasing trend is observed in Figure 6.22. In particular an improvement of 104% is obtained increasing the CB amount from 10 phr to

30 phr. It is well-known that tear strength, such as tensile strength and abrasion resistance, tends to increase with the rising of carbon black content, until to achieve a maximum value around 50-60 phr. A further addition of the fillers provokes a detriment of these properties due to aggregation phenomena.
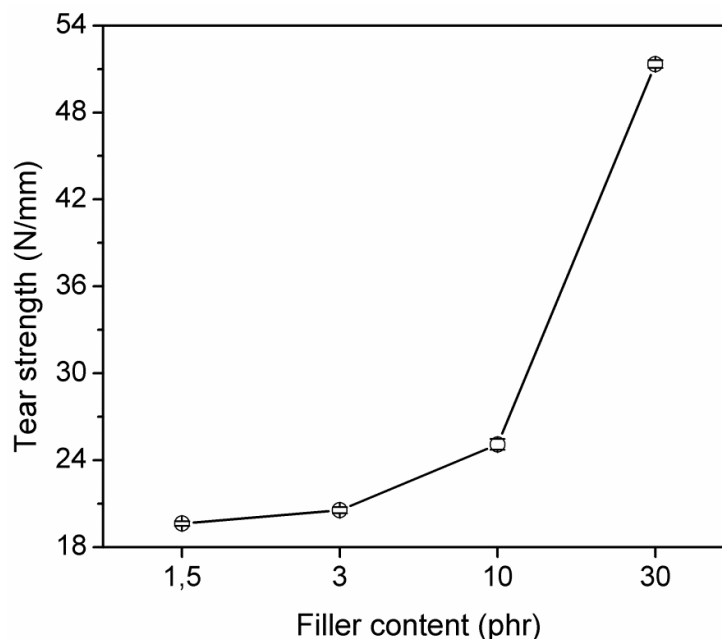

Fig. 6.22 Tear strength of CB-filled compounds vs. carbon black content

Comparing these results with the tear strength values obtained by using the nanoclays, it is evident that the vulcanizates having equal amounts of fillers give different tear strength. Particularly, the compounds with silica and carbon black show lower values. Although, it is established that spherical particles can blunt the crack tip more effectively than the plate-shaped filler having aspect ratio particles [18], such a small amounts of CB and S used in this experiment may not be sufficient to effectively blunt the tear tip. In particular, it is necessary to add 10 phr carbon black to obtain similar tear strength as the composite with 10 phr C15.

The higher values obtained for OMMT-filled samples can be due to the layer structure of the clay which can strongly restrict the motion of rubber molecules and hinders the propagation of the crack during tearing [19].

References

[1] S. Varghese and J. Karger-Kocsis, *J. Appl. Polym. Sci*, **91**, 813 (2004).

[2] M.S. Kim, G.H. Kim and S.R. Chowdhury, *Polym. Eng. Sci.*, **47**, 308 (2007).

[3] P.L. Teh, Z.A. Mohd Ishak, A.S. Hashim, J. Karger-Kocsis and U.S. Ishiaku, *J. Appl. Polym. Sci*, **94**, 2438 (2004).

[4] L.N. Carli, C.C. Roncato, A. Zanchet, R.S. Mauler, M. Giovanela, R.N. Brandalise and J.S. Crespo, *Appl. Clay Sci.*, **52**, 56 (2011).

[5] Q. Liu, Y. Zhang and H. Xu, *Appl. Clay Sci.*, **42**, 232 (2008).

[6] A. Das, F.R. Costa, U. Wagenknecht and G. Heinrich, *Eur. Polym. J.*, **44**, 3456 (2008).

[7] M.S. Kim, G.H. Kim and S.R. Chowdhury, *Polym. Eng. Sci.*, **47**, 308 (2007).

[8] V. Thakur, A. Das, R.N. Mahaling, S. Rooj, U. Gohs, U. Wagenknecht and G. Heinrich, *Macromol. Mater. Eng.*, **294**, 561 (2009).

[9] N. Rattanasom, A. Poonsuk, T. Makmoon, *Polym. Test.*, **24**, 728 (2005)

[10] N. Tabsan, S. Wirasate and K. Schiva, *Wear,* **269**, 394 (2010).

[11] A. Bandyopadhyay, V. Thakur, S. Pradhan and A.K. Bhowmick, *J. Appl. Polym. Sci*, **115**, 1237 (2010).

[12] X.P. Wang, A.M. Huang, D.M. Jia and Y.M. Li, *Eur. Polym. J.*, **44**, 2784 (2008).

[13] K.G. Gatos, L. Százdi, B. Pukánszky and J. Karger-Kocsis, *Macromol. Rapid Commun.*, **26**, 915 (2005).

[14] S. Chakraborty, S. Bandyopadhyay, R. Ameta, R. Mukhopadhyay, A.S. Deuri, *Polym. Test.*, **29**, 181 (2010).

[15] M. Arroyo, M.A. López-Manchado and B. Herrero, *Polymer*, **44**, 2447 (2003).

[16] N. Rattanasom, S. Prasertsri, T. Ruangritnumchai, *Polym. Test.*, **28**, 8 (2009).

[17] M.A. López-Manchado, J.L. Valentín, J. Carretero, F. Barroso and M. Arroyo, *Eur. Polym. J.*, **43**, 4143 (2007).

[18] A.M. Riley, C.D. Paynter, P.M. McGenity and J.H. Adams, *Plast. Rubb. Proc. Appl.*, **14**, 85(1990)

[19] Y. Liang, W. Cao, Z. Li, Y. Wang, Y. Wu and L. Zhang, *Polym. Test.*, **27**, 270 (2008).

Conclusions

This PhD thesis focused on the study of rubber compounds for industrial applications.

The first part of this scientific work regarded the production and the characterization of rubber compounds based on ethylene vinyl acetate with a high content of VA. Particularly, the attention was concentrated on the material flame resistance properties. Unfortunately, the final end-use of this compound requires flame retardancy but also no emissions of obscuring and toxic smoke. Consequently, the most common fire retardant additives used in polymers based on halogen were excluded.

The first difficult met concerned the production method of the compounds. The mixing of the ethylene vinyl acetate with the other ingredients by using the two-roll mill revealed itself very difficult. This is principally due to the features of EVA with high vinyl acetate content which presents as highly sticky rubber and it attaches on the rolls during the compounding. This made difficult a continuous cutting and folding from the operator, necessary to favour a uniform dispersion of the ingredients.

Several commercial products micro and nano-sized were added to the EVA-based compounds. The use of intumescent products, often used in plastic EVA whose improve significantly flame retardancy, demonstrated poor effectiveness in the rubber compounds studied. On the contrary, aluminium tri-hydroxide seems to have a fundamental importance in the combustion reduction of the EVA-based rubber compounds.

Two kinds of organo-modified nanoclays were also tested. The cone calorimeter and the LOI provided different results. In particular, cone calorimeter demonstrated that the organic-modifier did not influence the combustion behaviour of the sample. On the contrary, the flame retardancy is strictly dependent on the surfactant present within clay layers. Cloisite 30B provided the higher LOI values probably for the higher dispersion degree achieved in the matrix, confirmed by the XRD analysis. This is due to the presence of the hydroxyethyl polar groups which increases the compatibility of this clay with the highly polar 70 VA-EVA rubber.

The second part of this thesis was devoted to the study of mechanical performances of natural rubber/polybutadiene blend. First of all several nanoclays were added to the rubber compounds and their effects on tensile properties were considered.

Observing that the organo montmorillonites gave the best results an in-depth study about these nanoclays was carried out and a comparison with the effectiveness of conventional fillers, such silica and carbon black, was executed.

The curing characteristics of the compounds were considered and several tests to determine the optimum curing time were carried out.

Considering overall mechanical performances the NR/BR blend filled with Cloisite 15A exhibits the highest improvement of mechanical properties in respect to the one loaded with Cloisite 30B. This behaviour is due to a higher compatibility between the rubber matrix and the clay favourite by the filler strong apolar character.

The blends filled with silica demonstrated higher elasticity for all the loadings tested. However, increasing the silica content its typical tendency to aggregate became evident and a detriment of tensile and tear strength were observed.

A good dispersion of silica in apolar rubber without the use of compatibilizer is very difficult to achieve, and in this case the use of the two-roll mill placed in an unfavourable situation.

Cloisite 15A-filled samples showed better mechanical performance in respect to carbon black-loaded blends, at the same level loading. This is mainly due to the interaction mechanism developed between filler and matrix. In fact, while carbon black forms strong covalent bonds with rubber chains, nanoclays exhibit physical absorption. Consequently the carbon black interaction mechanism limits strongly the movement of rubber chains and, as observed in this thesis, with loading increasing the higher tensile strength is accompanied by a detriment of the elastic characteristics.

However, the differences between the mechanical performances of the samples filled with Cloisite 15A and the ones filled with carbon black were not so high as reported in several other scientific works. This is probably due to the use of the two-roll mill.

It is clear that to exploit the nanofiller advantages the first step is to achieve a their optimum dispersion, near to exfoliation condition.

Finally, a consideration about the economical aspect must to be done when the aim is an industrial production of a material. In fact, nowadays the cost of organo-montmorillonites is very high, near to 15 euro/kg, probably for their still poor diffusion in the industry and the expensive and longer procedures necessary to obtained the organo-modify.

On the contrary, the conventional fillers, such as silica, carbon black but also aluminium tri-hydroxide are very cheaper, less than 1 euro/kg. It is obvious that to justify the use of nanoclays for a scale production, the compound performances must to be strongly satisfactory but obtained using very small amounts of nanofillers.